University of Montana
ScholarWorks at University of Montana

Graduate Student Theses, Dissertations, & Professional Papers

Graduate School

1981

Stratigraphy sedimentology and diagenesis of the Precambrian upper Newland Limestone central Montana

Gerald A. Zieg
The University of Montana

Follow this and additional works at: https://scholarworks.umt.edu/etd
Let us know how access to this document benefits you.

Recommended Citation
Zieg, Gerald A., "Stratigraphy sedimentology and diagenesis of the Precambrian upper Newland Limestone central Montana" (1981). *Graduate Student Theses, Dissertations, & Professional Papers*. 7449.
https://scholarworks.umt.edu/etd/7449

This Thesis is brought to you for free and open access by the Graduate School at ScholarWorks at University of Montana. It has been accepted for inclusion in Graduate Student Theses, Dissertations, & Professional Papers by an authorized administrator of ScholarWorks at University of Montana. For more information, please contact scholarworks@mso.umt.edu.

COPYRIGHT ACT OF 1976

THIS IS AN UNPUBLISHED MANUSCRIPT IN WHICH COPYRIGHT SUBSISTS. ANY FURTHER REPRINTING OF ITS CONTENTS MUST BE APPROVED BY THE AUTHOR.

MANSFIELD LIBRARY
UNIVERSITY OF MONTANA
DATE: 1981

STRATIGRAPHY, SEDIMENTOLOGY, AND DIAGENESIS OF THE PRECAMBRIAN UPPER NEWLAND LIMESTONE, CENTRAL MONTANA

by

Gerald A. Zieg

B.A., University of Montana, 1979

Presented in partial fulfillment of the requirements for the degree of

Master of Science

UNIVERSITY OF MONTANA

1981

Approved by:

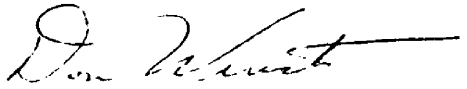

Chairman, Board of Examiners

Dean, Graduate School

June 18, 1981
Date

UMI Number: EP38250

All rights reserved

INFORMATION TO ALL USERS
The quality of this reproduction is dependent upon the quality of the copy submitted.

In the unlikely event that the author did not send a complete manuscript
and there are missing pages, these will be noted. Also, if material had to be removed,
a note will indicate the deletion.

UMI EP38250

Published by ProQuest LLC (2013). Copyright in the Dissertation held by the Author.

Microform Edition © ProQuest LLC.
All rights reserved. This work is protected against
unauthorized copying under Title 17, United States Code

ProQuest LLC.
789 East Eisenhower Parkway
P.O. Box 1346
Ann Arbor, MI 48106 - 1346

ABSTRACT

Zieg, Gerald A., M.S., Spring, 1981 Geology

Stratigraphy, Sedimentology, and Diagenesis of the Precambrian Upper Newland Limestone, Central Montana

Director: Don Winston

The Precambrian Newland Limestone was deposited below wave base in the Helena embayment part of the Belt basin. The lower Newland consists of mainly tan calcareous shale interrupted by scattered turbidite sandstone beds, and reflects an environment of pelagic deposition. The upper Newland consists of two carbonate-terrigenous cycles, each containing microspar toward its base, silty microspar in its middle, and silty shale toward its top. Asymmetric ripple cross laminations in silty microspar and silty shale record the passage of bottom currents that carried terrigenous material into the basin. Terrigenous influx may reflect a wetter climate, uplift of fault blocks along the embayment margin, or shoaling upward allowing migration of a silty shale facies basinward. In a tentative facies model, the Belt strata of the Helena embayment are interpreted as a complete transgressive-regressive sequence. The carbonate-terrigenous cycles may reflect the beginning of regression in the Helena embayment.

An eastward-thinning clastic wedge of the base of the Greyson Shale and the eastward flow direction of turbidites in the lower Newland in Deep Creek Canyon indicate an uplifted fault block to the west during Newland and Greyson deposition, perhaps restricting the Helena embayment from the main Belt basin. Along the northern margin of the Helene embayment, much of the Newland was pervasively dolomitized and partially silicified early during diagenesis, due to either meteoric water-fresh water mixing, or silica precipitation in Mg-rich $SO_4^{=}$ deficient water allowing dolomite precipitation.

Rope-shaped microspar parallel to bedding, plate-shaped microspar oblique to bedding, concave- and convex-upward hemispheroids of microspar, and thinly laminated structures and mottling in microspar were formed by pressure solution. The symmetry of the forms about vertical planes and axes suggest that overburden stress rather than tectonic stress caused the pressure solution.

ACKNOWLEDGMENTS

Many people helped make this thesis possible and I thank you all. Special thanks go to Don Winston, Johnnie Moore, Dee Taylor, Shirley Pettersen, Dave Godlewski and Cominco American, to George Cameron, Andy Sorenson, my parents and grandparents, and especially to my wife, Susan.

TABLE OF CONTENTS

Page

ABSTRACT ii

ACKNOWLEDGMENTS iii

LIST OF TABLES . . . . . .

LIST OF FIGURES . . . . . .

CHAPTER

I. INTRODUCTION 1

General Geology 2

Previous Studies 10

Methods 15

II. STRATIGRAPHIC DESCRIPTIONS 16

Rock Types 16

Correlation of Upper Newland Stratigraphy 28

Unit I 28

Unit II 31

Unit III 31

Unit IV 32

Unit V 36

Unit VI 37

Unit VII 38

Basal Greyson Shale 42

Upper Newland Carbonate-Terrigenous Cycles 42

Lower Newland Limestone 46

CHAPTER Page

Lower Newland Summary 54

Thickness of the Newland Limestone 55

III. SEDIMENTOLOGICAL INTERPRETATION 56

Conclusions 61

The Chamberlain-Newland Problem and Other Speculations 64

Summary 70

IV. NEWLANDIA AND RELATED STRUCTURES 72

Introduction 72

Morphologic Descriptions 73

Plates 73

Ropes 86

Hemispheroids and Ovoids 91

Thinly-laminated Structures 96

Mottling 99

Forms at Other Locations 99

Previous Interpretations 105

Interpretations 107

Conclusions 114

V. DIAGENESIS 116

Pressure Solution 116

Dolomitization 117

Silicification 118

CHAPTER Page

Calcitization 118

Diagenetic Relationships at Little Birch Creek . .121

Interpretation 125

Discoid Nodules 127

Conclusions 129

REFERENCES 131

APPENDIX I: SECTION LOCATIONS 137

APPENDIX II: ROCK TYPES 139

APPENDIX III: SECTION PROFILES 152

LIST OF TABLES

Page

Table 1. 18

LIST OF FIGURES

Figure		Page
1.	Regional correlation diagram	4
2.	Location diagram	6
3.	Pre-Flathead configuration of Belt strata in the Helena embayment	9
4.	Relative compositions of shale and carbonate	21
5.	Sandstone composition diagrams	24
6.	Relative abundance of major rock types	27
7.	Depositional environments of major rock types	27
8.	Correlation of the upper Newland	30
9.	Clast of microspar in a microspar matrix, Univ IV, Smith River section	35
10.	Load structures in silty microspar, Unit IV, Little Birch Creek section	35
11.	Discontinuous beds and nodules of silty microspar, Unit IV, Little Birch Creek section	35
12.	Ripple cross-lamination set in silty microspar, Unit VII, Newlan Creek section	40
13.	Discontinuous and nodular beds of silty microspar, Unit VII, Newlan Creek section	40
14.	Upper Newland carbonate-terrigenous cycles	44
15.	Isoclinal soft sediment fold, lower Newland, Smith River section	49
16.	Debris flow, lower Newland, Smith River section	49
17.	Flute casts on the sole of a calcite quartz sandstone bed, lower Newland, Deep Creek section	49
18.	Depositional and structural history of the lower Newland in the Smith River section	52

Figure Page

19. Intraclast of microspar and molar-tooth structure in intrasparite, Unit VII, Newlan Creek section . . . 59

20. Ooids and oolitic lithoclasts in calcitic quartz sandstone, lower Newland, Newlan Creek section . . . 59

21. Deformed ooid and molar tooth clast in sandy sparite, Unit VII, Little Birch Creek section 59

22. Probable and known Precambrian faults along the margins of the Helena embayment and associated slumps and clastic wedges 63

23. Tentative facies model for Belt strata of the Helena embayment 69

24. Plates oblique to bedding 75

25. Ropes 77

26. Concave-upward hemispheroids 79

27. Thinly-laminated structure 81

28. Mottling 83

29. Symmetric orientation of curved plates 85

30. Soles of beds of ropes and plates 85

31. Ropes and plates in outcrop 88

32. Matrix between plates 88

33. Solution boundary between ropes 90

34. Stylolitic boundary between ropes 90

35. Concave-upward hemispheroids in outcrop 93

36. Bottoms of concave upward hemispheroids 93

37. Variations in ovoids and hemispheroids 95

38. Thinly-laminated structure in outcrop 98

Figure Page

39. Mottling and thinly-laminated structure in outcrop . . 98

40. Oriented mottling, Deep Creek Canyon 102

41. Cut slab showing oriented mottling and microspar plates 102

42. Silicified rings, Deep Creek Canyon 104

43. Cross section of silicified ring center 104

44. Cross section of silicified ring 104

45. Evolution of plates and ropes 109

46. Thin section view of silicified ring 112

47. Chert-cored intraclasts 120

48. Dolomite rhombs in chert 120

49. Radial axial calcite 123

50. Granoblastic quartz in radial axial calcite 123

51. Rhombs of calcite in chert 123

CHAPTER I

INTRODUCTION

The stratigraphy of Belt sedimentary rocks of the northern and central parts of the Helena embayment is only generally known from the regional correlations of McMannis (1963). In the southern part of the embayment, the LaHood Formation has been studied in detail by Alexander (1955), McMannis (1952, 1955, 1963), Hawley (1973), Boyce (1975), and Bonnet (1979). These studies have suffered from lack of knowledge of the rest of the Belt stratigraphy of the Helena embayment.

As a first step for future understanding of a stratigraphic framework and of a depositional model of the Helena embayment Belt sedimentary rocks, I have measured and described five sections of Newland Limestone in the central and northern parts of the embayment, identified the major rock types in these sections, divided the upper part of the Newland Limestone into correlative units based on these rock types, and interpreted the sedimentology of the upper part of the Newland Limestone on the basis of characteristics of the individual lithologies and the stratigraphic framework revealed by the correlations. I have also described and interpreted parts of the lower part of the Newland Limestone.

In addition, I have described and interpreted some of the diagenetic features in the carbonates in the upper part of the Newland Limestone, including a new interpretation of forms described by Walcott (1914) as Algonkian algal flora. Finally, I have speculated on the relationship of

other Helena embayment Belt formations to the Newland Limestone, developed a tentative facies model for Helena embayment Belt deposition, and speculated on the nature of the embayment's margins and the relationship between the Helena embayment and the main Belt basin.

General Geology

Walcott (1899) demonstrated that the Newland Limestone is overlain by the following sequence; the Greyson Shale, the Spokane Formation, the Empire Formation, and the Helena Dolomite. Walcott (1899) further demonstrated that the Chamberlain Shale underlies the Newland Limestone and rests on the Neihart Quartzite, which in turn rests on Precambrian crystalline basement. Smith and Barnes (1966) determined that the Newland Limestone is probably correlative with the Prichard Formation to the east (Fig. 1) and with the calcareous Altyn and Waterton Formations to the northwest. Harrison (1972) supports this correlation.

The Newland Limestone is exposed only in the Helena embayment part of the Belt basin (Harrison, 1972, Fig. 2). This is an eastward extending arm of the basin whose exposures are bounded on the north by the crest of the Little Belt Mountains and on the south by the Perry line, an east-west trending fault zone that was active during Belt deposition (McMannis, 1963). Helena embayment exposures are interrupted on the west by the Boulder batholith and the Elkhorn volcanics, and extend at least as far east as the Big Snowy Mountains, where Reynolds (1979) has identified Newland shale underlying the Flathead Quartzite of post-Belt age.

Figure 1. Correlation of the lower Belt, the Ravalli Group, and the lower part of the Middle Belt Carbonate of the Belt Supergroup from the Helena embayment to central western Montana. After Harrison (1972).

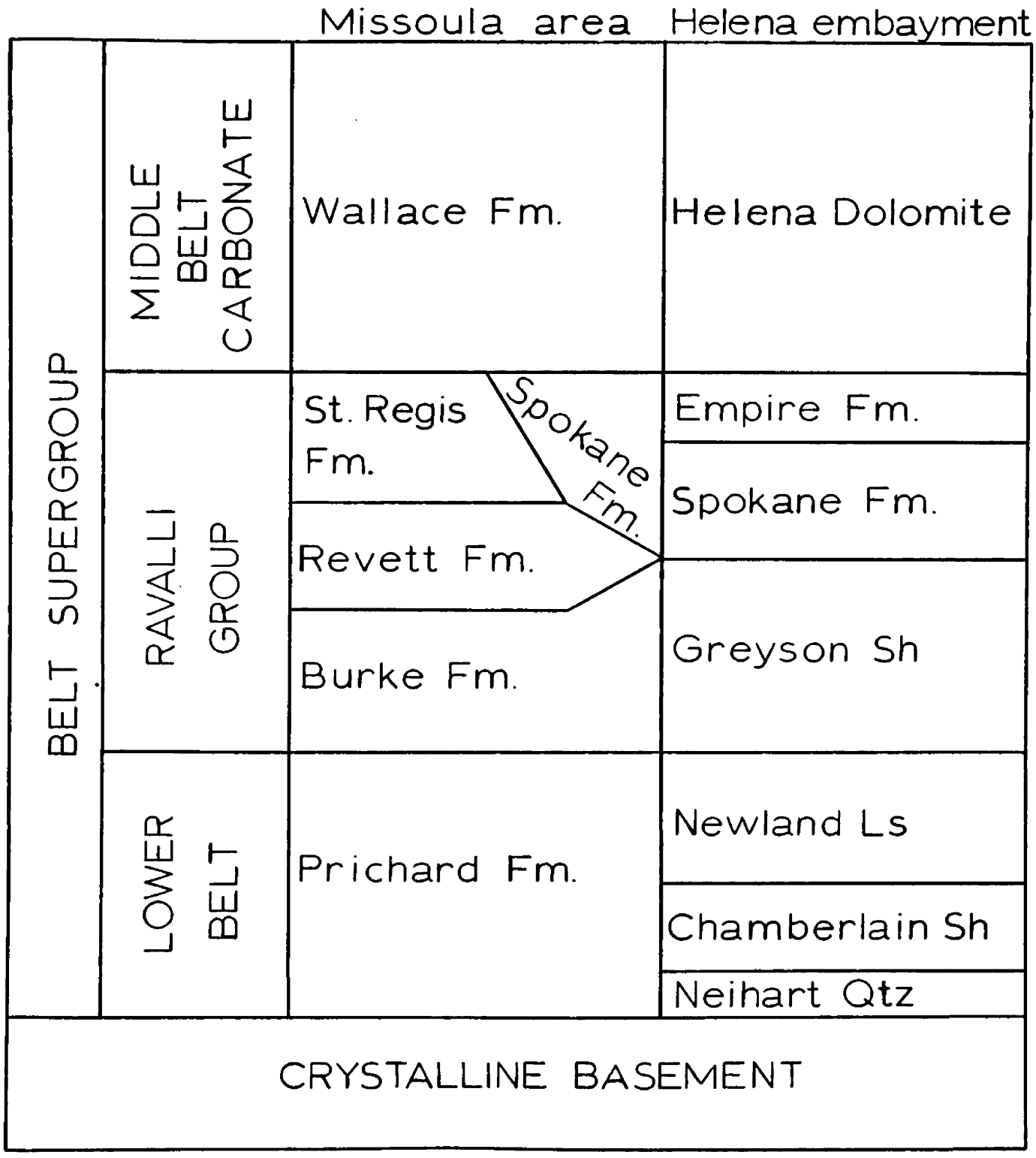
Missoula area
Helena embayment
BELT SUPERGROUP
MIDDLE BELT CARBONATE
Wallace Fm.
Helena Dolomite
RAVALLI GROUP
St. Regis Fm.
Spokane Fm.
Empire Fm.
Spokane Fm.
Revett Fm.
Burke Fm.
Greyson Sh
LOWER BELT
Prichard Fm.
Newland Ls
Chamberlain Sh
Neihart Qtz
CRYSTALLINE BASEMENT

Figure 2. Location diagram. WSS= White Sulphur Springs; 1 = Newlan Creek section; 2 = Decker Gulch section; 3 = Smith River section; 4 = Little Birch Creek section; 5 = Deep Creek section; A = Big Belt Mountains; B = Little Belt Mountains; C = Bridger Mountains; D = Castle Mountains; E = Crazy Mountains; F = Big Snowy Mountains. The stippled pattern within the dashed boundaries in the upper diagram indicates Newland Limestone exposures, and the dashed line in the lower diagram shows the approximate eastern limit of the Belt basin. The eastward extension of the dashed line encloses the Helena embayment.

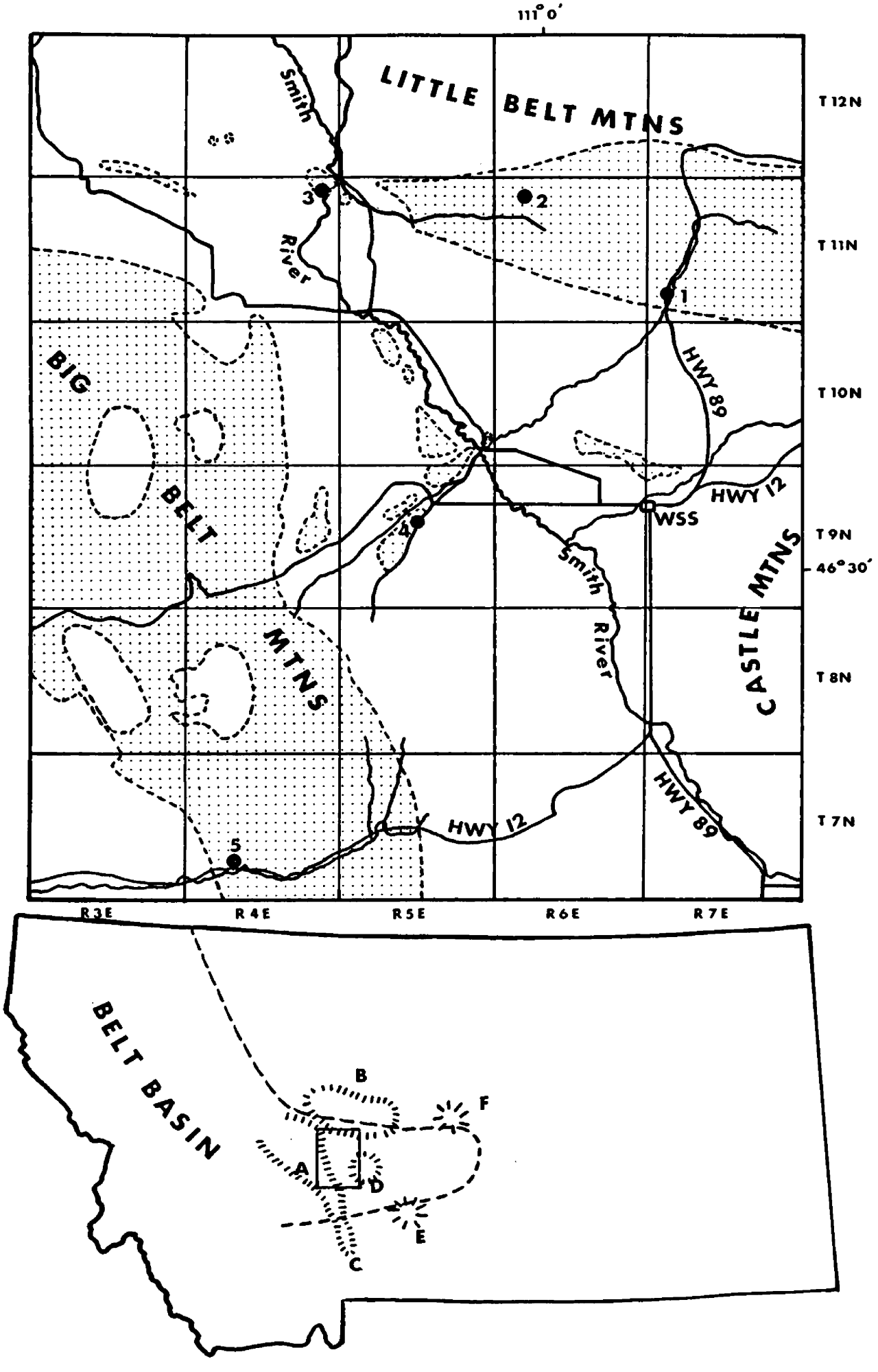
111° 0'
LITTLE BELT MTNS
Smith River
BIG BELT MTNS
CASTLE MTNS
Smith River
HWY 89
HWY 12
HWY 12
HWY 89
WSS
1
2
3
4
5
T 12N
T 11N
T 10N
T 9N
46° 30'
T 8N
T 7N
R3E
R4E
R5E
R6E
R7E
BELT BASIN
A
B
C
D
E
F

During the Proterozoic, the northern edge of the Helena embayment warped gently down to the south, while block faulting along the Perry line formed the southern edge of the embayment. After Belt deposition, uplift of the embayment's northern and southern margins bowed the Belt strata into an east-west trending syncline. Pre-Middle Cambrian erosion beveled the Belt strata most deeply on the northern and southern margins of the embayment (Walcott, 1899; McMannis, 1963; Fig. 3). Cretaceous and early Tertiary folding and thrusting uplifted the western and central parts of the Helena embayment (Woodward, 1981). The greatest uplift occurred along the northwest-southeast trending Big Belt anticlinorium. Erosion of the uplifted area exposed much of the Belt strata in the western and central parts of the embayment. Tertiary deposition, accompanied by basin and range style block faulting (Reynolds, 1979), covered much of the previously exposed Belt strata.

As a result of these tectonic events, the northernmost exposures in the Helena embayment are Neihart Quartzite, the overlying Chamberlain Shale, and possibly the Newland Limestone. The Neihart Quartzite and Chamberlain Shale are exposed only in the Neihart, Moose Creek, and Sheep Creek areas in the Little Belt Mountains, and their southward extent is unknown. McMannis (1963), Harrison (1972), and Verrall (1955) assume that the Neihart and Chamberlain extend underneath the Newland Limestone throughout the embayment. Groff (1967) suggested that perhaps these strata represent nearshore facies of the Newland Limestone. The NewlandLimestone and the Greyson Shale outcrop throughout the embayment. The Big Belt

Figure 3. Configuration of Belt strata in the Helena embayment just prior to Cambrian deposition. pCl = LaHood Formation; Cf = Flathead Quartzite; pCs = Spokane Formation; pCg = Greyson Shale; pCn = Newland Limestone; pCc = Chamberlain Shale; pCni = Neihart Quartzite; Am = Archean metamorphics. After Walcott (1899) and McMannis (1963).

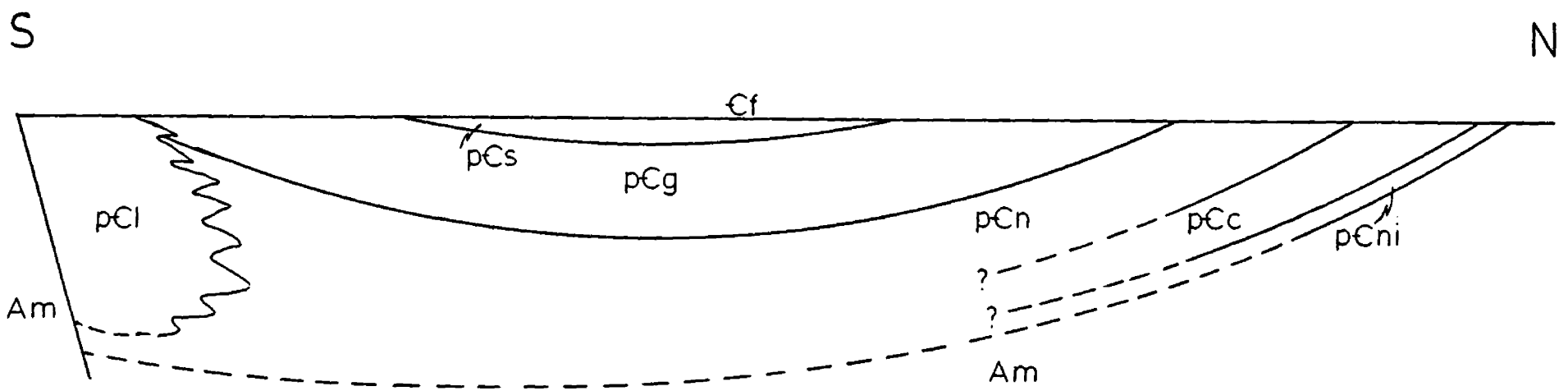
S
N
Cf
pCs
pCg
pCl
pCn
pCc
pCni
Am
?
?
Am

Mountains contain dominantly Newland Limestone exposures. The Spokane Formation outcrops only toward and in the center of the embayment and in the main Belt basin to the west. The LaHood Formation is exposed along the southern margin of the embayment.

Since the base of the Newland Limestone is nowhere exposed except along the northern margin of the embayment, the thickness of the Newland is uncertain throughout most of the embayment. Lack of sufficient knowledge of Newland stratigraphy and structural complications in areas where its base is exposed have made thickness determinations of the Newland along the northern edge of the embayment tenuous. Walcott (1899) estimated the thickness of the Newland at 2000 feet (610 meters) in the northern part of the embayment. Nelson (1963) measured 9500 feet (2896 meters) of Newland in Deep Creek Canyon in the center of the embayment, and Groff (1967) estimates its thickness in the same area to exceed 18,000 feet (5486 meters). McMannis measured 5000 feet (1524 meters) of Newland in the Horseshoe Hills.

Previous Studies

Studies of Belt rocks in the Helena embayment have been limited to description and mapping of formations, sedimentology of the LaHood Formation, microfossil description, clay mineralogy, and scattered age dating. Belt lithologies of the northern and central parts of the Helena embayment have been recognizable as mappable formations since early work by Weed and Pirsson (1896) who termed them the Belt shale formations of the Algonkian.

Weed (1899) established the type section of the Neihart Quartzite, and Walcott (1899) established the type sections for the Chamberlain Shale, Newland Limestone, Greyson Shale, Spokane Formation, Empire Formation, Helena Dolomite, and Marsh Formation (abandoned name). The Newland Limestone type sections are along Newland Creek (now Newlan Creek) and in Sawmill Canyon four miles south of Neihart. Since 1899, the Newland Limestone has been mapped and briefly described by Mertie, Fisher and Hobbs (1951), Nelson (1963), Skipp and Peterson (1965), Birkholz (1967), Hruska (1967), McClernan (1969), Phelps (1969), Dahl (1971) and Keefer (1972). Keefer (1972) remapped the Belt shales and carbonates near Neihart and measured 512+ feet (156+ meters) of Greyson Shale underlain by 567 feet (173 meters) of Newland Limestone, in turn underlain by 2021 feet (616 meters) of Chamberlain Shale. Nelson (1963) divided the Newland Limestone in the Deep Creek section into an upper limestone-bearing member and a lower shaly member.

Studies of Belt strata in the southern part of the Helena embayment have been focused on the sedimentology of the LaHood Formation, which has been studied extensively by Verrall (1955), Alexander (1955), McMannis (1952, 1955, 1963), Hawley (1973), Boyce (1975), and Bonnet (1979). McMannis (1963) correlated the Belt formations across the Helena embayment. Attempts to correlate in detail Newland sections across the southern part of the embayment have been unsuccessful, due to the repeated interruption of typical Newland lithologic sequences by coarse clastic debris shed from the upraised block south of the Perry Line.

Walcott (1899) found carbonaceous films parallel to bedding in the Greyson shales which he believed were remains of crustaceans and annelid trails. Identical carbonaceous films occur throughout the Newland, so a summation of later work on them is presented here. Walter, Oehler and Oehler (1976) re-examined these features and conclude that they are composed principally of carbon with associated crystals rich in iron and sulfur. They interpret the films as body fossils of red, green or brown algae. Horodyski (1980) reports similar abundant films from the Chamberlain and Newland shale along Belt Creek and Jefferson Creek a few miles south and southeast of Neihart. From thin sections cut parallel to bedding, he describes filamentous, spheroidal and ellipsoidal microfossils. He notes their similarity to microfossils from the middle and upper Proterozoic in the Soviet Union, Sweden, Australia, and Canada.

Walcott (1914) described forms from the Little Birch Creek section which he considered to be algal and classified them as the new genera Newlandia, Copperia, Greysonia, and Kinneyia (these forms are further discussed in Chapter IV).

Maxwell (1964) and Maxwell and Hower (1967) have determined illite polytypes of shale samples from the Neihart Quartzite, Chamberlain Shale, Newland Limestone, Greyson Shale, and Spokane Formation near Neihart. They report that all these shales are dominantly composed of the 1Md illite polytype, along with chlorite and, in one sample from the Spokane Formation, kaolinite. No measurable quantities of 3M dioctahedral micas occur in the samples. They report increasing quantities of the 2M polytype

westward, indicating increasing metamorphism in that direction. According to Hoffman and Hower (1979) smectite changes to illite at about 200 C^{o} and illite begins to change to 2M polytype mica at about 275 C^{o}. Thus the presence of the 1Md illite polytype, which is a less ordered and lower temperature illite polytype (Yoder and Eugster, 1955; Velde, 1965), indicates that the maximum temperature reached by the shales during burial ranged between 200-275 C^{o}.

The Newland Limestone is probably younger than 1700 m.y.b.p. (million years before present) and older than 1325 m.y.b.p. The maximum age for Belt strata in the northern part of the embayment is established by K/Ar dates on minerals from the Precambrian crystalline basement near Neihart. Hayden and Wehrenberg (1960) report K/Ar dates of 1320 and 1340 m.y.b.p. (without correction for argon leakage) for samples of potassium feldspar from a pre-Belt granitic dike two miles north of Neihart. With correction for argon leakage, these dates recalculate to about 1630 m.y.b.p. Burwash and others (1962) calculate a biotite K/Ar date of 1750 m.y.b.p. and a hornblende K/Ar date of 1790 m.y.b.p. from a sample of pre-Belt biotite-hornblende gneiss collected about 7 miles north of Neihart. Catanzaro and Kulp (1964) report biotite and hornblende K/Ar dates from the pre-Belt Pinto metadiorite north of Neihart that range from 1700 (biotite) to 1820 (hornblende) m.y.b.p. They attribute any younger dates from the Pinto metadiorite as a result of resetting of K/Ar ratios during intrusion of Cretaceous magmas. Catanzaro and Kulp (1964), on the basis of U/Pb ratios, calculate the age of the latest metamorphism of the Precambrian crystalline basement around Neihart at 1920 $\pm$ 20 m.y.b.p.

K/Ar dates on the Precambrian crystalline basement south of the Helena embayment are similar to those near Neihart. Hayden and Wehrenberg (1960) report a biotite K/Ar date of 1630 m.y.b.p. from a sample of biotite-plagioclase-quartz gneiss from the pre-Belt Pony gneiss near Norris, Montana, and a potassium feldspar K/Ar date of 1770 m.y.b.p. from a sample of granite gneiss collected along the Cooke City Highway south of Red Lodge. Giletti (1966) reports a 1600 m.y.b.p. age for the latest metamorphism of the Precambrian crystalline basement in southwestern Montana, based on K/Ar and Rb/Sr whole rock, biotite, muscovite, and potassium feldspar dates. However, Harrison (1972) suggests that K/Ar dates of the Precambrian crystalline basement probably reflect uplift rather than rock-forming events. Thus, the maximum age of the Belt strata in the Helena embayment is probably less than about 1700 m.y.b.p., the approximate time of uplift of the Precambrian crystalline basement on which it lies. Younger dates may reflect re-setting of K/Ar ratios due to intrusion of Cretaceous and Tertiary magmas.

Whole rock samples from the Neihart Quartzite, Chamberlain Shale, Newland Limestone, and Greyson Shale in the Little Belt and Big Belt Mountains (Obradovich and Peterman, 1968), plot on the basis of Rb/Sr and Sr^{87}/Sr^{86} analyses around 1325 $\pm$ 15 m.y.b.p. for the entire section. Unpublished Sr^{87}/Sr^{86} analyses by Peterman (according to Eby, 1977) from whole rock samples from the same section indicate what Peterman interprets to be a regional metamorphic event also of an age of 1325 $\pm$ 15 m.y.b.p. Any metamorphism of the Belt strata in at least the northern part of the

Helena embayment is improbable because of the survival of the 1Md illite polytype in these rocks reported by Maxwell and Hower (1967). Obradovich and Peterman (1968) also report whole rock and glauconite Rb/Sr dates of about 1100 m.y.b.p. for the Empire Formation, Helena Dolomite, Shepard Formation, and McNamara Formation in the Sun River area. Thus the depositional age of the Newland is greater than 1325 $\pm$ 15 m.y.b.p.

Methods

Five sections (Fig. 2) were measured with a Jacob's staff and a Brunton compass and were sampled. Intervening outcrops were studied where possible. Correlations were made on the basis of lithology and lithologic sequences.

Thin sections and acetate peels were made from pertinent samples, and cut surfaces of carbonate samples were etched with HCl. Carbonates were stained with alizarin red S solution and alizarin red S and potassium ferrocyanide solution to determine calcite and dolomite content. Some carbonate minerals were identified by X-ray diffraction analysis of both powdered specimens and sawed rock chips. Standard X-ray diffraction techniques were used by Steve Black to determine the clay mineralogy of the shales. Field data, mineralogical data, section profiles, and section locations are compiled in the appendix at the back of this volume.

CHAPTER II

STRATIGRAPHIC DESCRIPTIONS

Rock Types

Identification and description of the major rock types of the Newland Limestone make it possible to correlate lithologic sequences and interpret their environments of deposition. The major rock types in the Newland Limestone (Table 1) are tan calcareous shale, black calcareous shale, silty shale, gray microspar, black chert-bearing microspar, silty microspar, nodular black microspar, calcitic quartz sandstone, laminated quartz sandstone, and black chert (for detailed descriptions of these and the minor rock types of the Newland Limestone, see Appendix II).

Most rock types of the Newland Limestone are fine grained, restricted in mineralogy, and sedimentary structures are mostly small scale. Calcite and dolomite grains of the carbonate-rich rock types are less than about 30 microns in size. Only sparry calcite or dolomite cement in sandstone and diagenetically recrystallized calcite are up to 50 microns or more in size. The compositions of silt and sand grain populations are generally quartz rich with small percentages of plagioclase, orthoclase, microcline, muscovite, biotite, metamorphic rock fragments, chert, ooids, carbonate clasts and intraclasts, and oolitic lithoclasts. Sand grains are generally moderately to well rounded. The clay-sized fraction of all the rock types is dominantly

Table 1. Bedding thicknesses, color, and common associations of the major rock types of the Newland Limestone.

NAME	BEDDING	COLOR		COMMON ASSOCIATION
		FRESH	WEATHERED	
tan calcareous shale	tnl, tkl .3-.5 cm	T, G	T, G	lower part of the Newland Limestone
black calcareous shale	tnl, tkl .3-.5 cm	DG, Bl	DG, Bl	interbedded with silty microspar
silty shale	tnl, tkl .2-1 cm	G, DG	B, G, Gr, Ru	upper part of the Newland Limestone and Greyson Shale
gray microspar	tnb (6-8cm) with tnl, tkl .2-1cm	DG	LG	upper part of the Newland Limestone
black chert-bearing microspar	tkl, tnb .5-6 cm	DG, LG	B, DG	upper part of the Newland Limestone
silty microspar	tnb-mb 4-25 cm, with tkl .3-1 cm	DG	T, LG	upper part of the Newland Limestone
nodular black microspar	tnl, tkl .2-1 cm	DG, Bl	DB, Ru	scattered nodules in silty shale
calcitic quartz sandstone	tnl-mb .2-25 cm	LG, DG	LG	dominantly with tan calcareous shale
laminated quartz sandstone	tnb (6-10 cm)with tnl-tnb .2-5 cm	LG, Bl, B	LG, Bl, B	with silty shale
black chert	nodules, lenses, bedded stringers	Bl, DB	Bl, DB	occurs in black chert-bearing microspar

tnl=thinly laminated; tkl=thickly laminated; tnb=thinly bedded; mb=medium bedded; T=tan; G=gray; Gr=green; B=brown; Bl=black; Ru=rusty; L=light; D=dark

composed of illite with lesser amounts of chlorite. Sedimentary structures, in order of decreasing abundance, are ripple cross-laminations (all formed by migration of asymmetric ripples), soft sediment folds, load structures, and single occurrences of flute casts and convolute bedding. Lastly, carbonaceous films, though not everywhere abundant, do occur throughout the Newland Limestone.

Each major rock type in the Newland Limestone is characterized as follows. Shale ranges from carbonate rich to carbonate free, and tan calcareous shale ranges from calcite rich to dolomite rich (Fig. 4). Tan calcareous shale is the most abundant rock type in the Newland Limestone (Fig. 6) and comprises nearly all of the lower Newland and parts of the upper Newland. Black calcareous shale interleaves with silty microspar, and unlike tan calcareous shale, it is nowhere dolomitic. Silty shale is mostly non-calcareous and ranges from thinly-laminated clay-rich shale to shale containing silt-to-argillite couplets and cross-laminated sandstone lenses. Silty shale is also the dominant rock type of the Greyson Shale.

The major carbonate rock types in the Newland Limestone range from nearly pure gray microspar, both calcitic and dolomitic (Fig. 4), to silty microspar containing silty laminations, cross-laminations, and in places cross-laminated calcitic quartz sandstone lenses. Thicker bedded silty microspar contains abundant cross-laminations and interbeds of black calcareous shale. Beds over 10 cm thick generally grade upward from silt-poor to cross-laminated silt-rich microspar. Conversely, laminations and thin beds grade upward from silt-rich to

Figure 4. Relative compositions of shale and carbonate in the Newland plotted on calcite-dolomite-terrigenous component triangles.

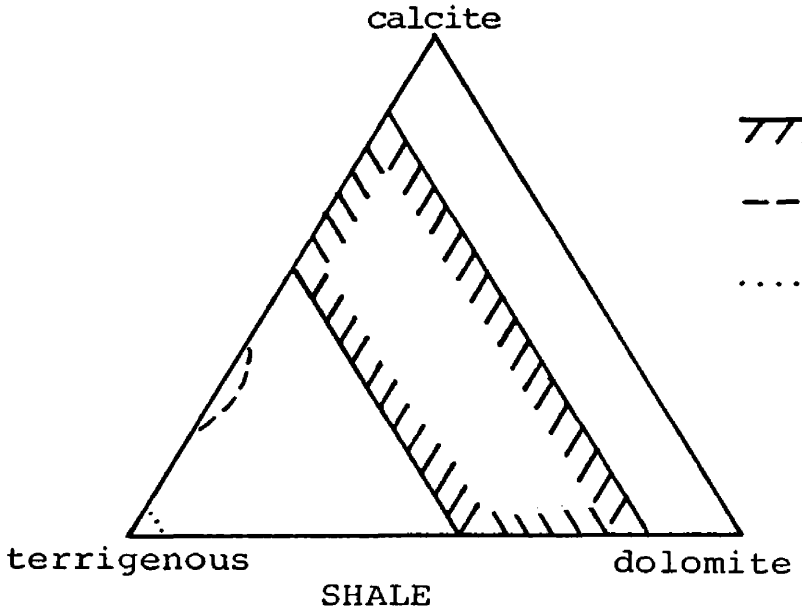
calcite
terrigenous
dolomite
SHALE
tan calcareous shale
black calcareous shale
silty shale

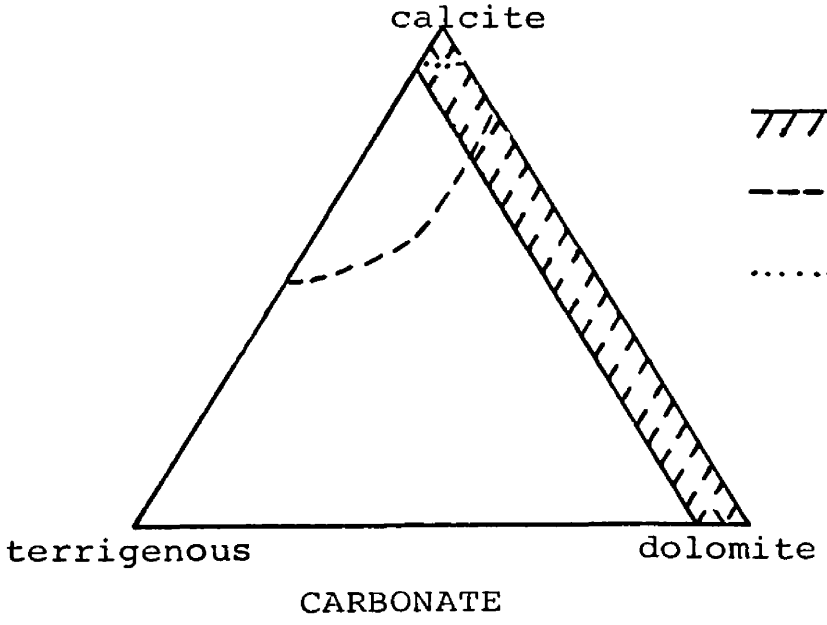
calcite
terrigenous
dolomite
CARBONATE
gray microspar and black chert-bearing microspar
silty microspar
nodular microspar

silt-free microspar. Silty layers often overlie scoured surfaces, and in places are deformed into load structures. Beds of silty microspar less than 10 cm thick contain interbedded tan calcareous shale, and laminations typically grade upward from silt-rich bottoms to pure carbonate tops.

Black-chert bearing microspar ranges from light tan-, brown-, and gray-weathering where dolomitic to dark gray-weathering when calcitic. Black chert nodules and stringers along bedding make black chert-bearing microspar distinct from the gray microspar rock type.

Nodular black microspar is non-dolomitic and bedding is seldom visible. In some nodules with visible bedding, the microspar contains silty laminations and cross-laminations like those in the silty microspar rock type. The disc-shaped nodules range from 10 cm to 60 cm in diameter, and are typically scattered in silty shale.

Laminated quartz sandstone (Fig. 5) occurs in thin laterally discontinuous beds up to 15 cm thick in silty shale. Typically, the beds contain sets of alternating light-gray calcite-cemented laminations, black clay- and organic residue-bearing laminations, and in a few places, brown iron-oxide cemented laminations. Laminations range from 0.1 cm to 1.5 cm thick, and light-gray laminations are most abundant. Sand grains are generally in grain-to-grain contact and show no size grading. The sandstone contains no carbonate grains.

Calcitic quartz sandstone contains clasts to mainly quartz with a few carbonate grains, including oolites and oolitic lithoclasts, and metamorphic rock fragments, feldspar grains, muscovite grains,

Figure 5. Sandstone clastic components quartz-carbonate-feldspar + mica are plotted on a ternary diagram, (upper diagram), and matrix composition is plotted against grain size in the lower diagram.

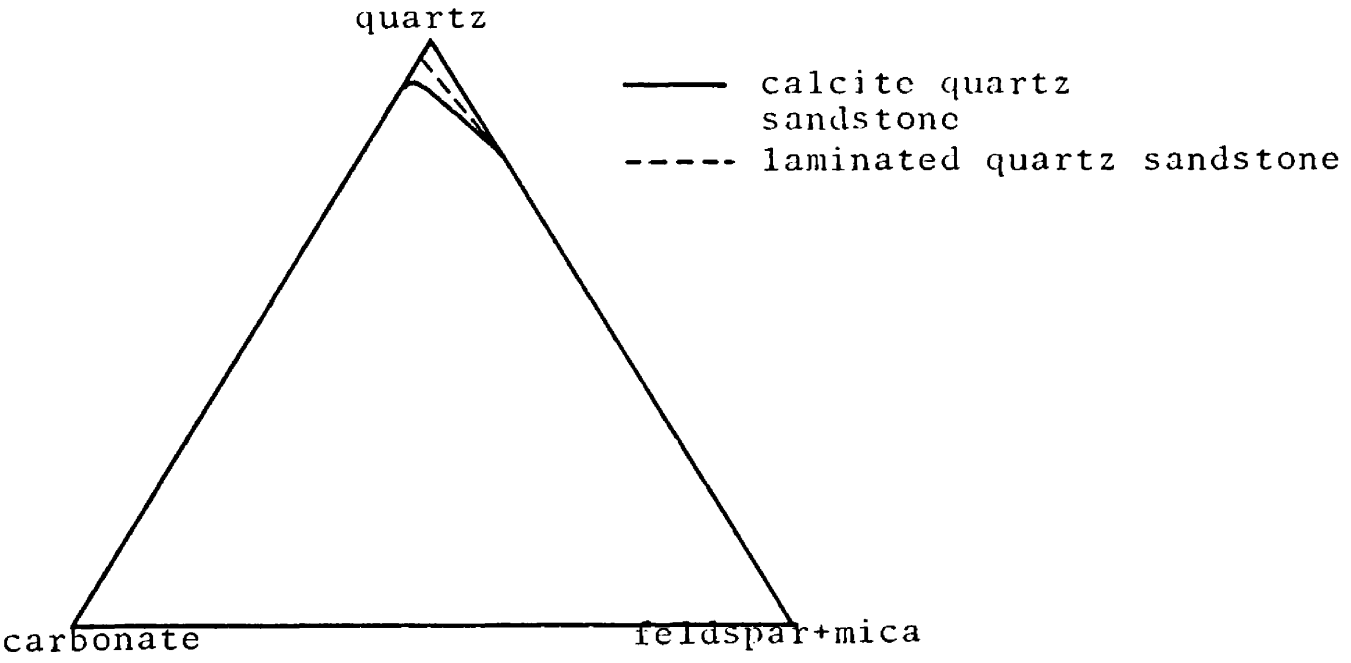
quartz
calcite quartz sandstone
laminated quartz sandstone
carbonate
feldspar+mica

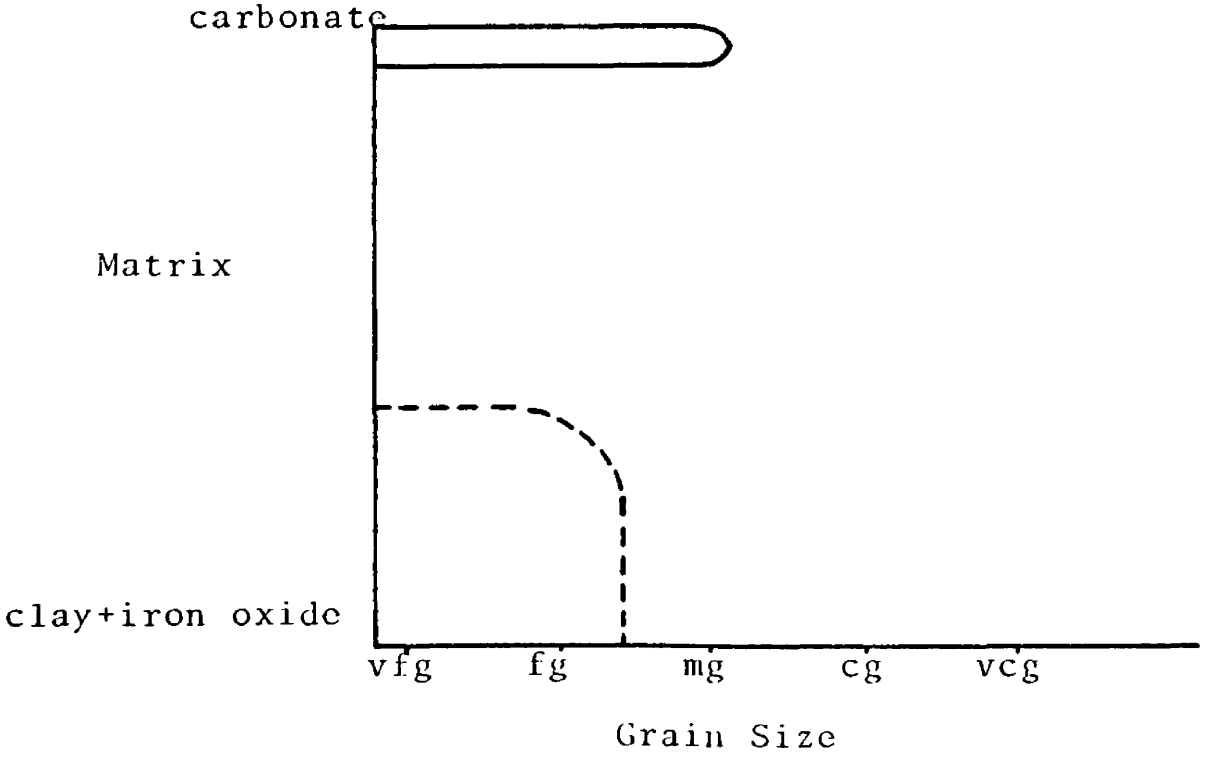
carbonate
Matrix
clay+iron oxide
vfg
fg
mg
cg
vcg
Grain Size

and a few zircon and biotite grains. The fine- to medium-grained clasts are matrix supported in sparry carbonate cement. Calcitic quartz sandstone contains no internal bedding except for occasional cross-laminations, and in some places the sandstone fines upward. Calcitic quartz sandstone is most abundant in tan calcareous shale in the lower part of the Newland Limestone, but occurs as both beds and as cross-laminated lenses in silty microspar in the upper part of the Newland Limestone. The only flute casts observed are on the sole of a calcitic quartz sandstone bed.

Based on sedimentary structures, the rock types of the Newland Limestone were deposited in current-free to current-dominated depositional environments (Fig. 7). The lack of desiccation features indicate that all these environments were subaqueous. Tan calcareous shale was deposited in a current-free environment, and its thin, even laminations indicate pelagic deposition. Calcitic quartz sandstone, based on its graded bedding, lack of internal structures, matrix-supported grains, and flute casts, was probably deposited by turbidity flows into the pelagic environment of tan calcareous shale deposition. Gray microspar and black chert-bearing microspar contain little terrigenous material, but scattered aggregates of medium-grained sandstone in black chert-bearing microspar indicate at least some current activity during microspar deposition. Although sets of ripple cross-laminations less than 0.5 cm thick indicate some traction transport, abundant continuous evenly spaced thin laminations suggest a dominantly still water environment of micrite mud deposition.

Figure 6. Estimated relative abundance of the major rock types of the Newland Limestone. TCS = tan calcareous shale, GM = gray microspar; BCM = black chert-bearing microspar; SM = silty microspar; SS = silty shale; BS = black calcareous shale; LQSS = laminated quartz sandstone; CQSS = calcite quartz sandstone; NBM = nodular black microspar.

Figure 7. Depositional environments of the major rock types of the Newland Limestone with respect to current activity.

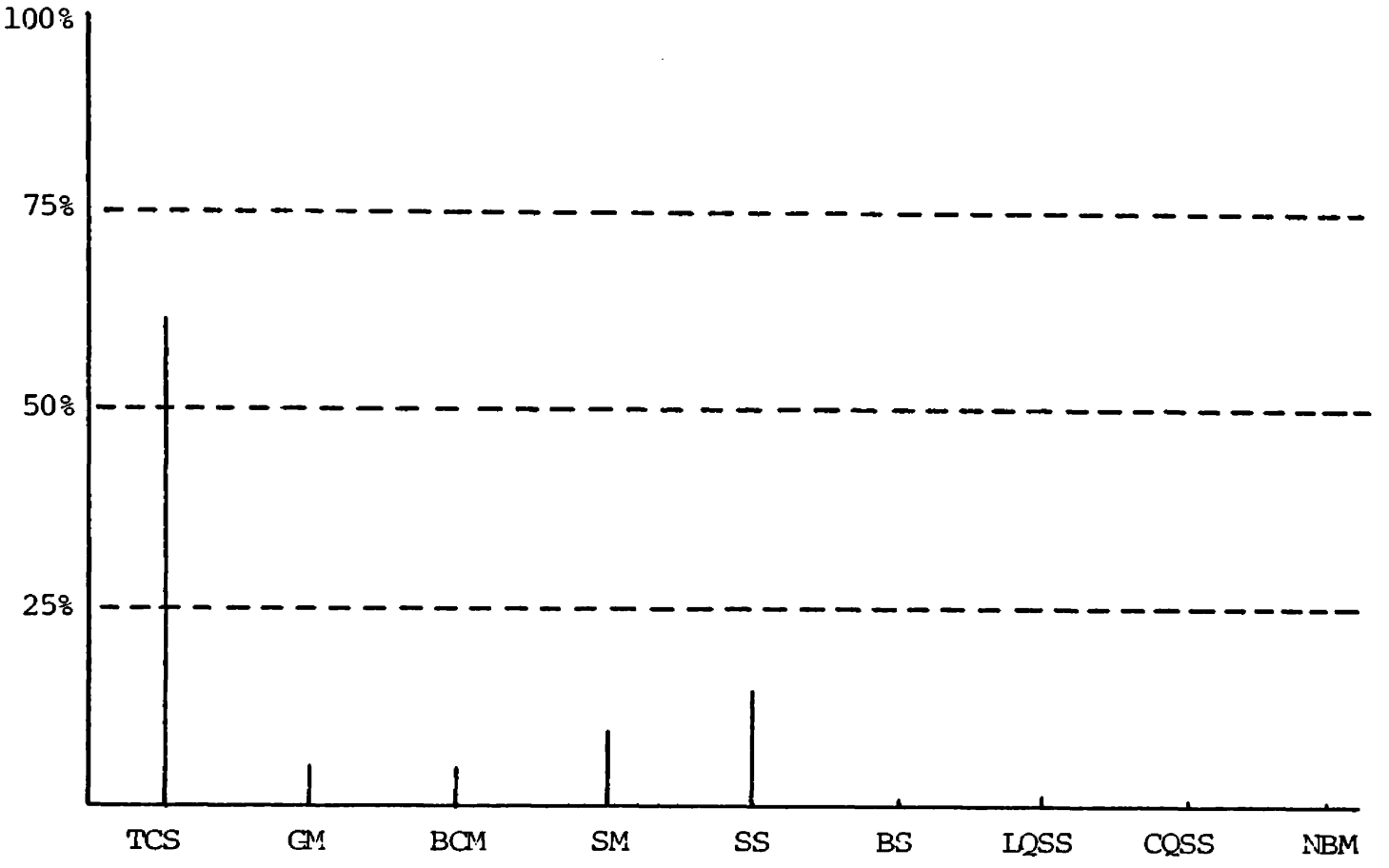
100%
75%
50%
25%
TCS
GM
BCM
SM
SS
BS
LQSS
CQSS
NBM

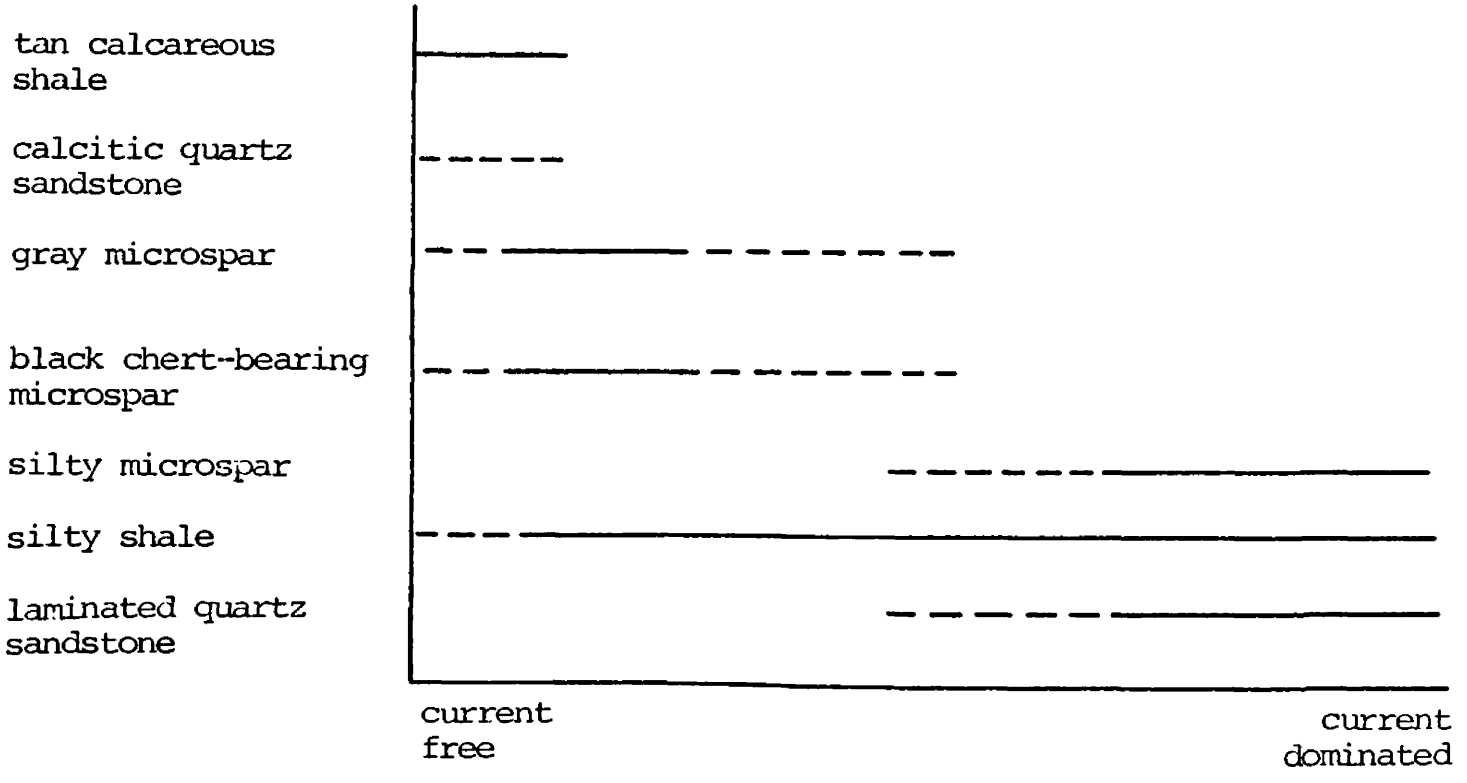
tan calcareous shale
calcitic quartz sandstone
gray microspar
black chert-bearing microspar
silty microspar
silty shale
laminated quartz sandstone
current free
current dominated

The abundant cross-laminated silt and fine-grained sand and graded silt-to-argillite or silt-to-carbonate couplets in most silty microspar and silty shale indicate that they were deposited in current dominated environments, but where these structures are absent in silty shale, a still water environment of deposition probably prevailed.

Correlation of Upper Newland Stratigraphy

The upper part of the Newland Limestone differs from the lower thinly-laminated tan calcareous shale part in that it consists mainly of medium- to thin-bedded microspar intervals and silty shale intervals. The upper part of the Newland Limestone can be divided into seven distinct lithologic units on the basis of the major rock types. Although individual rock types vary from place to place in lithology and thickness, each extends across the area and forms the basis for the rock stratigraphic correlations described in this section (Fig. 8). Detailed descriptions of the measured sections used in these correlations are given in Appendix III.

Unit I

Unit I is an interval of gray microspar, dolomitic gray microspar, and silty microspar up to 30 m thick. This unit is cut out by faulting at both the Newlan Creek and Smith River sections. At Decker Gulch, Unit I consists of 3 m to 5 m of dolomitic microspar beds 5 cm to 12 cm thick. At Little Birch Creek, Unit I is 12 m thick, and consists of 6 cm to 12 cm beds of gray microspar and silty microspar. The microspar beds are separated by thinly-laminated tan calcareous shale

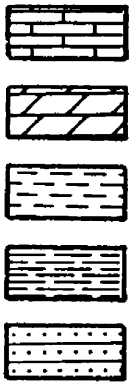

Figure 8. Correlation of the upper Newland. The major carbonate rock types are grouped together under microspar and dolomitic microspar. 'X's indicate covered intervals. DC = Deep Creek section; LBC = Little Birch Creek section; NC = Newlan Creek section; DG = Decker Gulch section; SR = Smith River section; and BG = basal Greyson Shale. The Roman numerals indicate correlative units discussed in the text.

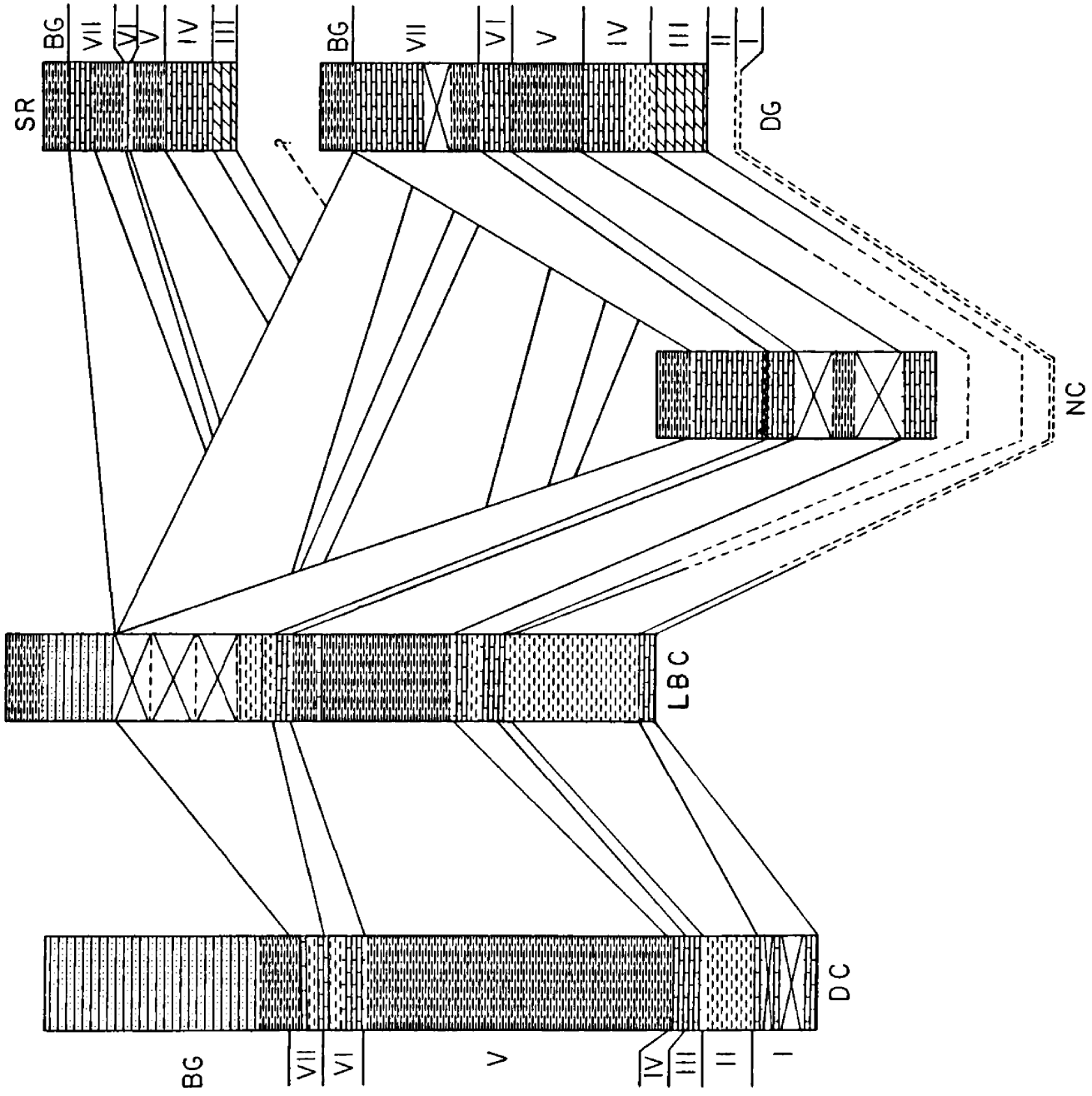
SR
BG
VII
VI
V
IV
III
?
BG
VII
VI
V
IV
III
II
I
DG
NC
LBC
DC
BG
VII
VI
V
IV
III
II
I

partings, and many beds contain ripple cross-laminations of silt and fine sand grains near their tops. Some beds contain pressure solution features. In the Deep Creek section, several carbonate intervals which may be correlative with Unit I appear repeated by faulting. Each interval is about 30 m thick and contains gray microspar beds, some of which are mottled. Since microspar intervals occur below Unit I in the Little Birch Creek section, I believe that the upper of the three microspar intervals, from the 655 m to 684 m interval of the Deep Creek section, is correlative with Unit I.

Unit II

Unit II is tan calcareous shale overlying Unit I. The shale is dolomitic below the Decker Gulch section where it is about 30 m thick and in the Little Birch Creek section where it is 122 m thick and is interlaminated with red and white non-calcareous shale (see Appendix II) near its base. In the Deep Creek section, Unit II is 61 m thick, less dolomitic, and contains a few intervals of dark gray-, brown-, green-, and pink-weathering silty shale.

Unit III

Unit III is a distinctive black chert-bearing microspar interval. No other unit contains so much black chert. Unit III is faulted out at Newlan Creek. At Decker Gulch, it is 30 m thick, the microspar is completely dolomitic, and chert is more abundant than in any other section. A few thin beds of calcitic quartz sandstone occur near the top of the

unit at Decker Gulch. In the Smith River section, Unit III is 23 m of dolomitic black chert-bearing microspar. It weathers lighter gray and contains less black chert than at Decker Gulch.

In the Little Birch Creek section, Unit III is about 6 m of dark gray-weathering nondolomitic black chert-bearing microspar containing abundant diagenetic mottling and pressure solution structures (see Chapter IV). Irregular clots of medium-grained sandstone up to 2 cm in diameter occur in and against the black chert nodules.

In Deep Creek Canyon, Unit III is 15 m of nondolomitic gray microspar containing sparse black chert, abundant pressure solution structures, and diagenetic mottling (see Chapter IV). The unit is thickened here by internal folding.

Unit IV

Unit IV is characterized by gray- and tan-weathering silty microspar interbedded with tan calcareous shale or black calcareous shale. Although at Newlan Creek the bottom of Unit IV is faulted out, the middle and upper part is thickly-laminated to thinly-bedded slightly dolomitic silty microspar containing abundant ripple cross-laminations and a few thin interbeds of calcitic quartz sandstone. Compressional soft sediment deformation structures in some of the tan silty microspar beds consist of imbricated broken laminations, laminations truncated against bedding planes, and compacted broken laminations. Discoid nodules of radial-fibrous calcite with cone-in-cone structure are exposed in Unit IV near the head of Lake Creek about six miles east of the Newlan Creek

section. The nodules are in two 30 cm to 60 cm beds, are closely packed, and range in size from several centimeters to 40 cm in diameter. These are further discussed in Chapter V.

Unit IV in Decker Gulch is 48 m thick and consists of a few meters of very thinly laminated (.1 cm) tan calcareous shale overlain by silty microspar similar to that along Newlan Creek. Small scale soft sediment isoclinal folds occur in Unit IV at several locations in the Decker Gulch area.

In the Smith River section, Unit IV consists of thickly-laminated thin- to medium-bedded medium gray- and tan-weathering silty microspar containing few ripple cross-laminations. All but the bottom 6 m and top 3 m of the 38 m thick unit contain abundant soft sediment folds formed by slumping. Folds are generally similar style, range from vertical to recumbant, and many are refolded. Truncation surfaces between adjacent beds are abundant. Folded and broken clasts of microspar are supported in a structureless microspar matrix in the centers of some folds. A bed of soft sediment deformed gray silty microspar clasts supported in a tan-weathering microspar matrix (Fig. 9) overlies the slumped carbonate. Overlying the bed of clasts is dolomitic tan calcareous shale which grades upward into the silty shale of Unit V. The slumped interval in Unit IV continues westward, but not eastward, indicating that the exposures in the Smith River section are the eastern margin of the slumped body.

In the Little Birch Creek section, Unit IV is 61 m thick and consists of thin- to medium- bedded gray- and tan-weathering silty

Figure 9. Clast of gray silty microspar supported in a tan-weathering microspar matrix. The row of angular fragments near the top of the photo have broken away from the main clast while the matrix was still soft. Upper Unit IV, Smith River Section.

Figure 10. Load structures formed by lenticular sets of ripple cross-laminations in a discontinuous bed of silty microspar. Unit IV, Little Birch Creek section.

Figure 11. Discontinuous beds and nodules of silty microspar with interbedded black calcareous shale. Note the ripple cross-lamination in the center of the nodule. Unit IV, Little Birch Creek section.

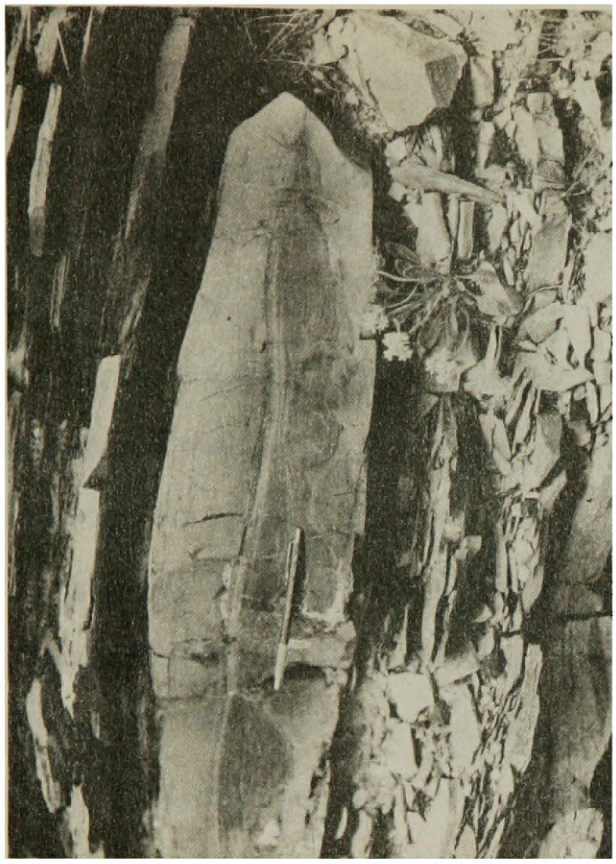

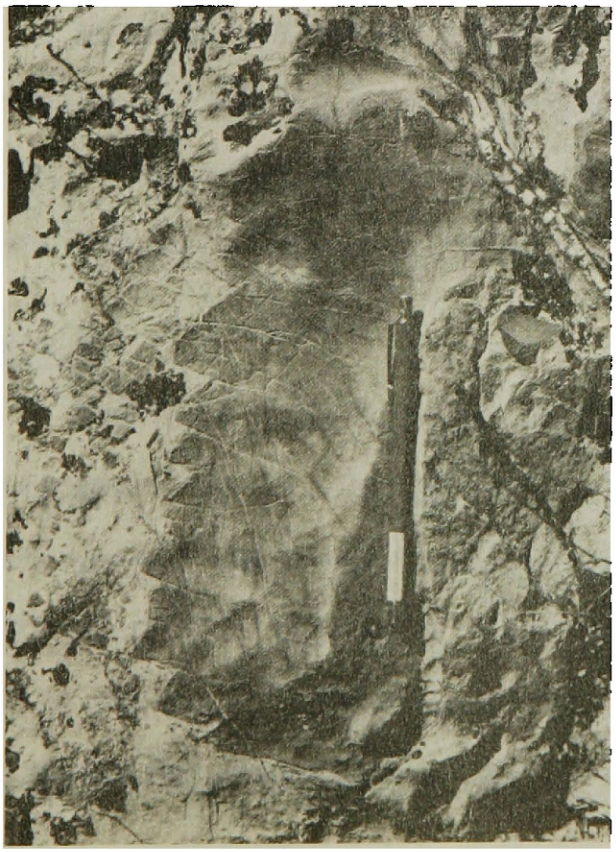

microspar containing abundant ripple cross-laminations (Fig. 10), load structures and detached load structures, and black calcareous shale interbeds. The middle and top of the unit contains intervals of tan calcareous shale. Some silty microspar beds pinch out laterally to black calcareous shale or occur as large bedded nodules (Fig. 11). Contacts of silty microspar with black calcareous shale are abrupt, the ends of the carbonate beds are rounded, and laminations in the microspar beds carry into the shales. These may be pull-apart structures or may be a result of carbonate dissolution. A thin bed of cross-laminated calcitic quartz sandstone at the base of Unit IV contains many chert grains, indicating chert in underlying Unit III may have formed before deposition of the overlying strata and may have been scoured from Unit III and redeposited in Unit IV.

No silty microspar occurs in Deep Creek canyon. Instead, Unit IV consists of 4.5 m of gray microspar beds containing several 2 cm to 5 cm thick interbeds of ripple cross-laminated calcitic quartz sandstone, overlain by a few meters of tan calcareous shale.

Unit V

Unit V is characterized by silty shale containing nodular black microspar. In the Newlan Creek section, the shale is fissile, weathers dark green, and contains scattered nodular black microspar. The lower part of Unit V is covered along Newland Creek and the upper part is silty shale. At Decker Gulch, the lower part of Unit V consists of brown and gray thinly- and irregularly-laminated silty and sandy

shale containing black microspar nodules. The upper part of Unit V at Decker Gulch is silty shale identical to that along Newlan Creek.

In the Smith River section, Unit V is very poorly exposed and consists of dark gray and brown fissile silty shale containing no carbonate nodules. At Little Birch Creek, Unit V is more than 90 m thick, and consists of dark gray-, brown- and rusty-weathering silty and sandy shale containing brown- and tan-weathering nodular black microspar and scattered beds of laminated quartz sandstone. The sandier the shale, the thicker and wavier the lamination sets become, and some contain alternating light pink and light green laminations. The sandy shale contains ripple cross-laminated sandstone lenses, many of which are loaded into underlying silty shale. The silty shale interval is capped by about 25 m of slightly calcareous fissile gray shale containing nodular black microspar. Scattered in the gray shale are thick laminations of fibrous white calcite with crystal long axes perpendicular to bedding and with well-developed cone-in-cone structure.

In Deep Creek Canyon, Unit V is 244 m thick and consists of only thinly laminated and fissile silty shale containing no sand grains, sandstone beds or lenses, or carbonate nodules.

Unit VI

In both the Newlan Creek and Decker Gulch sections, Unit VI is about 30 m thick and consists of thin beds of thinly- and thickly-laminated gray microspar, containing scattered pressure solution structures and mottling (see Chapter IV). It is generally well exposed,

is characteristically folded and faulted, and is called the 'contorted carbonate' by geologists working in the area.

In the Smith River section, Unit V is less than .8 m thick and consists of thinly-bedded dark gray microspar capped by a thin bed of intrasparite (see Appendix II). Local higher topography due to thickening of underlying Unit IV from emplacement of the slumped carbonate body may have limited later carbonate deposition here, resulting in thinning of Unit VI.

In the Little Birch Creek section, Unit VI is only 12 m thick, and consists of thin beds of thinly- to thickly-laminated gray microspar containing some silty laminations, few of which are ripple cross-laminated, and abundant pressure solution structures (see Chapter IV). In Deep Creek Canyon, Unit VI is about 27 m thick and consists of gray- to tan-weathering thin- to medium-bedded gray microspar containing a 3 m interval of fissile gray shale.

Unit VII

Unit VII changes greatly from place to place, but is characterized by microspar beds containing asymmetric ripple cross-laminations. In most places, the unit also contains tan calcareous shale intervals and gray shale (see Appendix II) intervals containing black microspar nodules.

At Newlan Creek, where Unit VII is in fault contact with Unit VI (Fig. 8), it is about 80 m thick and consists of silty microspar and interbedded black calcareous shale. The silty microspar contains abundant ripple cross-laminations (Fig. 12) and some load structures, and

Figure 12. Ripple cross-lamination set from silty microspar in Unit VII, Newlan Creek section. The sample is 7 cm tall.

Figure 13. Discontinuous and nodular beds of silty microspar interbedded with black calcareous shale. Unit VII, Newlan Creek section.

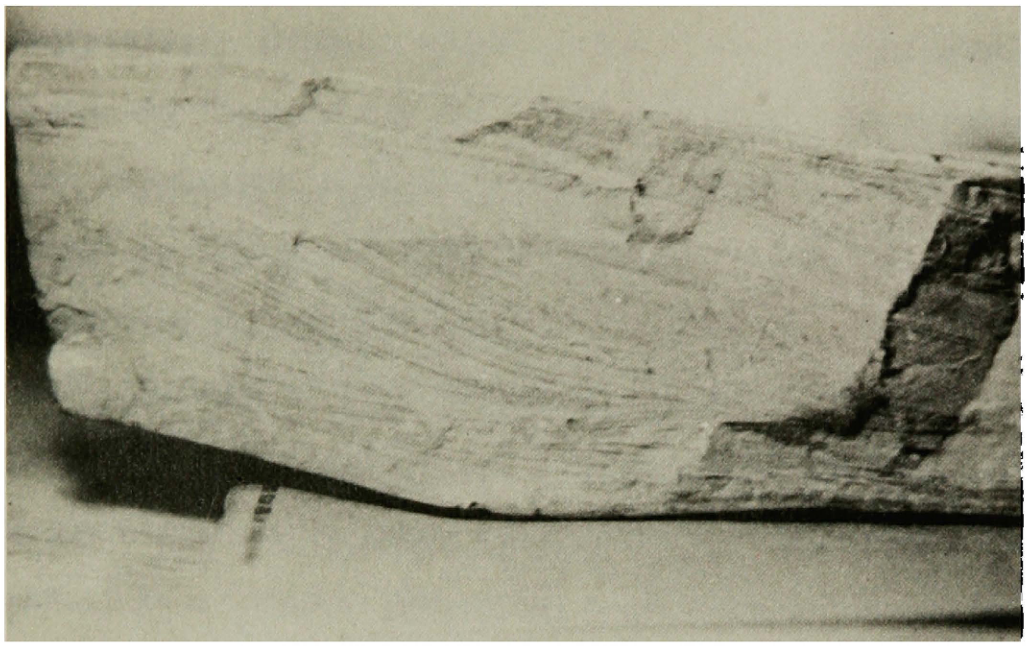

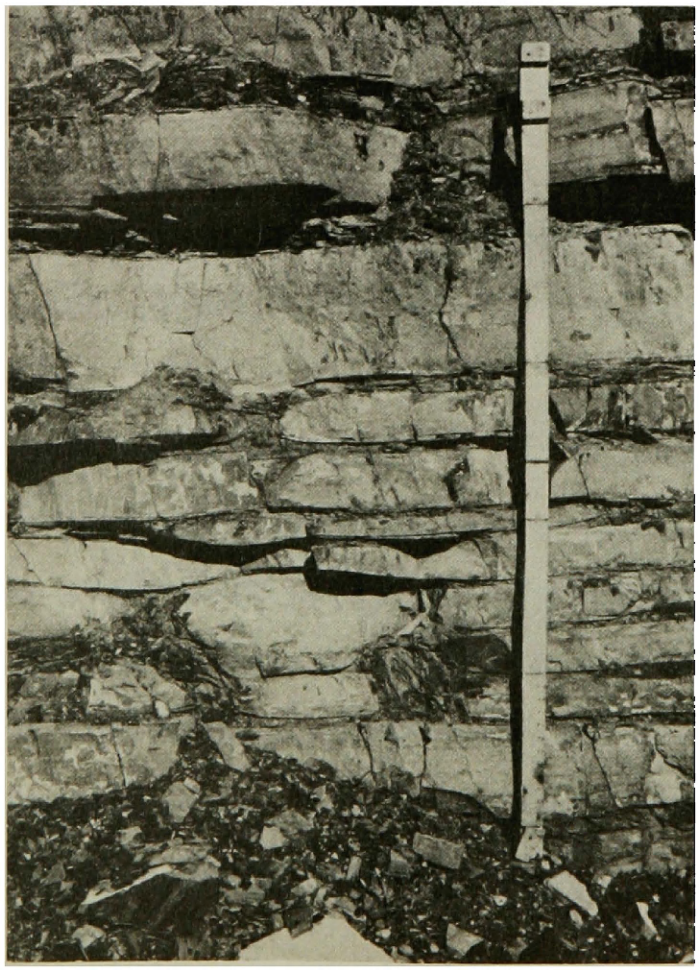

becomes progressively thicker bedded upward. One bedding plane surface has well-preserved linguoid current ripples arranged in an enechelon pattern. The ripplesare elongate in the direction of current flow with length-to-width ratios on the order of 5:2 and greater, and sand grains are concentrated on the leeward ends of the ripples. Some of the silty microspar beds are laterally discontinuous or nodular (Fig. 13).

In the Decker Gulch section, Unit VII consists of 30 m of very poorly exposed fissile gray shale overlain by 60 m of thinly-laminated thin beds of silty microspar containing ripple cross-laminations interbedded with tan calcareous shale. Three miles southwest of the Decker Gulch section in exposures along lower Whitetail Deer Creek, the gray shale in the lower part of Unit VII containsscattered black microspar nodules.

In the Smith River section, only the lower 24 m of Unit VII is exposed, and consistsof thinly- to thickly- laminated silty microspar with no ripple cross-laminations. The unit is in fault contact with the overlying Greyson Shale.

In the Little Birch Creek section, Unit VII consists of a few layers of thin-bedded silty microspar containing ripple cross-laminations, overlain by dark gray shale containing a few black microspar nodules and grading upward into tan calcareous shale, which comprises most of the 122 m thick unit. The silty microspar beds contain a megaripple of sandy sparite (see Appendix II). Unit VII at Deep Creek is 50 m thick. Its base consists of 8 m of thin- to medium- bedded gray microspar with

a few 2 cm to 5 cm thick interbeds of ripple cross-laminated calcitic quartz sandstone, overlain by 5 m of gray shale with abundant carbonaceous films and a few black microspar nodules. Above this, 3 m of light brown-weathering microspar is overlain by 34 m of dominantly tan calcareous shale with some silty shale. The silty shale, like that of Unit V lower in the Deep Creek section, contains no sand grains or current-formed sedimentary structures.

Basal Greyson Shale

At the Newlan Creek, Decker Gulch, and Smith River sections, the basal Greyson Shale consists of silty shale. In each section, the abundance of ripple cross-laminations in the silty shale is roughly equivalent to their abundance in the silty microspar of underlying Unit VIII.

At Little Birch Creek and along Deep Creek, the base of the Greyson Shale consists of thickly-bedded quartzite overlain by silty shale. At Little Birch Creek, the quartzite is 60 m thick and fine to medium grained. In the Deep Creek section, the quartzite is 183 m thick, is underlain by 75 m of silty shale, and the lower part of the quartzite contains conglomerate layers with clasts of metamorphic rock and Newland carbonate. Ten miles to the east, in the head of Deep Creek Canyon, the quartzite is fine grained and is only 3 m thick.

Upper Newland Carbonate-terrigenous Cycles

The upper Newland units can be grouped into two similar cycles, each increasing upward in terrigenous material (Fig. 14). At the base

Figure 14. Idealized upper Newland cycles. In each cycle, terrigenous material increases upward. Thickness of the idealized section is about 365 meters.

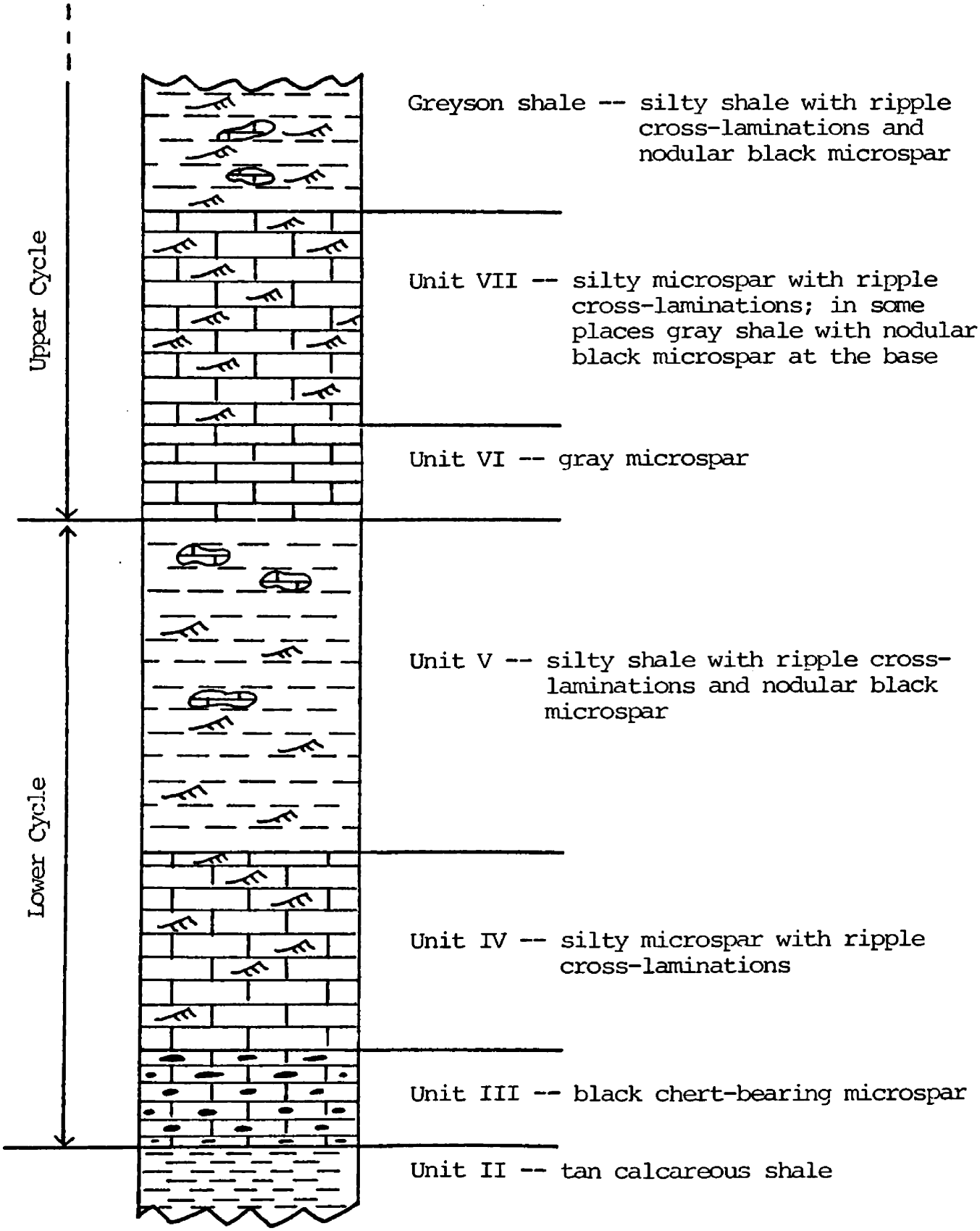
Upper Cycle
Lower Cycle
Greyson shale -- silty shale with ripple cross-laminations and nodular black microspar
Unit VII -- silty microspar with ripple cross-laminations; in some places gray shale with nodular black microspar at the base
Unit VI -- gray microspar
Unit V -- silty shale with ripple cross-laminations and nodular black microspar
Unit IV -- silty microspar with ripple cross-laminations
Unit III -- black chert-bearing microspar
Unit II -- tan calcareous shale

of each cycle is gray microspar or black chert-bearing microspar containing few or no ripple cross-laminations, overlain in the middle of the cycle by silty microspar containing ripple cross-laminations, in turn overlain toward the top of the cycle by silty shale containing ripple cross-laminations. At Little Birch Creek and in Deep Creek Canyon, quartzite instead of silty shale occurs in the upper part of the upper cycle, and in Deep Creek Canyon, where no silty microspar occurs, the middle parts of the cycles consist of gray microspar with interbeds of ripple cross-laminated calcitic quartz sandstone between 1 cm and 5 cm thick.

Because symmetrical wave ripples are absent, I believe the asymmetrical ripple cross-laminations were produced by bottom currents transporting silt and sand in traction transport across clay and micrite surfaces below wave base. Strong currents are evidenced by the linguoid ripples, megaripples, and scoured surfaces in the silty microspar. Bottom currents appear to have accompanied each onset of terrigenous influx in the cycles, though the medium-grained sandstone clots in the black chert-bearing microspar of Unit III at Little Birch Creek indicate the currents may have preceded terrigenous influx.

During deposition, each cycle began with micrite mud deposition, to which was added an influx of clay, silt and some sand until finally carbonate deposition was completely replaced by deposition of silty shale. The second cessation of carbonate production marks the base of the Greyson Shale.

Tan calcareous shale in the cycles probably reflects a period of low carbonate production and low terrigenous influx in a quiet, bottom current-free environment dominated by pelagic deposition. Silty shale without sand grains and ripple cross-laminations reflects a similar environment without carbonate production and perhaps greater terrigenous influx. However, gray shale with nodular black microspar appears to reflect periods of carbonate-free deposition interrupting the carbonate-dominated part of the cycles. The gray shale may be instead a product of pressure solution of a former carbonate interval (see Chapter V). Pressure solution of a former carbonate body underneath the gray microspar of Unit VI explains the abrupt contact between the two cycles. Some nodules of black microspar contain silt laminations and ripple cross-laminations, indicating that silty microspar once underlay the gray microspar.

Lower Newland Limestone

The lower part of the Newland Limestone is widely but poorly exposed and generally appears as tan calcareous shale float. In better exposures it consists mainly of thin, evenly laminated tan calcareous shale, with local intervals of thin-bedded gray microspar and dolomitic gray microspar, and calcitic quartz sandstone.

A number of good exposures occur in the Newlan Creek section. In a quarry at the mouth of Miller Gulch noncalcareous argillite (see Appendix II) is exposed, and contains abundant small scale compressional soft sediment folds. Most other exposures of lower Newland in the

Newlan Creek section consist of dolomitic tan calcareous shale. The upper part of the lower Newland contains scattered beds of dolomitic gray microspar and calcitic quartz sandstone.

At Decker Gulch and in the surrounding area, the lower Newland is mostly covered by float, but appears similar to the tan calcareous shale at Newlan Creek. Float from jasparized zones in the lower Newland, noted by Phelps (1969) and McClernan (1967), occurs throughout the area.

In the Smith River section, much of the lower Newland is well exposed. Below the measured part of the section, the shale is less well exposed, tan-weathering, and calcareous. Above this occur sequences of dolomitic mudstone, gray shale, quartz sandstone, black dolomite, and molar-tooth structure-bearing dolomite (see Appendix II). These rock types are absent in any other lower Newland exposures.

In the lowest 30 meters of the Smith River measured section, the calcareous shale is more thickly laminated than below, and is dolomitic and silicified. The next 60 meters of section consist of dolomitic mudstone containing abundant soft sediment folds (Fig. 15) formed by slumping. Fold amplitudes range from several centimeters to as much as one meter. Most folds are similar style, isoclinal, and recumbent, and some of these are themselves folded. Others are truncated by planes along which other sediment has flowed. Failure of folds characteristically occurs along fold limbs.

The mudstone also contains nodules of gray laminated chert (see

Figure 15. Isoclinal soft sediment fold in dolomitic mudstone. Lower Newland, Smith River section.

Figure 16. Debris flow of chert pebbles matrix-supported in dolomitic mudstone. Lower Newland, Smith River section.

Figure 17. Flute casts on the sole of a calcitic quartz sandstone bed, lower Newland, Deep Creek section.

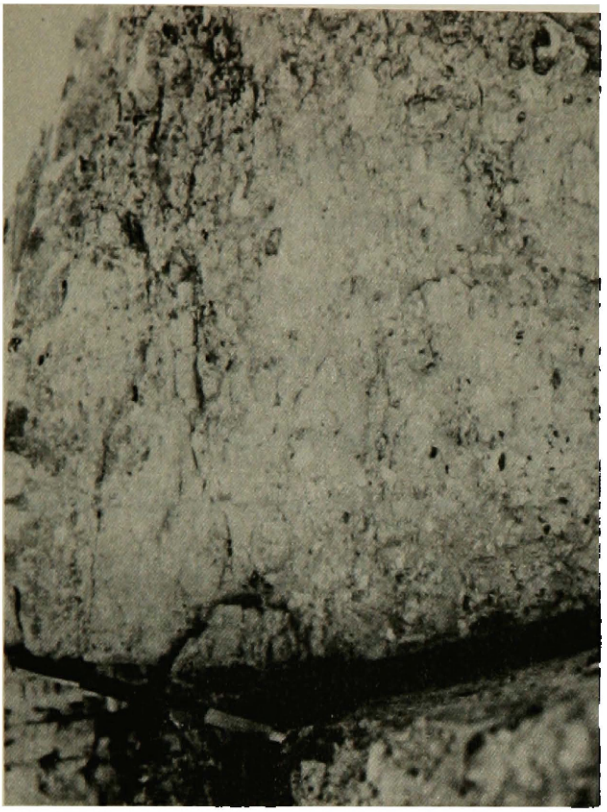

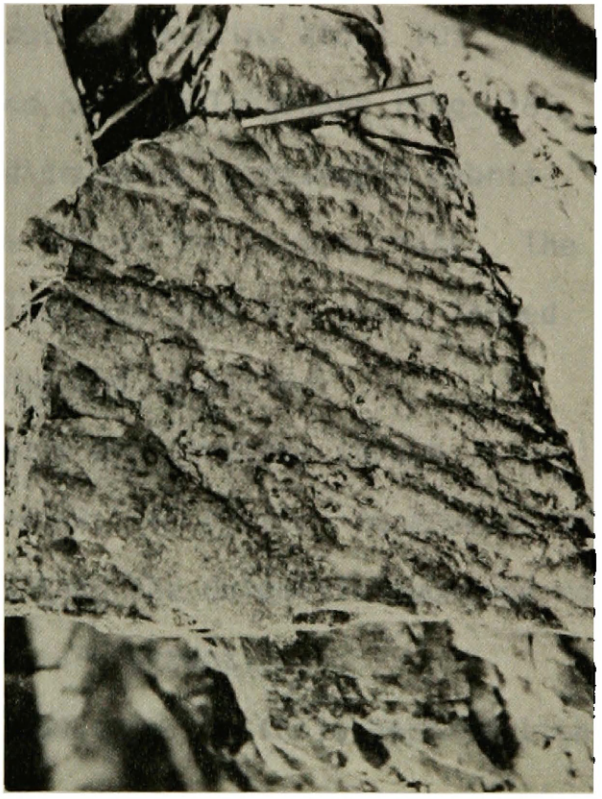

Appendix II) up to .5 meters thick and 2 meters long. The chert nodules are mostly brecciated around their edges, and rounded chert sand grains and cobbles are supported in the mudstone matrix far from any exposed chert nodules. Many matrix-supported chert sand grains occur in thick ungraded laminations in the mudstone and were probably deposited as density flows. A 0.5 m calcareous mudstone layer capping the zone of most intensely deformed mudstone contains about 10% rounded matrix-supported gray chert sand and pebble grains (Fig. 16). The clastic components fine upward, and probably represent a debris flow or density flow that rode over the top of the slumped mass. The chert clasts in the deformed mudstone indicate that the chert formed in the sediments before they were slumped and lithified.

Above the slumps the mudstone appears undisturbed, though it still contains laminations with chert sand grains. In places, it appears more like the tan calcareous shale rock type than the dolomitic mudstone rock type suggesting that the two lithologies are gradational.

About 30 meters above the slumped mudstone the shale becomes light gray, fissile, and noncalcareous, and is capped by molar tooth-bearing dolomite. A thrust fault subparallel to bedding, which dips thirty to forty degrees to the south, cuts the molar tooth-bearing dolomite and is expressed by sheared shale, brecciated dolomite, and drag folds in the shale. Above this the section is repeated, but consists of beds that were deposited beyond the limit of the slump (Fig. 18 bottom). Here, the debris flow, which contains intraclast-bearing lithoclasts and chert sand and pebbles, overlies tan calcareous shale with gray

Figure 18. Depositional and structural history of the lower Newland in the Smith River section. Vertical scale is about 85 m/inch.

1) Dolomitic mudstone was slumped onto tan calcareous shale and covered by a turbidite flow of dolomitic mudstone with chert pebbles.

2) Gray shale with quartz sand turbidite lapped onto the slumped mound.

3) After gray shale deposition, molar tooth-bearing dolomite and overlying Belt strata were deposited.

4) A Cretaceous or early Tertiary thrust stacked the section. Strata above and to the right of the dashed line were then eroded.

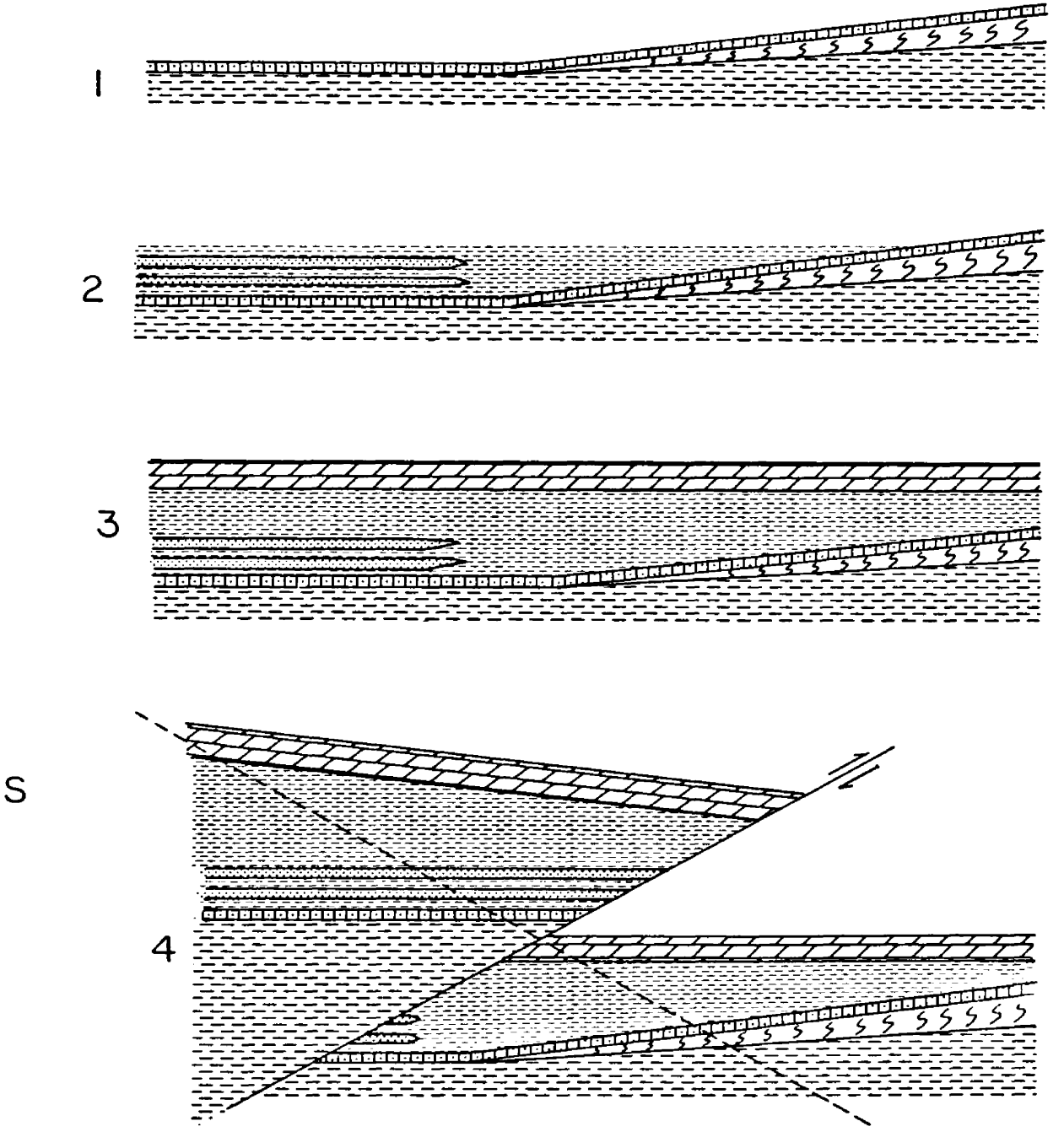
1
2
3
S
4
N

microspar beds and nodules instead of slumped dolomitic mudstone. The gray shale interval is wedge shaped, thickens downdip, and has steeper dips at its base, where it contains several quartz sandstone beds. The wedge shape of the gray shale interval probably results from late Cretaceous or early Tertiary internal folding and thrusting. The quartz sandstone beds probably were deposited as turbidites that flowed down the same slope as the slump. They may be absent in the gray shale underneath the thrust fault because the quartz sand turbidite flows circumvented the slumped area, which may have been topographically higher (Fig. 18).

At the Little Birch Creek section, no lower Newland shale is exposed. On the west side of Little Birch Creek and stratigraphically below Unit I of the eastward dipping upper Newland section, are poor exposures of two gray microspar intervals.

In Deep Creek Canyon, the lower Newland is well exposed. The thinly- to thickly-laminated calcareous shale is much less dolomitic than at the Smith River, Decker Gulch, and Newlan Creek sections, and lacks evidence of soft sediment slumping. Variations in the shale consists mainly of lamination thicknesses and the ratio of dark to light laminations. Darker laminations are more prevalent lower in the section.

The tan calcareous shale in the upper part of the lower Newland in the Deep Creek section contains many gray microspar beds and intervals. At the base of the gray microspar-bearing part of the lower Newland, a sequence of green claystone-tan calcareous shale-gray

microspar-tan calcareous shale-black siltstone (see Appendix II) is caught and overturned underneath a thrust fault. Below this, the tan calcareous shale contains several 6 cm to 60 cm thick calcitic quartz sandstone beds, one of which has flute casts on its sole (Fig. 17).

Lower Newland Summary

The lower Newland is dominantly composed of tan calcareous shale, reflecting a pelagic depositional environment interrupted by occasional calcitic quartz sandstone turbidite sheets. During the deposition of the upper part of the lower Newland, some micrite muds were deposited.

Minor lithologies that may be useful in future correlations in the lower Newland are gray microspar and noncalcareous argillite in the northern part of the embayment, and gray microspar, green claystone, black siltstone, and changes in dark and light lamination ratios in the tan calcareous shale in the southern part of the embayment. Correlations within the lower Newland are not yet possible because of the uniformity of the thick shale sequences and their poor exposure.

The dolomitic mudstone, gray shale, quartz sandstone, and molar tooth-bearing dolomite in the lower Newland in the Smith River section are absent in the other sections, and were probably deposited in the Smith River section due to its proximity to the edge of the embayment. Cobble-sized lithoclasts in the debris flow, quartz pebbles in the quartz sandstone, and the slumping all indicate a site of deposition near the edge of the embayment. Also, molar-tooth bearing dolomite is elsewhere exposed only in the Neihart, Moose Creek, and Little

Sheep Creek areas to the northeast and east. These areas are all along the northern edge of exposures of Helena embayment Belt strata.

Thickness of the Newland Limestone

The thickness of the Newland Limestone in the Decker Gulch and Newlan Creek area is about 900 m, based on thicknesses of measured sections and estimates of the thickness of the lower Newland. The base of the Newland is covered to the south, but the Newland appears to thicken considerably southward. In my estimation, Nelson's (1963) measured thickness of 2896 m for the Deep Creek section is probably excessive due to stacking and internal folding of portions of the section by Cretaceous and Tertiary thrust faults.

CHAPTER III

SEDIMENTOLOGICAL INTERPRETATION

The Newland sediments were probably deposited below wave base, as indicated by the lack of desiccation features and wave ripples. The lower Newland is mostly thinly- and evenly-laminated tan calcareous shale, reflecting pelagic sedimentation. Current-transported coarse-grained sediment in the lower Newland occurs only in slumps, as in the Smith River section, or in calcitic quartz sandstone turbidites.

The gray microspar intervals in the upper part of the lower Newland mark a turning point in Newland sedimentation. The lack of clay and silt in the microspar when compared to the calcareous shale suggests a period of either intense carbonate production or reduced clay and silt influx into the basin. After micrite mud deposition (Unit I, Fig. 8), pelagic carbonate, clay, and silt deposition resumed (Unit II, Fig. 8). Overlying this are the two carbonate-terrigenous cycles of gray microspar overlain by silty microspar and capped by silty shale.

The three processes that may have developed the carbonate-terrigenous cycles are carbonate precipitation, bottom currents, and terrigenous influx. Biological calcite precipitation by unicellular or filamentous algae, or periodic calcite saturation of the embayment water due to increased water salinities, probably caused the micrite mud

deposition in the bottoms of the cycles. In restricted basins, the typical sequence of mineral precipitation with increasing salinity is calcite, followed by gypsum, followed by halite (Till, 1978). In the Helena embayment, where there is no strong evidence for any gypsum or halite precipitation, either salinity levels required for gypsum precipitation were never reached, or sulfate-reducing bacteria inhibited gypsum precipitation by breaking down the sulfate ions. Oolites and oolitic lithoclasts in calcitic quartz sandstone turbidites and in sandy sparite (Fig. 20, Fig. 21) may reflect higher salinities near shore. Shoaling upward of the Newland sediments, suggested by the increased currents during upper Newland deposition, may have caused carbonate precipitation. Embayment waters may have increased in salinity during shoaling upward, causing calcite precipitation, or perhaps algal blooms occurred in the shallower water during shoaling upward.

The silty microspar intervals in the middle of the cycles reflect simultaneous calcite precipitation, bottom currents and terrigenous influx. Increases in salinity or decreases in temperature of near shore water may have increased its density with respect to water farther offshore, resulting in bottom currents flowing basinward carrying terrigenous material. Terrigenous influx may reflect increased shoaling upward of the Newland sediments, allowing bottom currents to carry terrigenous material even farther into the basin, or may be the result of an increasingly humid climate causing increased erosion of the unvegetated Precambrian erosional surface. Silty shale deposition in

Figure 19. Intraclast of slightly dolomitic microspar (dark) and molar tooth structure (light) in intrasparite. Field of view is 3.84 mm X 2.3 mm. Plain light. Unit VII, Newlan Creek section.

Figure 20. Ooids and oolitic lithoclasts in calcitic quartz sandstone. Field of view is .96 mm X .576 mm. Crossed nicols. Lower Newland, Newlan Creek section.

Figure 21. Deformed ooid (top center) and molar tooth(?) clast (bottom center) in sandy sparite. Field of view is 2.4 mm X 1.44 mm. Plain light. Unit VII, Little Birch Creek section.

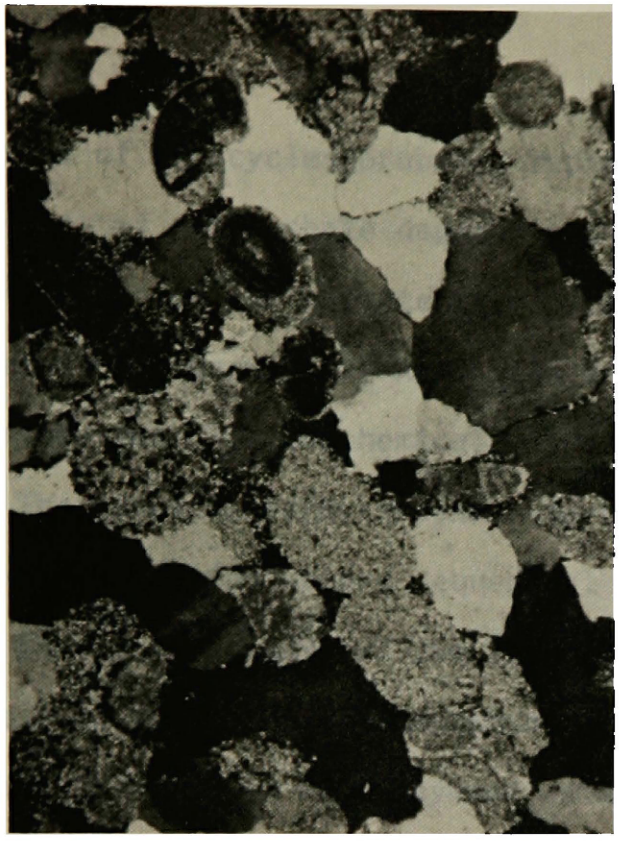

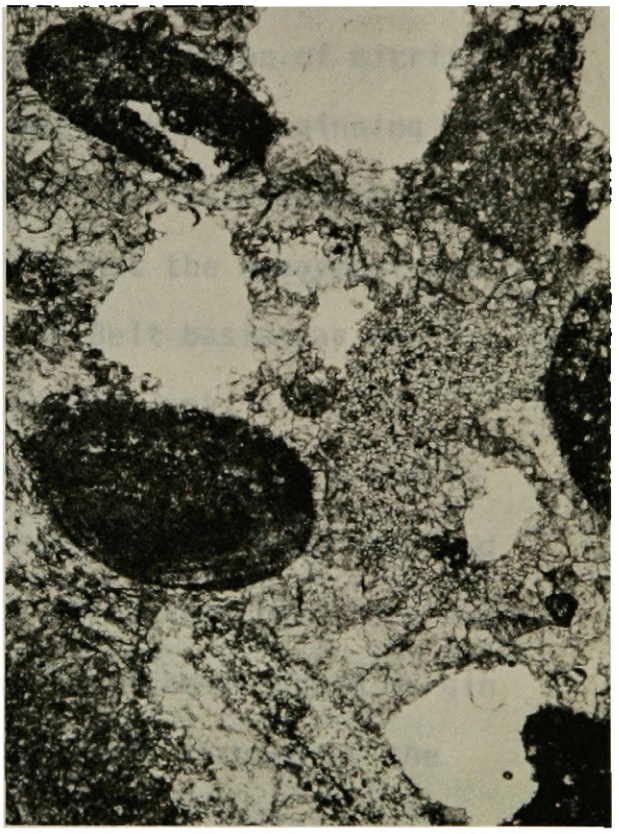

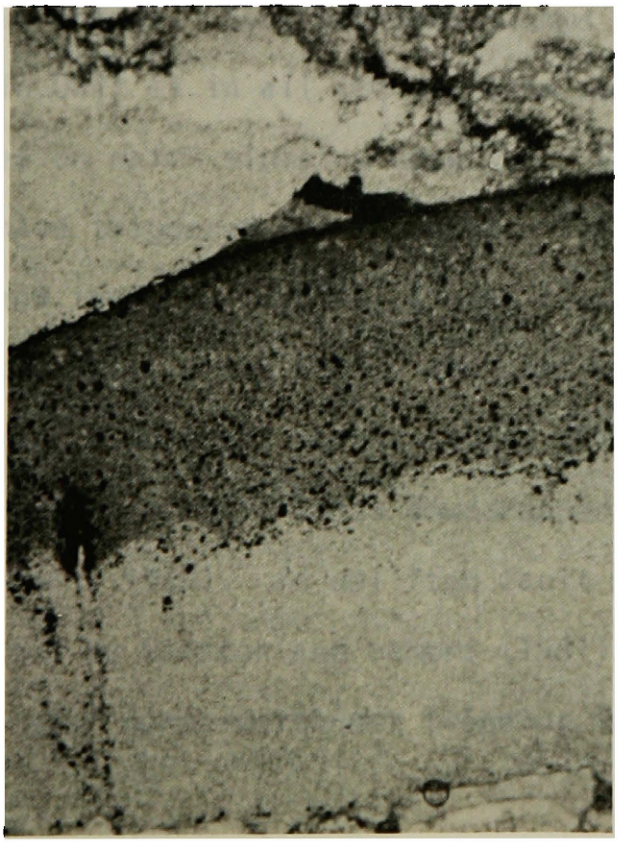

the tops of the cycles probably represents further shoaling. At the beginning of silty shale deposition, high terrigenous influx may have shut off biological calcite precipitation, or fresh water recharge along the embayment margin may have reduced water salinity below the level necessary for physico-chemical calcite precipitation.

The upper Newland carbonate-terrigenous cycles, then, may be sub-wave base shoaling upward sequences. The first deposition of micrite muds in the upper part of the lower Newland may mark the beginning of regression in the Helena embayment. Control of calcite precipitation by salinity changes in embayment water require that the embayment was at least partially restricted, or that the main Belt basin was restricted, whereas control by organic processes does not.

Faulting along the embayment margins probably also caused terrigenous influx. Soft sediment slumps are abundant in the lower Newland and in Unit IV in all the northern sections, indicating that there were slopes on which slumping occurred. Faulting along the northern margin may have triggered the slumping. The turbidite beds throughout the Newland indicate marginal slopes as well. The Volcano Valley Fault and the Sheep Creek Fault, now east-west trending Cretaceous or early Tertiary high-angle thrust faults (Fig. 22), may both be reactivated Precambrian normal faults downdropped to the south (Zieg, 1979; McClernan, 1969). An uplifted fault block west of the Helena embayment proposed by Winston and others (1981) is bounded on its eastern edge by a major north-northwest trending Precambrian fault that extended

through the present Missouri River Valley near Townsend (Fig. 22). The eastward and northeastward thinning of the basal Greyson quartzite and the eastward flow direction of turbidites in the lower Newland in the Deep Creek section, based on the orientation of flute casts, indicate that the turbidites and quartzites were shed from an upraised area to the west. Metamorphic rock cobbles in a conglomerate near the bottom of the basal Greyson quartzite, and metamorphic rock fragments and oolites in the turbidites indicate very shallow water and erosion of exposed basement rock to the west. An uplifted block to the west may have restricted the Helena embayment during much of its history, causing high salinities of embayment water and calcite precipitation.

Conclusions

The lower Newland Formation was deposited as a pelagic rain of silt and fine carbonate grains and represents the upper part of a transgressive sequence which developed in response to subsidence of the Helena embayment (McMannis, 1963). The pelagic sedimentation was interrupted by thin turbidite flows from the north and west, and massive ones from the south (McMannis, 1963). Along the northern margin of the embayment, soft sediment slumps probably resulted from margin faulting.

The upper Newland marks the beginning of a regressive sequence produced when the rate of filling exceeded the rate of subsidence. The sediments of the upper Newland represent sedimentation below wave base comprising two shoaling upward cycles in which periods of high carbonate production were swamped by terrigenous influxes. Calcite was

Figure 22. Diagram of probable and known Precambrian faults along the margins of the Helena embayment, and the extent of associated slumping and of clastic debris shed from the fault blocks. U = upthrown; D = downthrown; SCF = Sheep Creek Fault; VVF = Volcano Valley Fault; TL = Townsend Line; PL = Perry Line; SR = Smith River section; DG = Decker Gulch section; NC = Newlan Creek section; LBC = Little Birch Creek section. DC = Deep Creek section; SS = southern limit of soft sediment slumping; BGQ = approximate eastern boundary of basal Greyson quartzite; LH = approximate northern limit of LaHood deposition. Broken horizontal line pattern indicates Chamberlain Shale and overlying molar tooth-bearing microspar exposures, and the stippled pattern indicates Neihart Quartzite exposures. The scale is about eight miles to the inch.

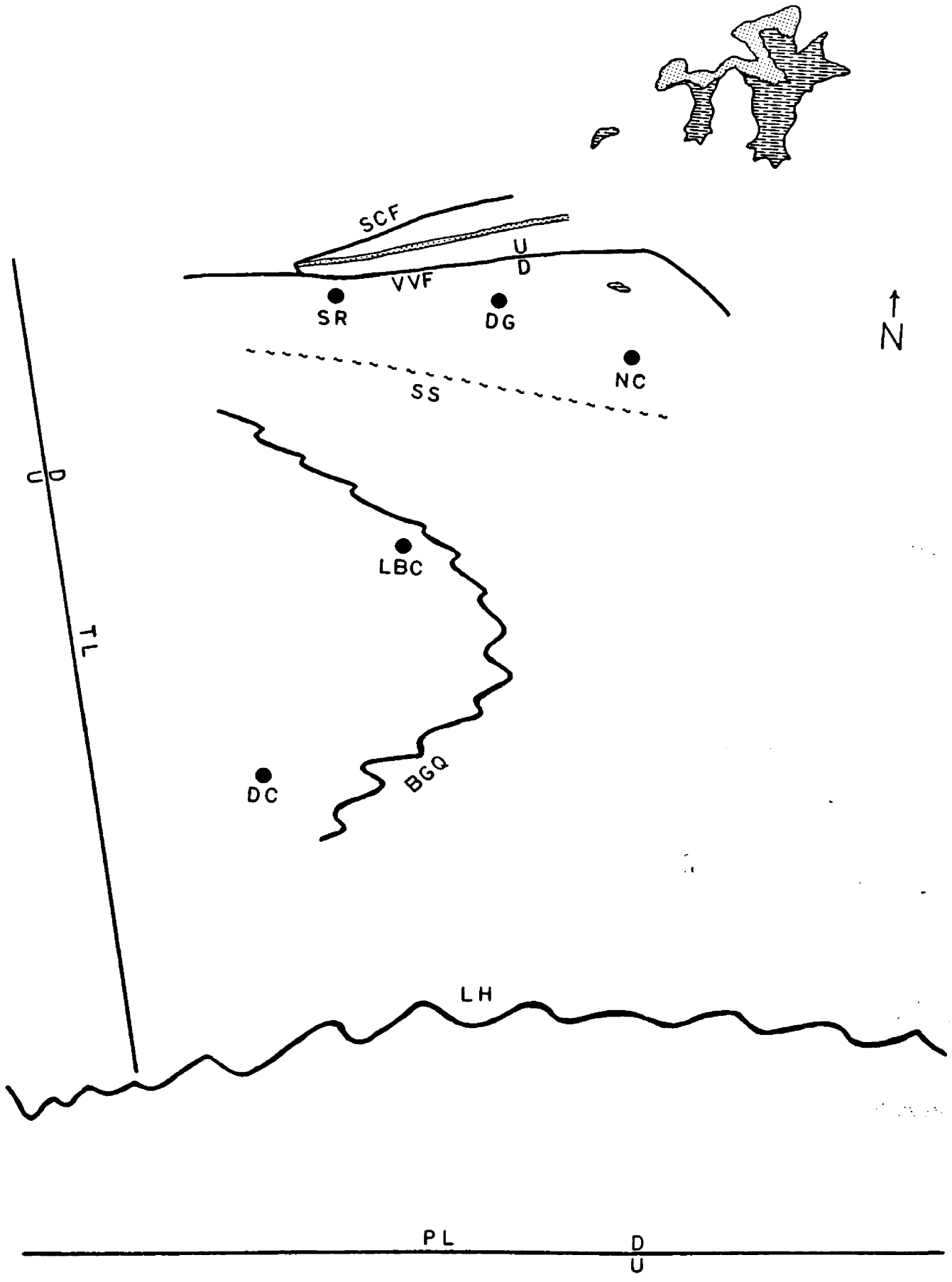
SCF
U
D
VVF
SR
DG
N
NC
SS
LBC
D
TL
BGQ
DC
LH
PL
D
U

precipitated by algae or due to high salinities, and terrigenous influx was either constant and migrated basinward during shoaling upward, or else resulted from a wetter climate or from uplift of fault blocks along the embayment margins creating a greater terrigenous supply. Either terrigenous influx or reduced salinities due to fresh water-embayment water mixing stopped carbonate production. The second onset of terrigenous influx and silty shale deposition marks the base of the Greyson Shale.

Uplift of a fault block to the west may have restricted the Helena embayment from the rest of the Belt basin during much of its depositional history. Further evidence for this might be found by comparing Ravalli Group and Middle Belt Carbonate sections along the western margin of the embayment with ones farther west.

Though the Helena embayment may have been isolated from the main Belt basin, the depositional styles are similar between correlative horizons. Both begin with transgression and a period of pelagic sedimentation, followed by regression culminating in nearshore and intertidal environments represented by the Spokane Formation and its western correlatives.

The Chamberlain-Newland Problem and Other Speculations

The two Newland Limestone sections established by Walcott (1899) along Newlan Creek and in Sawmill Canyon four miles south of Neihart may not be correlative. Instead, the Sawmill Canyon section carbonate may be stratigraphically below the lower Newland tan calcareous shale.

In the Neihart area, the 173 m thick interval of tan- and gray-weathering molar tooth-bearing dolomitic microspar (Keefer, 1972) with interbedded black shale is underlain by Chamberlain black shale (see Appendix II) and has been called Newland Limestone by Walcott (1899), Weed (1900), and Keever (1972). An overlying black-, brown-, red-, and purple-stained black shale interval over 156 m thick (Keefer, 1972) has been called Greyson Shale by Walcott (1899) and Keefer (1972), and Greyson Shale overlain by shale of the Spokane Formation by Weed (1900). However, molar tooth-bearing dolomitic microspar clasts occur in soft sediment breccia channels which cut Chamberlain-like black shale on an east-facing hillslopes overlooking the Little Sheep Creek drainage (section 36, R. 6 E., T. 12 N.) about six miles north of the Newlan Creek section and twelve miles southwest of the Neihart area exposures (Dave Godlewski, 1980, oral comm.). The dolomitic microspar clasts in the breccia channels have soft sediment folds, and the channels are similar to those filled with slope-derived breccias discussed by McIlreath and James (1979). The black shale containing the breccia channels continues upward several tens of meters and is overlain by about 300 m of lower Newland dolomitic tan calcareous shale. Thus the carbonate in the Neihart area may be a tongue in the Chamberlain Shale below the Newland Limestone, instead of correlating with the upper Newland carbonate as interpreted by Walcott (1899), Weed (1900), and Keefer (1972). No molar tooth-bearing dolomitic microspar occurs in any of the upper Newland sections and its occurrence in the lower Lewland in the Smith River section appears anomalous.

Black shale overlying the carbonate in the Neihart area is unconformably overlain by the iron oxide- and calcite-cemented Flathead quartzite of Cambrian age. Exposures of shale underlying the Flathead are characteristically stained various shades of red and purple by iron oxides weathering from the sandstone. The shale in the Neihart area called Greyson by Walcott (1899) and Keefer (1972) and additionally called Spokane by Weed (1900) may instead be the upward continuation of Chamberlain-like black shale deposited below the lower Newland calcareous shale stained red from weathering of the overlying Flathead Quartzite.

Since the molar tooth-bearing microspar and black shale overlying the type Chamberlain black shale in the Neihart area appear to lie below the tan calcareous shale of the lower Newland, perhaps they should be called an upper part of the Chamberlain Shale. Their dissimilarity with any Newland rock types in other Newland sections supports such a reinterpretation of the stratigraphic nomenclature.

If this recommendation is followed, all Belt exposures north of the Volcano Valley Fault (Fig. 22) may be limited to Neihart Quartzite, Chamberlain Shale, or molar tooth-bearing microspar underlying Newland Limestone, and are overlain by Flathead Quartzite. All exposures south of the Volcano Valley Fault, except the Little Sheep Creek exposure, are Newland, Greyson, or Spokane. This indicates that prior to Flathead deposition, the area south of the Volcano Valley Fault was probably downdropped, and that the fault was reactivated during the Cretaceous or early Tertiary. More work needs to be done to assess the merit of this reinterpretation of Helena embayment Belt stratigraphy.

A speculative facies interpretation for the Helena embayment Belt strata, based on interpretations of the Newland sedimentology and the reinterpretation of the molar tooth-bearing carbonates in the Neihart area, is shown in Figure 23. During lower Newland deposition, a pelagic rain of very fine-grained calcite, clay and some silt was deposited in the basin. To the south, LaHood sand and conglomerate probably flooded the southern margin of the embayment, and continued until sometime during Greyson deposition (McMannis, 1963). Along the northern edge of the embayment, molar tooth-bearing micrite mud and black shale of the Chamberlain were deposited, and north of this, the sands of the Neihart were deposited along the margin of the embayment. As lower Newland deposition continued, the sand, black mud, and molar tooth-bearing micrite mud migrated northward. The appearance of micrite mud (now gray microspar) in the upper part of the lower Newland may mark the beginning of regression in the embayment. The level of carbonate saturation in the embayment water increased for a time, allowing deposition of the micrite mud, and then pelagic deposition of clay, silt, and calcite resumed. Repeated intervals of gray microspar in the upper part of the lower Newland record that this happened several times.

Shoaling upward produced the two carbonate-terrigenous cycles, and the second period of silty shale deposition marks the base of the Greyson. Up to this time, Chamberlain- and Neihart-like facies were probably deposited along the northern margin of the embayment, as evidenced by molar-tooth clasts in Unit VII. Perhaps they changed to a

Figure 23. Tentative facies model for the Belt strata of the Helena embayment, from north to south. HH = Horseshoe Hills; DC = Deep Creek section; LBC = Little Birch Creek section; DG = Decker Gulch section; NH = Neihart; 1 = Neihart Quartzite; 2 = Chamberlain Shale; 3 = lower Newland Limestone; 4 = upper Newland Limestone; 5 = Greyson Shale; 6 = Spokane Formation. The heavy black line cutting through the diagram is the approximate present day erosional surface. The sketch below the main diagram is a scale outline of the cross-section. The north-south distance is about 140 km, and the maximum thickness shown is about 6 km.

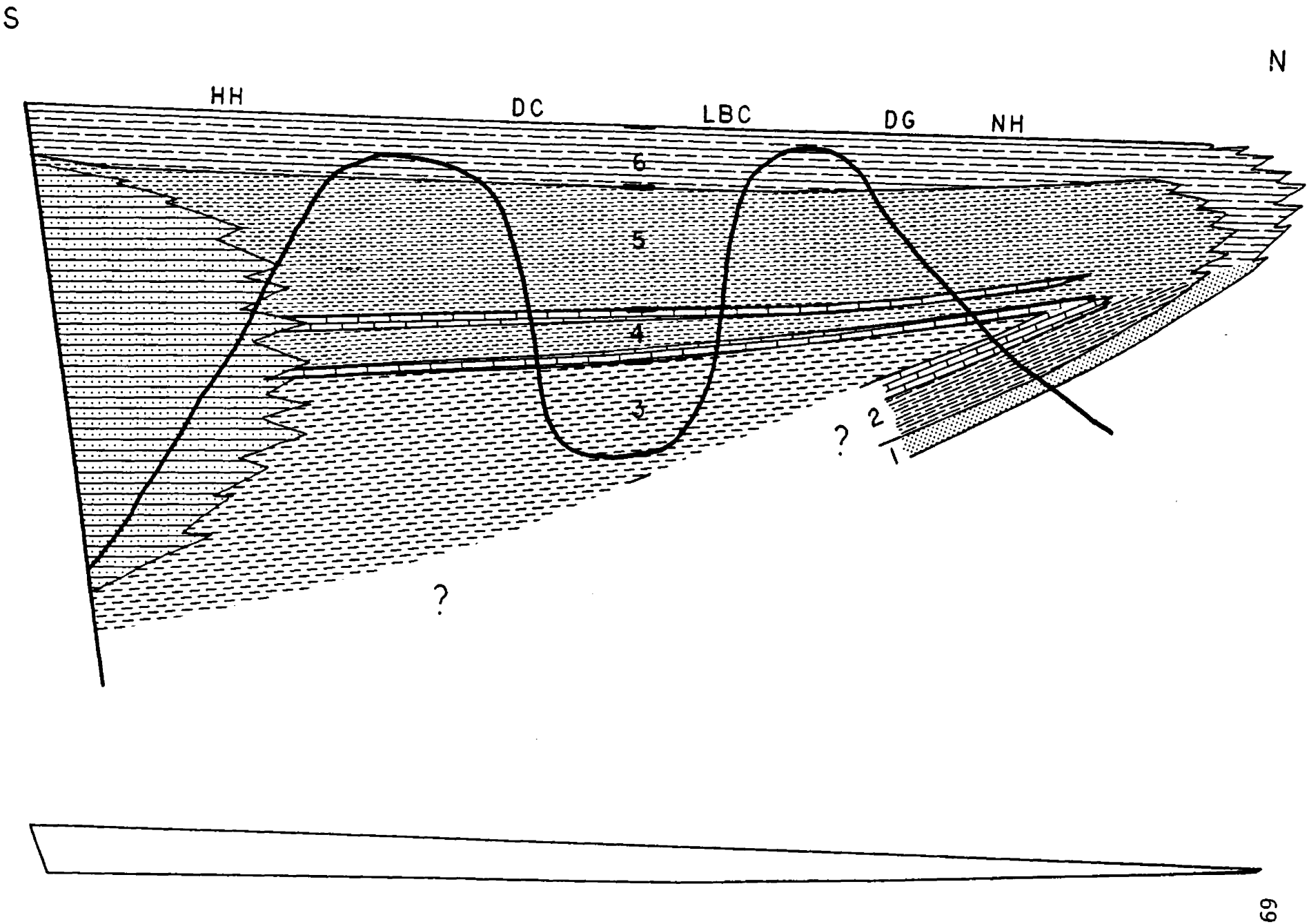
S
N
HH
DC
LBC
DG
NH
6
5
4
3
2
1
?
?

Greyson-like facies bordering a nearer shore, intertidal Spokane-like facies at the end of Newland deposition, and migrated basinward during regression in the embayment.

Summary

Interpretation of Newland deposition as subwave base is compatible with the interpretations of LaHood deposition of McMannis (1963) and Hawley (1973), who postulate the LaHood clastics were deposited in a subaqueous environment. However, Boyce (1975) interpreted the Newland as a tidal flat deposit, for which there is no supporting evidence in any of the Newland I studied.

Since the lower Newland tan calcareous shale appears to represent the deepest water depositional environment of any Helena embayment Belt sediments, the upper Newland-lower Newland boundary may mark the beginning of regression in the embayment. Uplift of a fault block to the west may have restricted the embayment and allowed carbonate saturation of embayment water and shoaling upward, resulting in the two carbonate-terrigenous cycles of the upper Newland, followed by Greyson and Spokane deposition. The Neihart Quartzite and the Chamberlain Shale may represent shoreward facies during transgression, and may have changed to Greyson- and Spokane-like facies at the beginning of regression.

Reinterpretation of the stratigraphic position of the molar tooth-bearing carbonate in the Neihart area as a pre-Newland carbonate not only enhances the symmetry of the transgressive-regressive cycle recorded in the Helena embayment Belt strata, but also supports an interpretation

of the Volcano Valley Fault as a reactivated Precambrian normal fault.

CHAPTER IV

NEWLANDIA AND RELATED STRUCTURES

Introduction

Beds of microspar cylindrical "ropes" parallel to bedding, microspar plates oblique to bedding, microspar concave-upward and convex-upward hemispheroids, and microspar containing thinly-laminated structures and mottling all occur in nondolomitic gray microspar and nondolomitic black chert-bearing microspar in Unit I, Unit III, Unit VI, and in the upper part of the lower Newland (Figs. 23-27). These structures were first described by Walcott (1914) who examined samples sent him by a local rancher from the Little Birch Creek section. Walcott (1914) concluded that the structures were algal remains and described five new genera and eight new species of Precambrian algal forms. The only two authors who have visited the outcrops question an algal origin for a part of the structures and suggest fracturing and weathering (Gutstadt, 1975) or groundwater dissolution along fractures after lithification (Fenton and Fenton, 1936) as an alternative origin.

Since the Little Birch Creek section contains the greatest number of the structures and is the holotype section for the taxa described by Walcott (1941), I studied structures from this section most extensively. From these studies, I believe all the forms can be explained as a result of pressure solution of the gray microspar and black chert-bearing microspar.

Morphologic Descriptions

Five distinct forms occur in the gray microspar and black chert-bearing microspar of the Little Birch Creek section. These are:

1) beds of microspar plates oriented oblique to bedding (Fig. 24);
2) beds of microspar cylindrical "ropes" parallel to bedding (Fig. 25);
3) microspar hemispheroids, both convex upward and downward, and ovoids (Fig. 26);
4) thinly-laminated structures in microspar (Fig. 27); and
5) light tan or gray mottles in darker microspar (Fig. 28).

Plates

Microspar plates are what Walcott named Newlandia major (1914). They consist of gray microspar in a clay-rich, calcite-deficient matrix and of black chert-bearing microspar in a clay-rich, black chert or radialaxial calcite matrix (Fig. 32). In cross-section perpendicular to their long axes, plate shapes range from planar to C-shaped and even S-shaped. The attitude of some plates reverses within a bed (Fig. 29). In other places, plate attitudes in a bed may dip opposite from plate attitudes in an adjacent bed. Plate intersections with bedding planes are sinuous but maintain overall consistent orientations in any given location. Thicknesses of plates range from 0.2 cm to 1.5 cm. Primary laminations within the plates are abruptly truncated but generally undeformed at matrix-microspar boundaries. Highly distorted laminations

Figure 24. Plates oblique to bedding. Laminated areas are microspar.

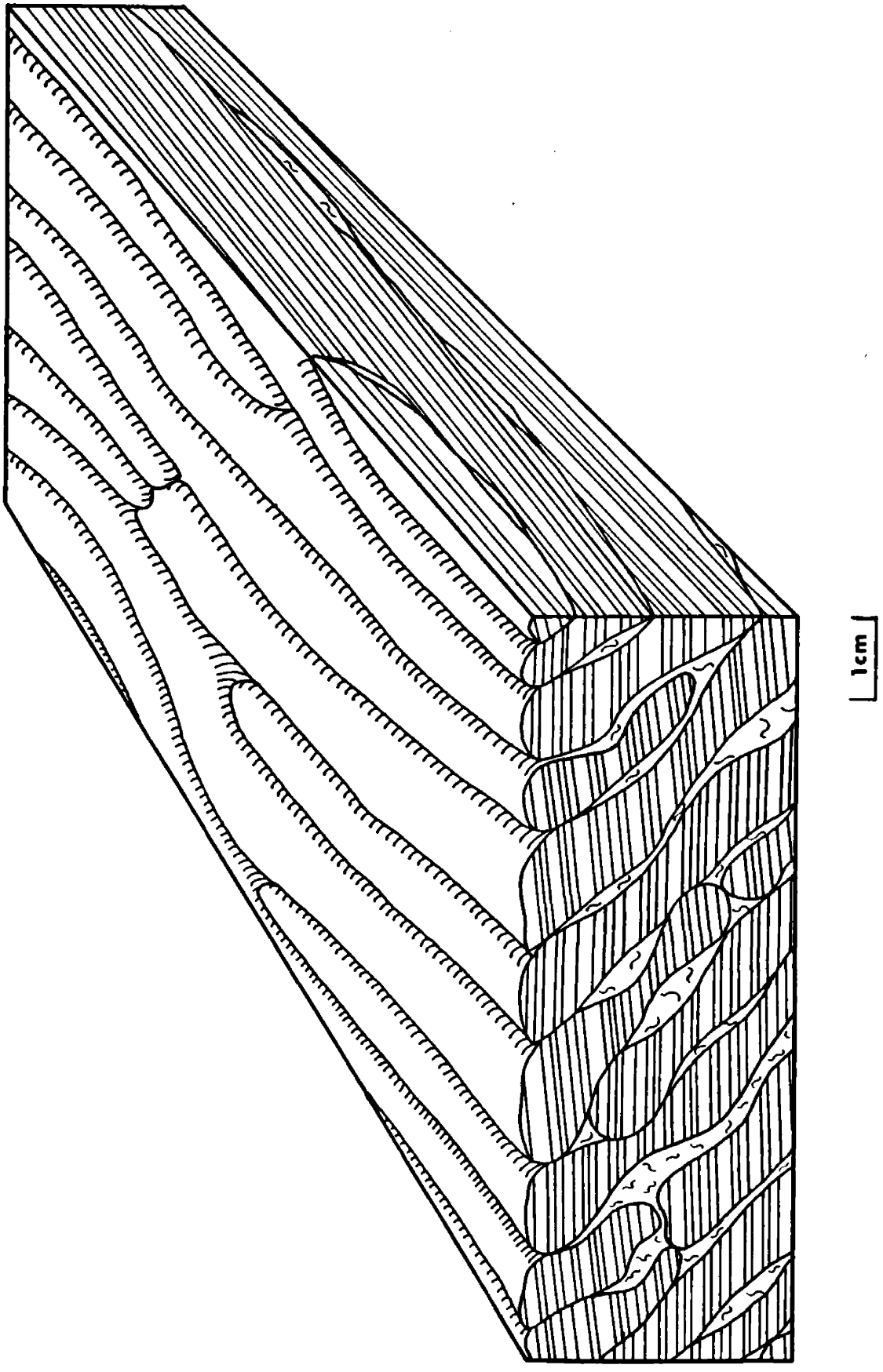
1cm

Figure 25. Ropes. Note the rotated ropes in the center of the bed. Block pattern indicates limonitic sparry calcite veinlets.

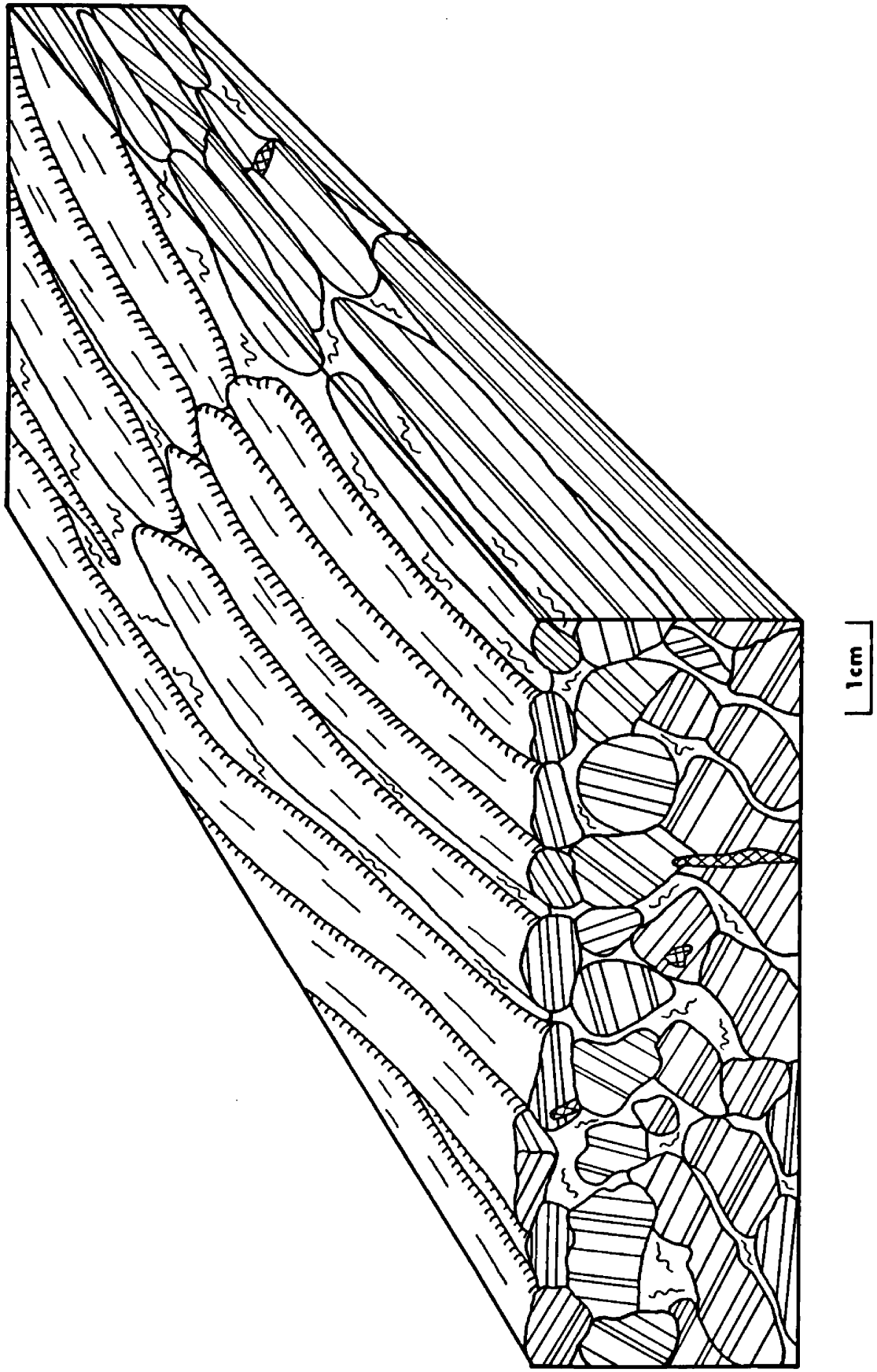
1cm

Figure 26. Concave-upward hemispheroids. Stippling indicates the dark part of the laminations.

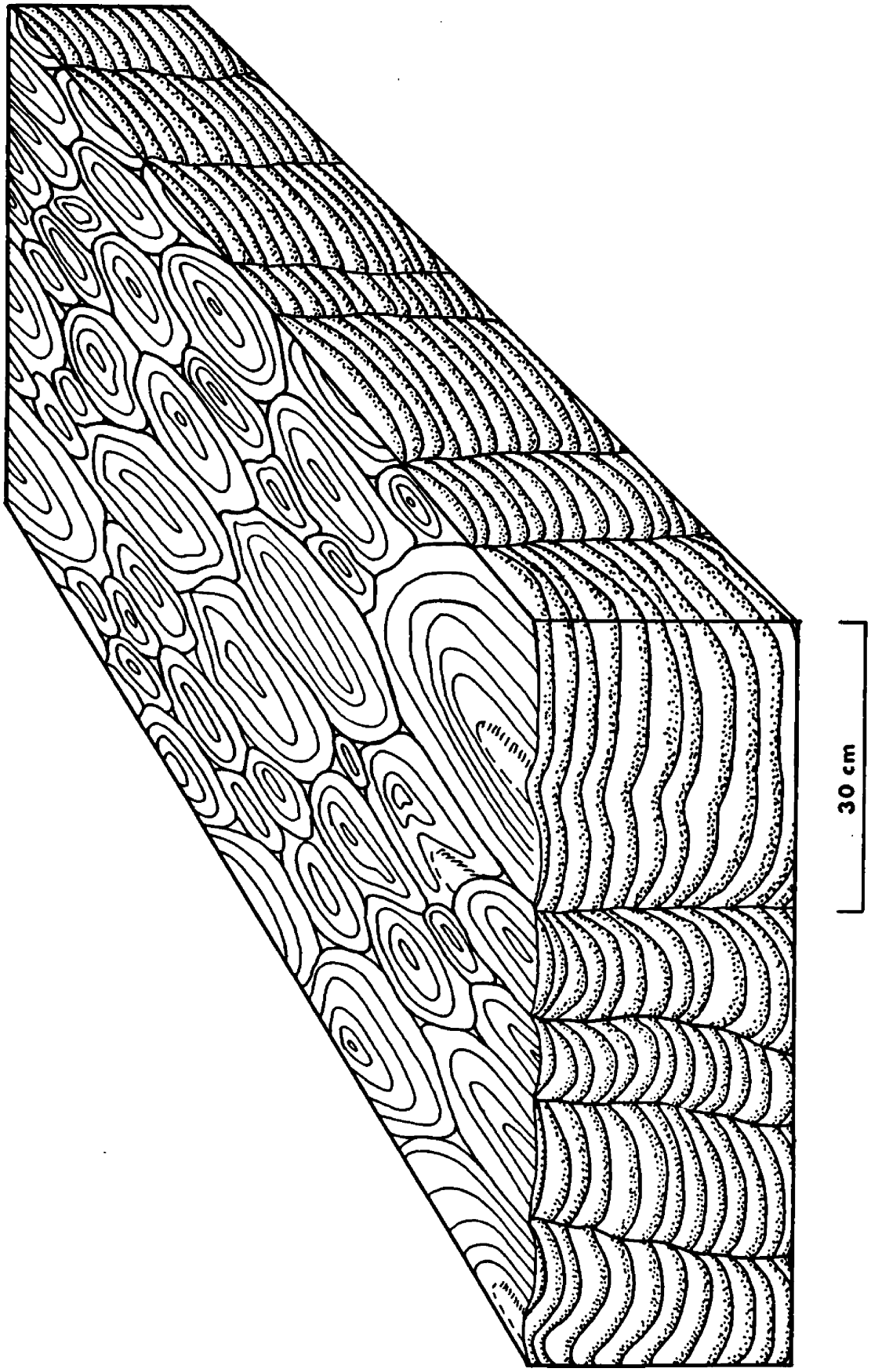
30 cm

Figure 27. Thinly-laminated structure. The dark area represents microspar, and the light area represents the tan- and light gray-weathering laminations. Note the stylolite on the near end of the right hand face of the block.

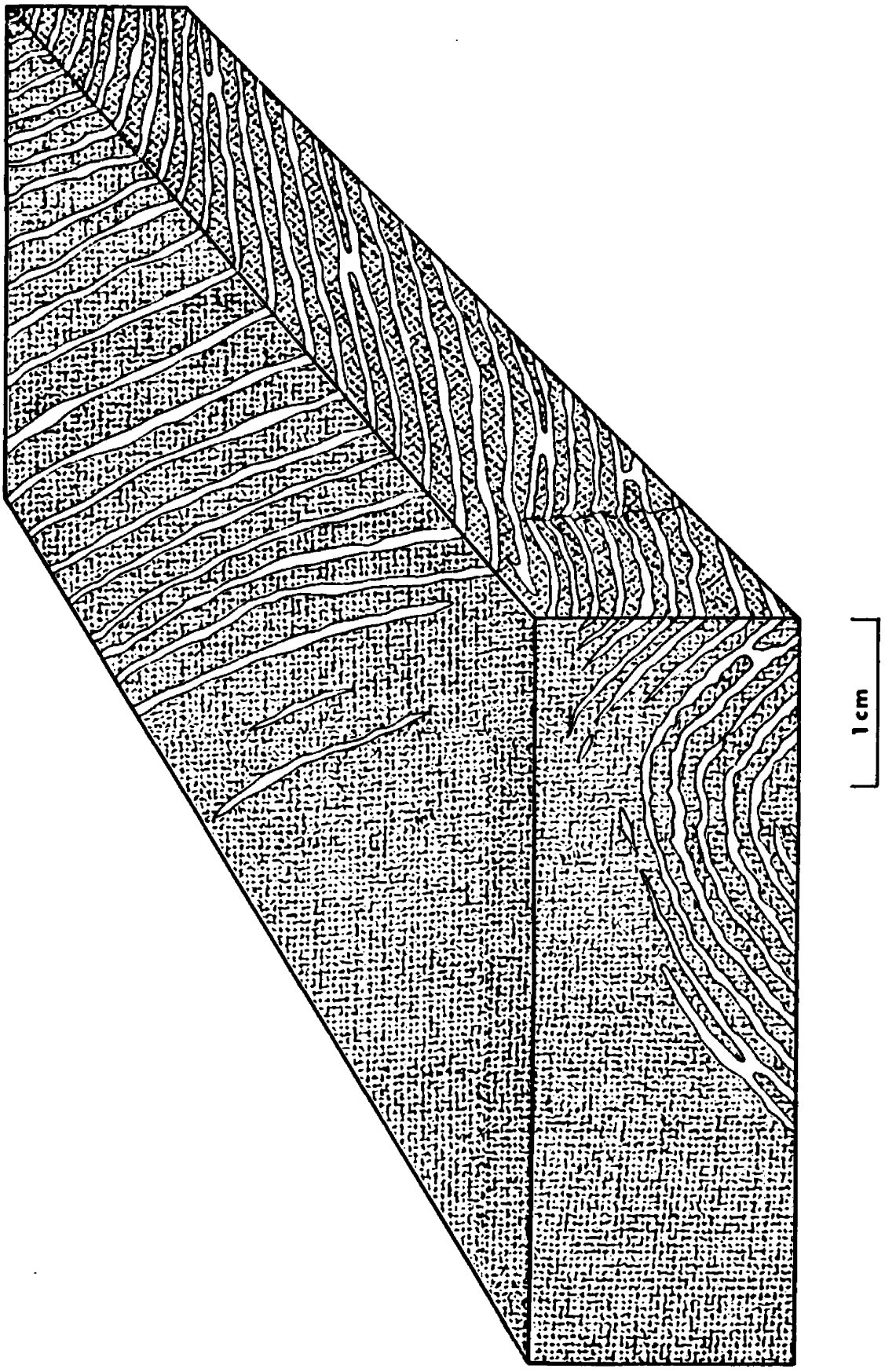
1cm

Figure 28. The light areas represent tan- and light gray weathering mottling in the darker microspar, represented by the dark pattern.

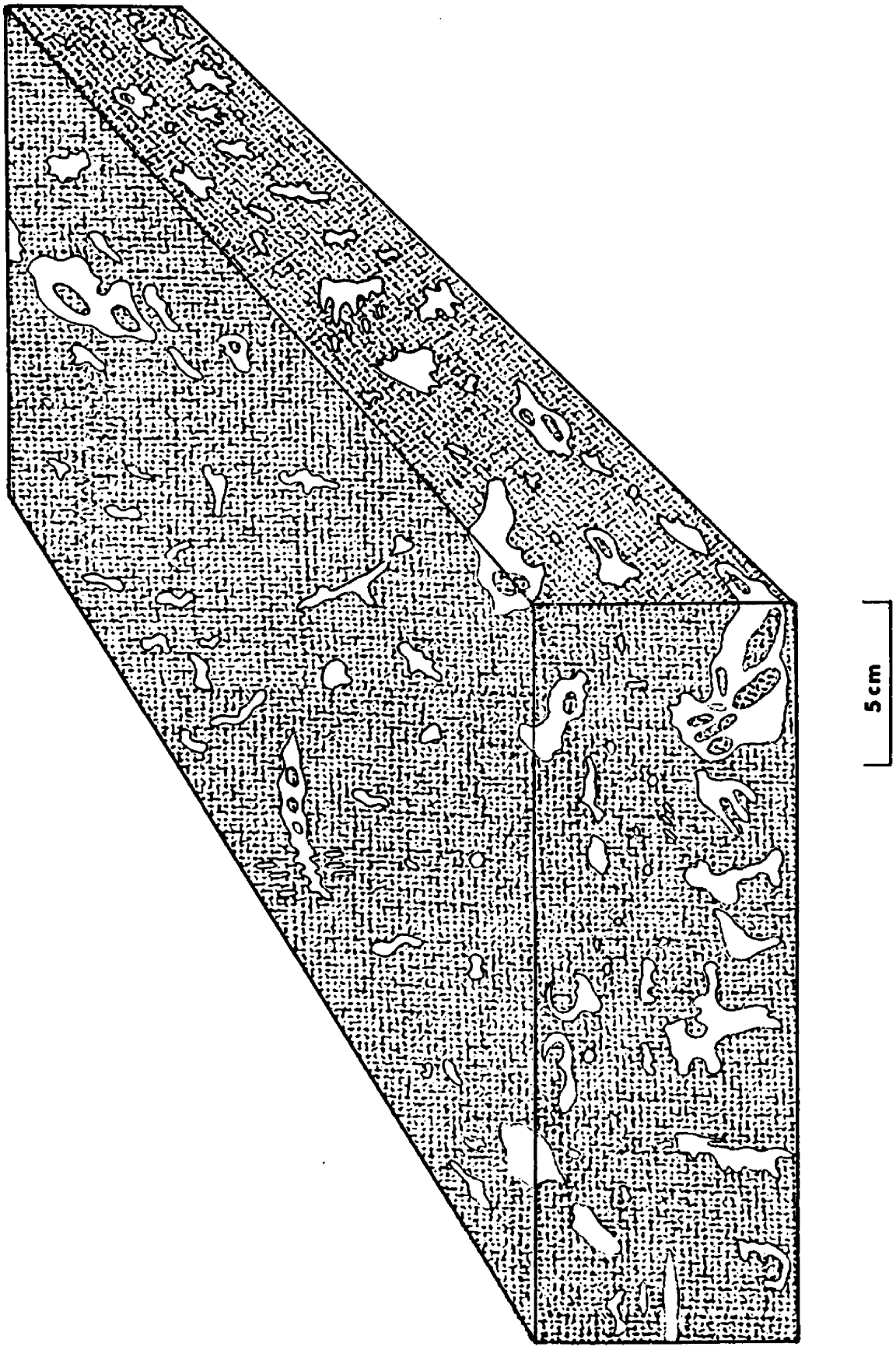
5cm

Figure 29. Symmetric orientation of curved plates. Unit III, Little Birch Creek section.

Figure 30. View of the soles of beds of ropes and plates, looking straight up from the base of the outcrop. The field of view covers about 1 vertical meter of the outcrop. Unit VI, Little Birch Creek section.

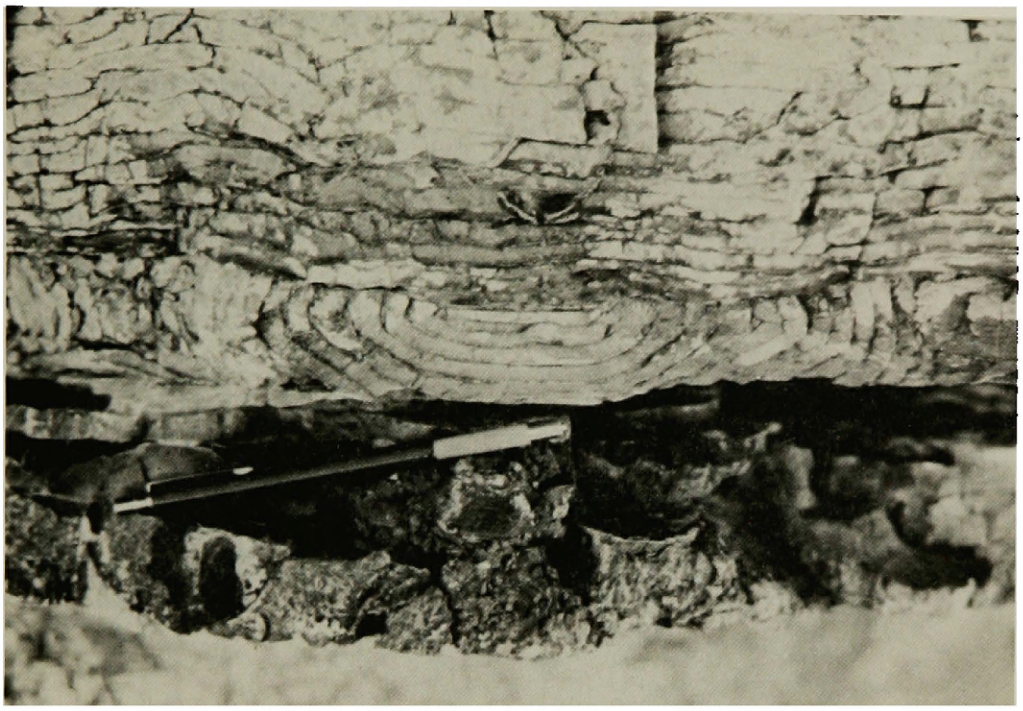

are preserved in the clay-rich matrix. Both offset of lamination sets and in a few places bending of laminations in the microspar next to microspar-matrix boundaries indicate normal movement between adjacent plates with net displacement of as great as several centimeters. Where plates touch one another, their boundaries are stylolitic. Stylolites also cut across plates, resulting in differing lamination attitudes on either side of the stylolitic boundaries. Irregular limonitic sparite veinlets cut through the microspar, but generally terminate at microspar-matrix boundaries, and typically thin into stylolitic boundaries.

Ropes

Ropes are what Walcott (1914) named Copperia tubiformis and Greysonia basaltica. The microstructure and lithology of ropes and their matrix is identical with that of plates, and in some instances they grade into one another (Fig. 31). An additional characteristic texture in ropes is embayment of one rope by another when viewed in cross-section (Fig. 25). Laminations truncated at these boundaries are undisturbed and the boundaries are stylolitic (Figs. 33, 34). Lamination orientations in adjacent ropes are characteristically discordant in the centers of beds and more nearly concordant near the tops and bottoms of beds. Offset of lamination sets and bending of laminations in the microspar against microspar-matrix boundaries indicate normal movement between adjacent ropes. Intersections of ropes and bedding planes are identical to those of plates and bedding planes (Fig. 33).

Figure 31. Cross-section view of ropes and plates in outcrop. Unit VI, Little Birch Creek section.

Figure 32. Thin section view of chert matrix (right, light) and clay, calcite, and chert matrix (left, dark) in contact, between radialaxial rimmed microspar plates (upper and lower edges of photo). Field of view is 3.84 mm X 2.3 mm, plain light, Unit III, Little Birch Creek section.

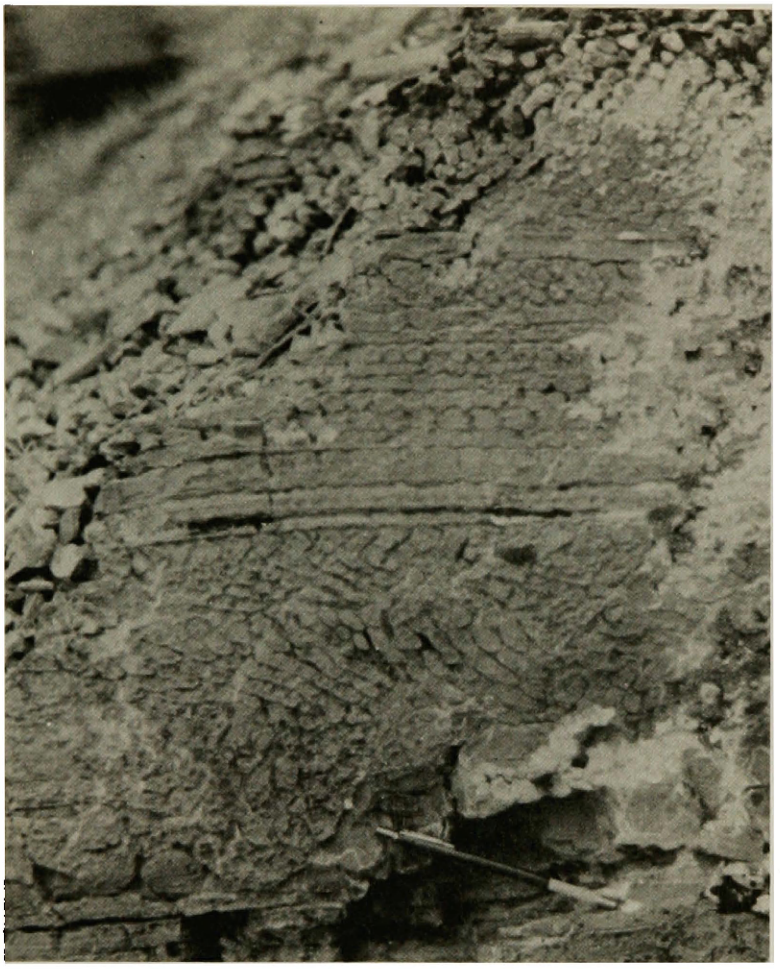

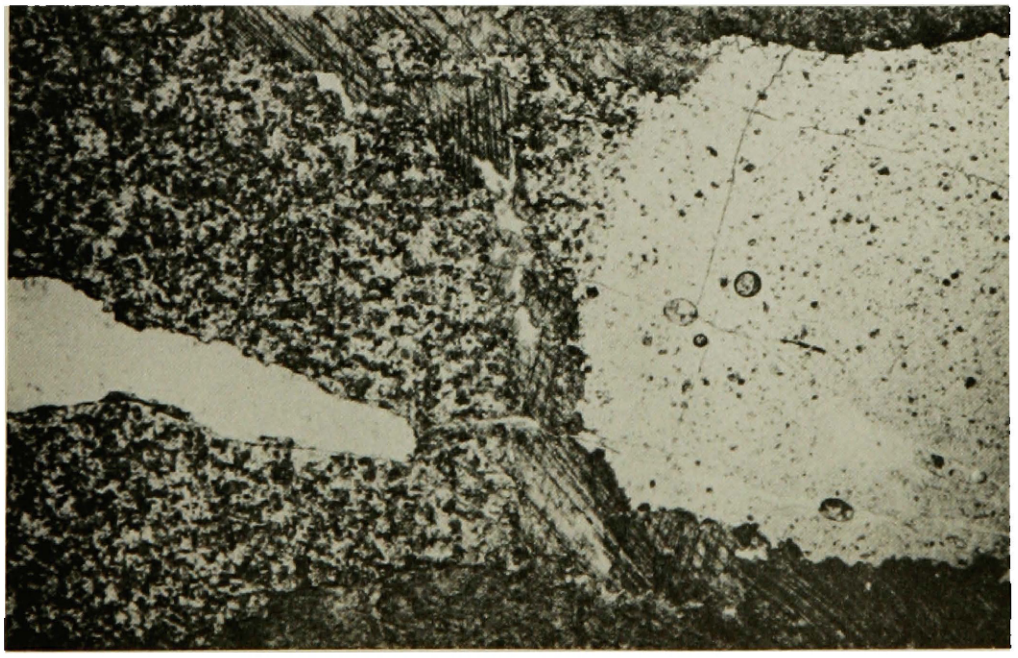

Figure 33. Thin section view of a solution boundary between two microspar ropes. Note the truncation of the silty laminations in the microspar against the solution boundary, and the stylolite in the microspar below the solution boundary. Field of view is 3.84 mm X 2.3 mm, plain light. Unit VI, Little Birch Creek section.

Figure 34. Stylolitic boundary between two microspar ropes. The stylolite widens into clay seams (dark) at its ends. Field of view is 3.84 mm X 2.3 mm, plain light. Unit VI, Little Birch Creek section.

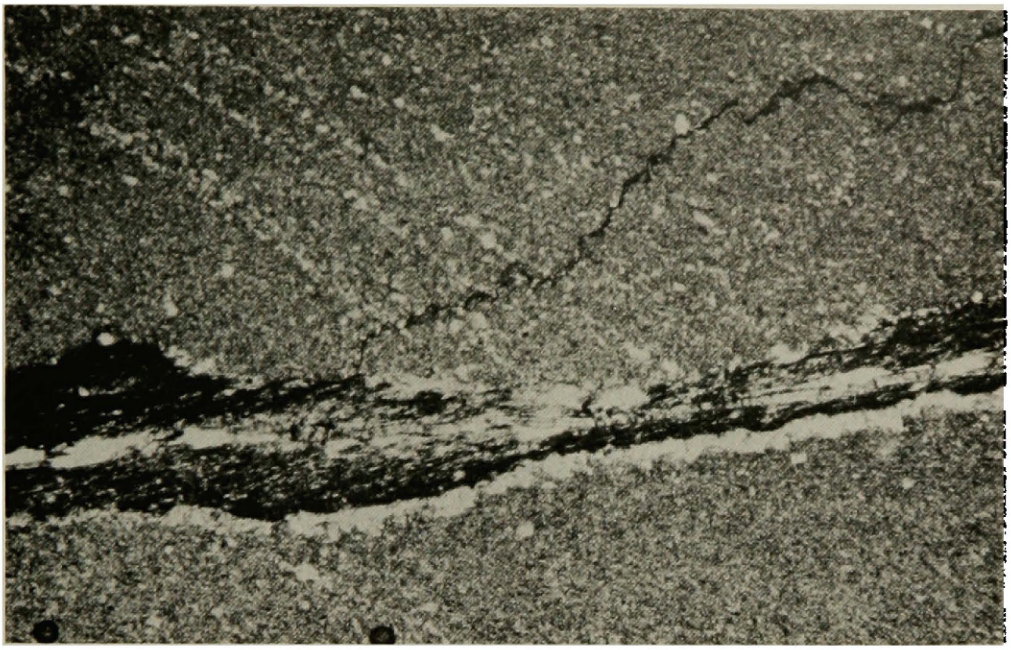

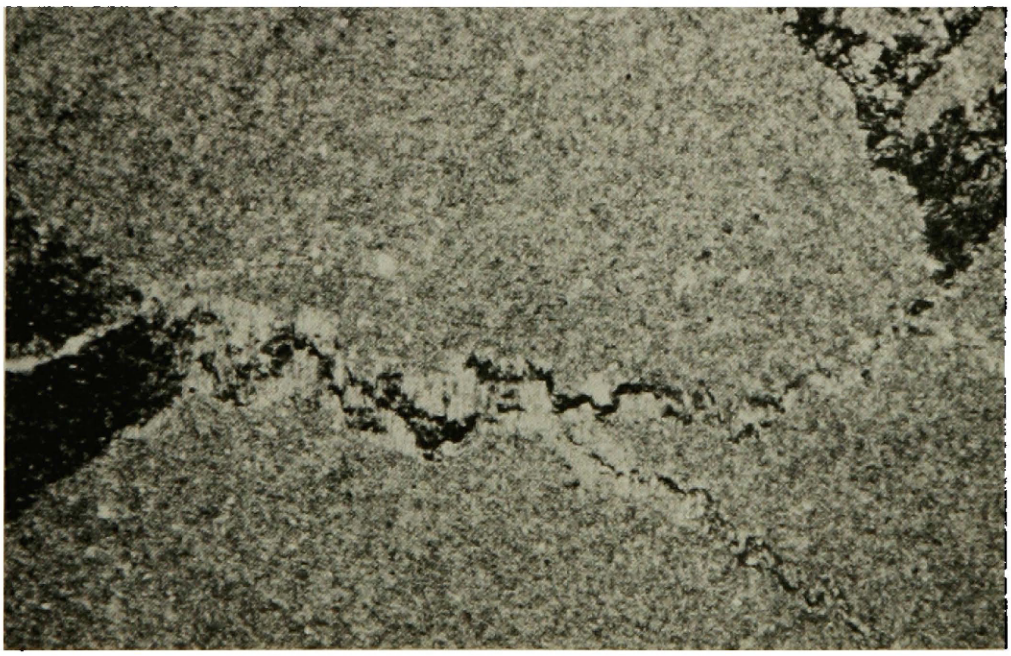

Orientations of some individual ropes rotate as much as 90 degrees within the bedding plane over a few tens of centimeters, and great changes in rope orientation also occur within a few vertical centimeters. Thicknesses of ropes range from 0.5 to 3.5 cm. Ropes range in length from less than a centimeter to several tens of centimeters.

Hemispheroids and Ovoids

Hemispheroids and ovoids occur only in gray microspar and are of the same composition as the ropes and curved plates. Concave-up hemisperhoids (Figs. 35, 36) are the dominant variety and are probably what Walcott (1914) named Newlandia concentrica (1914). They occur in stacks up to 0.5 meters high, in irregular aggregates, and isolated in individual beds. Where stacked, stylolites form the boundaries between stacks. Convex-upward hemispheroids and ovoids occur only isolated in single beds.

Lamination thicknesses range from 0.1 to 2 cm, and are characteristically less than 0.5 cm. Boundaries are sharp and even, and most are stylolitic. Laminations on both fresh and weathered surfaces change in color from dark gray to light gray upward in concave-upward hemispheroids, downward in convex-upward hemispheroids, and outward from the centers of the ovoids (Fig. 37).

In the concave-upward hemispheroids, quartz silt is locally finely cross-laminated. The thicknesses of silty laminations generally decrease toward the centers of inverted hemispheroids, while the thicknesses of silt-free microspar laminations increase toward the center of the forms.

Figure 35. Cross-section view of concave-upward hemispheroids in gray microspar, Unit VI, Little Birch Creek section.

Figure 36. Bottoms of concave-upward hemispheroids. Unit VI, Little Birch Creek section.

Figure 37. a) dark (stippled) and light color changes in ovoids (left) and in concave-upward and in convex upward hemispheroids.
b) Ovoids grading upward to convex-upward hemispheroids and downward to concave-upward hemispheroids. The horizontal dashed lines represent primary laminations.
c) Irregular arrangement of concave-upward Hemispheroids.
d) Abnormal morphologies in hemispheroids.

a
b
c
d

Microstylolite swarms are concentrated along the siltier edges of the inverted hemispheroids.

Some adjacent ovoids are overlain by convex-upward hemispheroids and underlain by concave-upward hemispheroids (Fig. 37). These stacks of ovoids and hemispheroids are elongate, parallel and separated by stylolitic planes. On bedding plane surfaces these appear similar to large ropes. Centers of ovoids characteristically exhibit thin laminations parallel to bedding that are truncated by the innermost concentric lamination of the ovoid, indicating that the truncating laminations are secondary.

Thinly-laminated Structures

Thinly-laminated structures occur in black chert-bearing microspar and are what Walcott (1914) named Newlandia lamellosa. The light tan- and gray-weathering laminations are thin but of slightly irregular thickness, and separate the dark gray microspar into even laminations about 0.1 cm apart. Many small irregularly shaped patches of the same composition as the tan-weathering laminations join together two or more laminations. The laminations are nearly all oblique to bedding and typically form hemispheroidal shapes (Fig. 38) unless distorted. The laminations are terminated at upper and lower bed boundaries, and are visible on bedding plane surfaces. This feature is probably what Walcott (1914) named Kinneyia simulans.

The light gray- and tan-weathering laminations and connecting patches are more clay and quartz rich than the host microspar. The

Figure 38. Hemispheroidal-shaped mottled thinly laminated structure. Unit III, Little Birch Creek section.

Figure 39. Mottling and thinly laminated structure. Unit III, Little Birch Creek section.

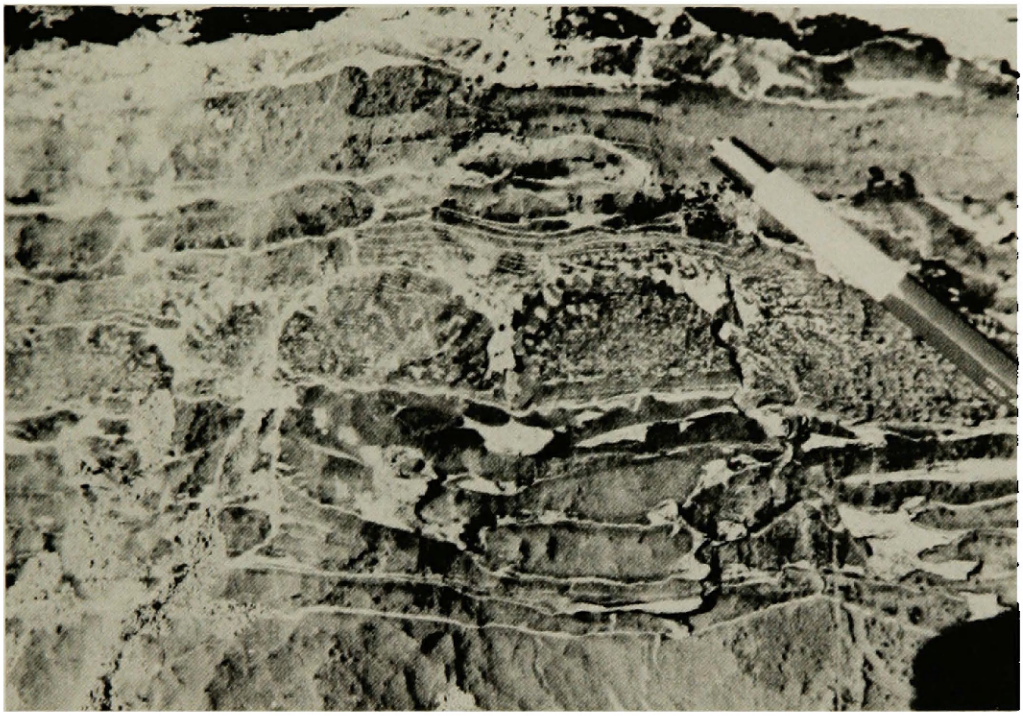

laminations contain silt-sized authigenic quartz and patches of coarser-grained secondary quartz. Stylolites, both concordant and disconcordant to the laminations, cut the microspar. Where discordant, they distort the laminations, bending them in the direction of stylolite growth.

Mottling

Light gray- and tan-weathering mottles, not discussed by earlier authors, occurs in dark gray black chert-bearing microspar and is clay and quartz rich and calcite deficient. In many places, mottling follows along laminations, increasing the size until the laminations are replaced by irregular mottles, indicating that mottling is a more spectacular form of the tan-weathering patches joining some of the thin laminations (Fig. 39). In other places, mottling appears unrelated to any other structure. Stylolites seem to control development of mottling because in some cases mottling abruptly ends against stylolites or changes style on either side of them. Material of identical composition as the mottles occurs as a matrix between ropes and curved plates in the black chert-bearing microspar where a black chert or radialaxial calcite matrix is not present.

Forms at Other Locations

Hemispheroids occur in Unit VI in the Newlan Creek section and the Decker Gulch section. Mottling also occurs in this unit in the Decker Gulch section, and in a gray microspar bed in the lower Newland in the Smith River section. Ropes and plates occur in the upper Newland

Formation in Johnson Canyon in the northern Bridger Range (Sheila Fountain, oral comm., 1980).

Oriented mottling (Fig. 40) and forms similar to curved plates (Fig. 41) occur in the Deep Creek Section. In addition, cherty concentric rings and radiating spokes on bedding surfaces (Fig. 42), averaging 40 cm in diameter, occur in Unit III in the Deep Creek section. In cross section, the rings surround unmottled cores (Fig. 43) while the rings themselves are made of frond-like mottling (Fig. 44). This form appears similar to Walcott's Newlandia frondosa (1914), and five miles northwest of the Deep Creek section, along Ray Creek, Nelson (1963) reports occurrences of Newlandia major, Newlandia lamellosa, and Newlandia frondosa.

Relationships Between Structures

In the Little Birch Creek section, hemispheroids and ovoids occur only in the bottom 0.5 meters of Unit VI. Inverted hemispheroids also occur in these beds, but completely dominate the outcrop for the next 2.5 vertical meters. Their average diameters diminish upward, until the forms abruptly change to beds of ropes and curved plates. The contact between inverted hemispheroids and the beds of curved plates and ropes is very sharp. In some cases, the contact is slightly discordant to bedding and ropes are sharply truncated by the hemispheroids. In Unit III at Little Birch Creek, thinly-laminated structures and mottling pass laterally into beds of ropes and curved plates over a distance of three meters.

Figure 40. Oriented mottling (light) enclosing gray microspar plates. Unit I, Deep Creek Canyon.

Figure 41. Cut slab showing oriented mottling (light) and microspar plates. Note the different attitudes of plates in different beds. Polished slab is 14 cm tall. Sample from Deep Creek Canyon.

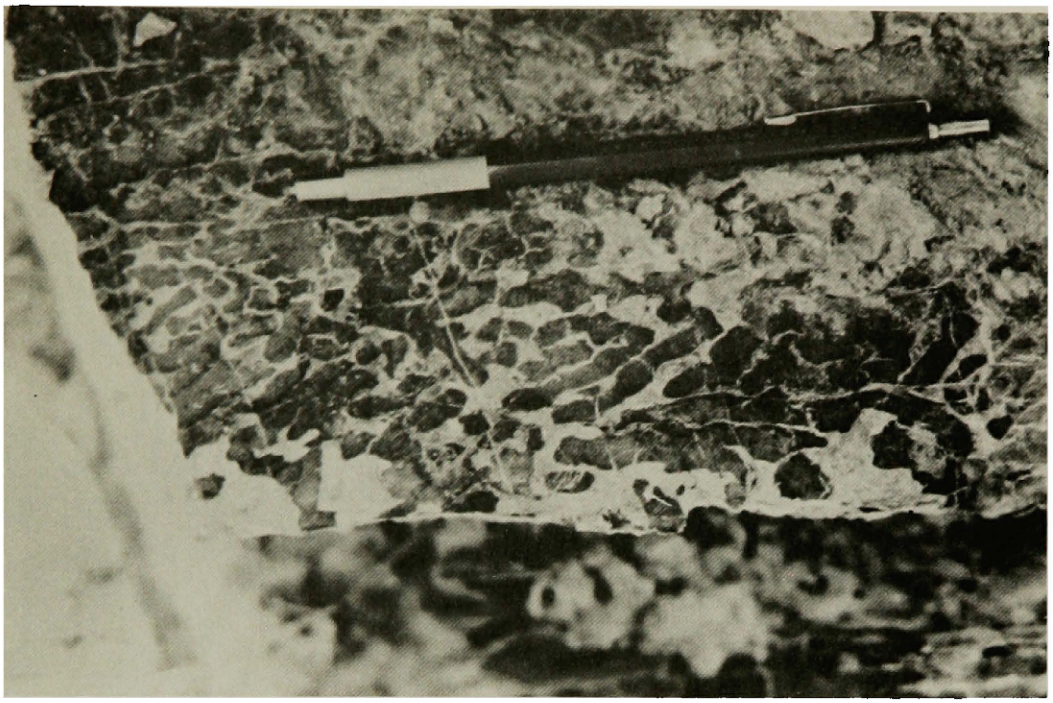

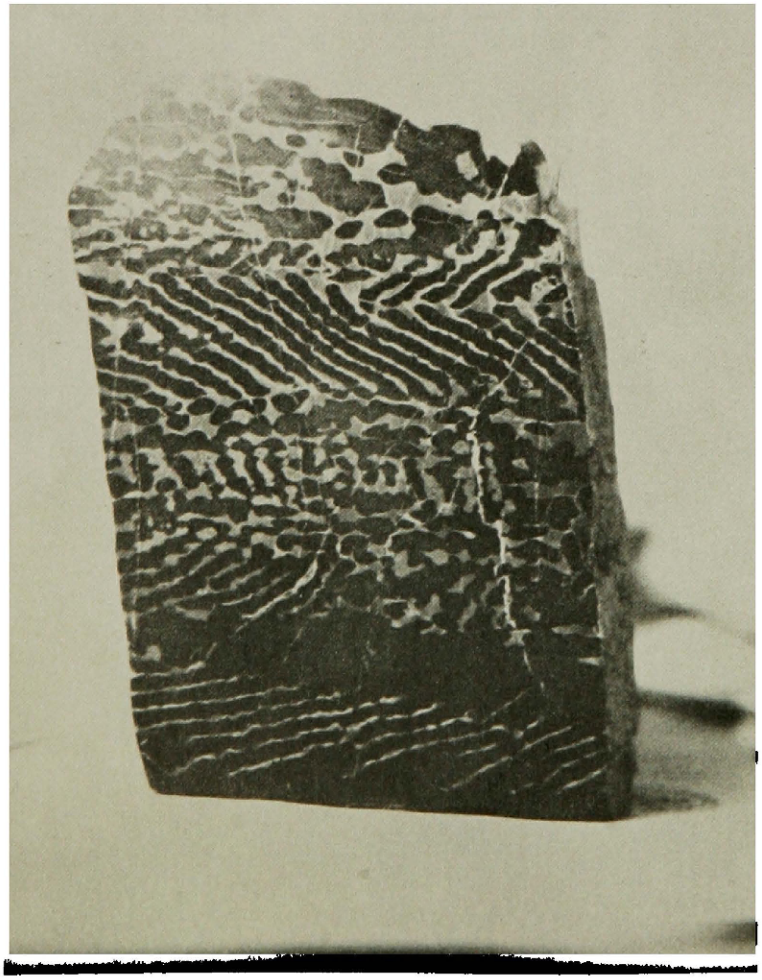

Figure 42. Silicitied rings on a gray microspar bedding plane surface. Unit III, Deep Creek section.

Figure 43. Cross section of the microspar center (dark) inside a silicified ring like that shown in Figure 41. Height of cut and etched face is 8.5 cm.

Figure 44. Same sample as in Figure 42, only rotated 90 degrees to show a cross section of the silicified ring. Silicified mottling is white, and microspar is dark. The mottles grade downward to stylolites. Height of the cut and etched face is 8.5 cm.

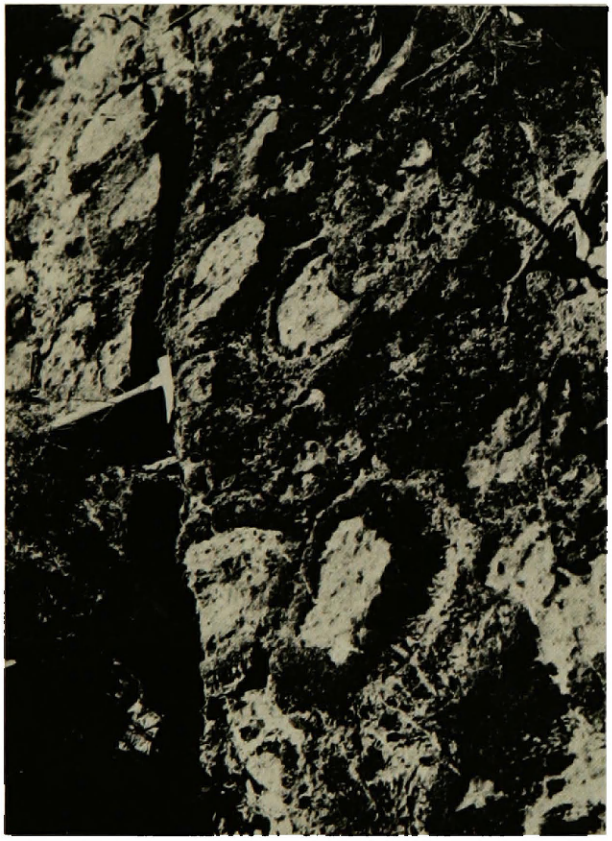

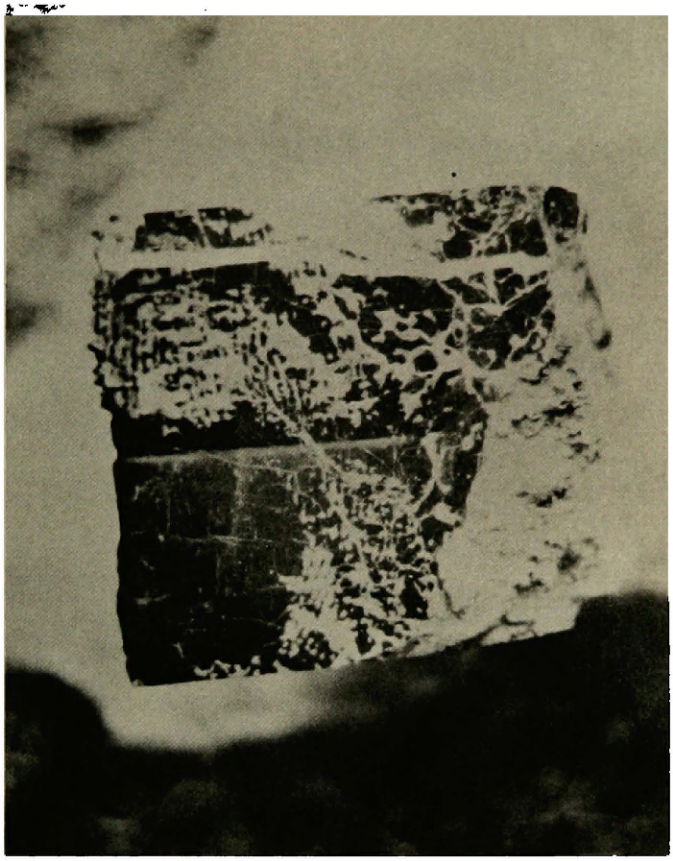

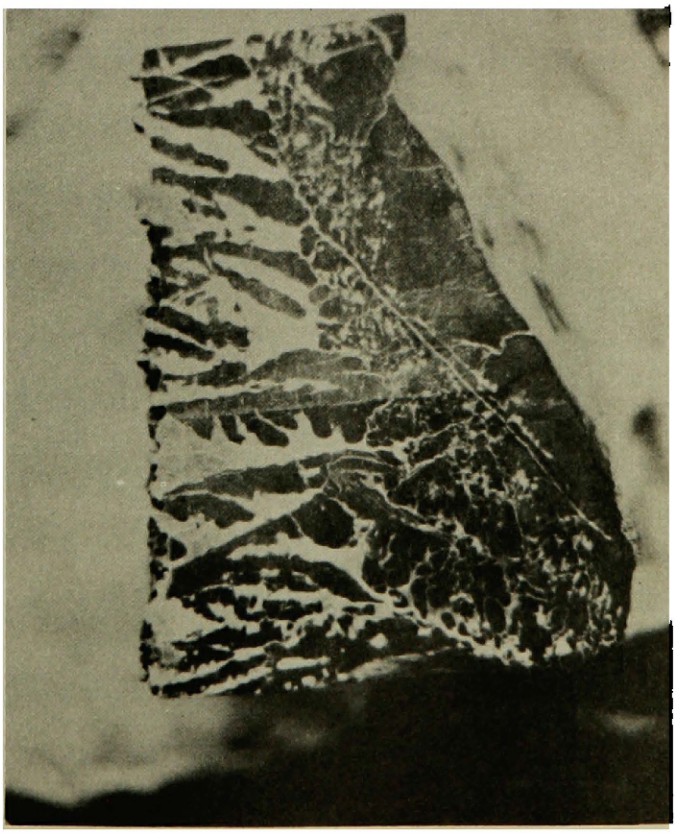

Forms transitional between ropes and plates, thinly laminated structures and plates, ropes or plates and hemispheroids, mottling and thinly laminated structures, and ropes or plates and mottling are present in the outcrops but are less abundant than the end members described above. Oriented mottling in Deep Creek Canyon is probably a transitional form between plates or ropes and mottling.

Previous Interpretations

Holtedahl (1921), Raymond (1935), and Glaessner (1962), none of whom visited the outcrops, have all questioned the validity of Walcott's taxa. Holtedahl (1921) noted a great similarity between Walcott's descriptions of the forms at Little Birch Creek and forms in the Permian limestones near Durham, England, which were accepted as secondary concretionary structures by his contemporaries. From Holtedahl's descriptions, forms in the Permian limestones seem much more discontinuous and variable than those along Little Birch Creek.

Fenton and Fenton (1936) visited the outcrops and concurred with Walcott (1914) that the genus Newlandia may be algal in origin and determined that Newlandia concentrica and Newlandia frondosa are really conspecific, as first suggested by Walcott. They determined that the other taxa developed from fracturing of the microspar with later dissolution of the carbonate by groundwater along fracture planes. They found Greysonia basaltica and Copperia tubiformis to be transitional.

Gustadt (1975) considers Greysonia basaltica, Copperia tubiformis, Newlandia major, and Camasia spongia pseudofossils, resulting from

fracturing and weathering of the microspar, and notes the gradational relationship of ropes and plates. Based on his observations of Walcott's collected specimens, and his own field observations, he considers Newlandia frondosa and Newlandia concentrica, as well as Newlandia lamellosa and Kinneyia simulans, transitional forms and dubiofossils. He notes a close resemblance of Newlandia lamellosa to cryptalgalaminate, a mat algal structure described by Aitken (1967).

Gutstadt found no Newlandia frondosa comparable to specimens in Walcott's collection, nor did he find any Camasia spongia. He found a single bed of Newlandia lamellosa and a great deal of Newlandia concentrica, Newlandia major, Greysonia basaltica, and Copperia tubiformis. I found much more Newlandia lamellosa than Gutstadt. From his photographs, location description and observations, he apparently found an isolated occurrence of the structure and never observed the outcrops containing abundant Newlandia lamellosa further up Little Birch Creek.

Forms called by Gutstadt Newlandia concentrica are called by Fenton and Fenton vasiform cone-in-cone structures. However, Fenton and Fenton interpret Newlandia concentrica as an algal form, but show no drawings or photographs of it. Based on the external and internal morphology of these structures, I believe Gutstadt's interpretation of these forms as Newlandia concentrica is consistent with Walcott's original classifications.

Interpretations

I believe these forms developed from pressure solution of microspar. Evidence for this is as follows: Stylolites occur along contacts between ropes, plates, ropes and plates, along laminations in hemispheroids, and between stacks of hemispheroids and stacks of hemispheroids and ovoids. Between ropes and plates, stylolites change into clay seams which contain greatly distorted laminations in some places. Stylolites and clay seams cut primary microspar laminations. The normal offset between adjacent ropes and plates, the rotation of ropes within the beds, and the distortion of preserved laminations in the clay seams indicate compaction of the beds after volume loss due to pressure solution. The gradational relationship between ropes and plates suggests that ropes developed from further pressure solution of plates (Fig. 45). After solution seams developed oblique to bedding to form plates, solution seams developed along laminations in the plates and formed ropes.

The truncation of primary planar microspar laminations by the concentric laminations of ovoids indicates that the concentric laminations are separated by pressure solution boundaries and the light to dark color changes within these secondary laminations result from concentration of insoluble residue along the boundaries. Pressure solution between stacks of hemispheroids is indicated by their stylolitic contacts.

The degree of mottling, and the thickness and orientations of laminations in thinly laminated structures, changes across stylolitic

Figure 45. Evolution of plates and ropes. Solution seams develop oblique to microspar bedding (top) to form plates (center). Further solution and compaction results in disoriented ropes (bottom).

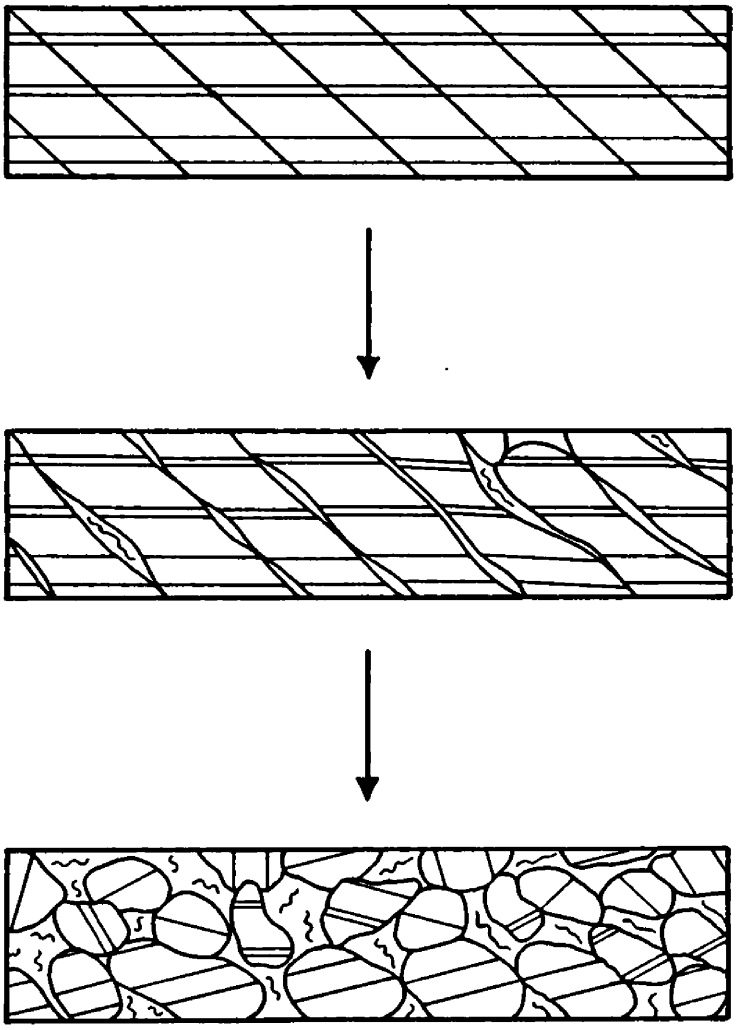

boundaries. This suggests that pressure solution began along the stylolites and continued into the microspar, forming the mottling and thinly laminated structures. The identical composition of mottling, thinly laminated structures, and the clay-rich matrix between many ropes and plates in the black chert-bearing microspar indicate that the mottling and thinly laminated structures result from pressure solution.

Evidence for a pressure solution origin for the rings of frond-like silicified mottling in the Deep Creek section is the concentration of clay in the silicified mottling (Fig. 46) and the gradation of the silicified clay-rich seams downward into stylolites (Fig. 43). The clay-rich oriented mottling separates the microspar into shapes similar to plates and ropes (Fig. 41) and in other places appear similar to thinly-laminated structure.

Tectonic explanations for the origin of ropes and plates do not explain the sinuous intersections of ropes and plates with bedding planes, the normal offset of lamination sets between ropes and curved plates, and the discordance between orientations of ropes and curved plates and the orientations of axial hinges and attitudes of fracture planes. Organic explanations for the origin of the forms do not explain truncation of primary microspar laminations by clay seams between ropes and plates and by concentric laminations of the ovoids, nor do they explain the identical compositions of the matrix between ropes and plates in black chert-bearing microspar and of mottling and thinly-laminated structure. The regularity and even spacing of laminations in

Figure 46. Thin section view of the boundary between microspar (dark) and clay- and insoluble residue-rich silicified mottling (light). Note the greater number of oriented muscovite blades on the right, and the muscovite flake lying across the microspar-mottle boundary. Field of view is 3.84 mm X 2.3 mm, crossed nicols, quartz plate. From silicified rings in Deep Creek Canyon.

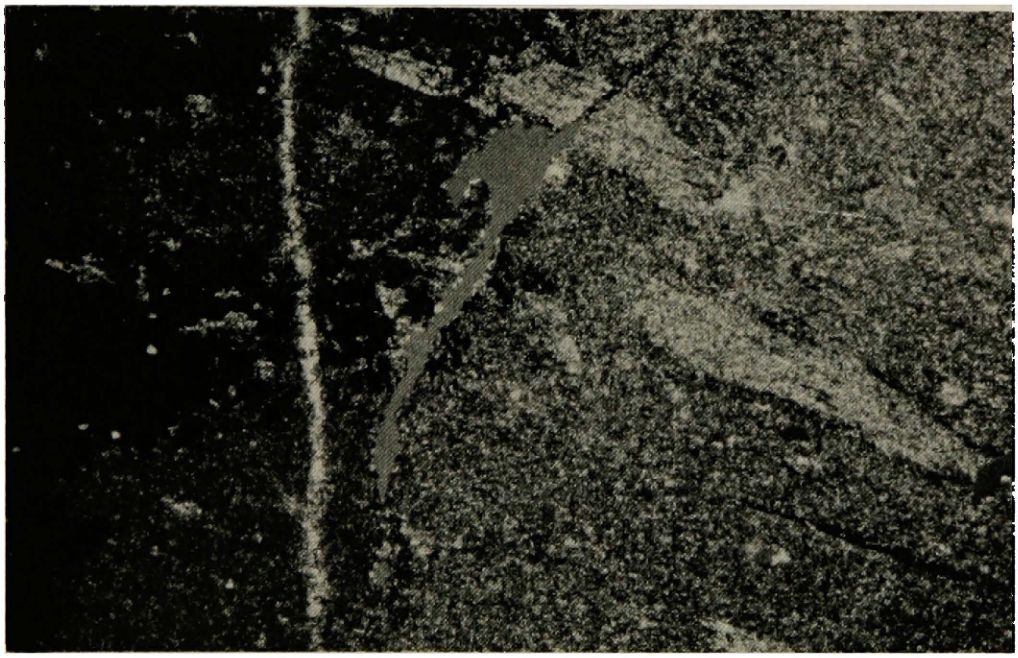

thinly laminated structures and hemispheroids, their lack of organic residues, their lack of crinkled lamination typical in stromatolites, and their association with ropes and plates also suggest an inorganic origin.

Wanless (1979) outlines a variety of features that result from pressure solution and the kinds of carbonate lithologies in which certain features should develop: Pressure solution in clean limestones with structurally resistant elements develop stylolites and grain contact solution sutures (sutured seam solution); in clean limestones without resistant elements pervasive solution and dolomitization results in a randomly mixed fabric of micrite or microspar and dolomite or in extreme cases a vaguely laminated dolomitic zone containing little clay or silt (non-seam solution); and in clayey limestones, microstylolites, microstylolite swarms and clay seams develop (non-sutured seam solution). A clayey limestone with structurally resistant elements will develop mixed suture-glide solution seams. However, the pressure solution forms in the upper Newland show stylolites, clay seams, and mottling, (which appears analagous to non-seam solution) all in the same lithology. Ropes and plates may develop first by non-sutured seam solution, and then act as structurally resistant elements, allowing sutured seam solution to occur where the forms come in contact. The process by which stylolites control mottling and thinly laminated structure is unclear.

As shown in Figure 28, attitudes of curved plates in a single bed may change to the opposite orientation over short lateral distances, and in many places their attitudes alternate back and forth in a sequence of

beds (Fig. 41). Though Wanless (1979) and Bathurst (1979) consider solution plane attitudes oblique to bedding a result of tectonic stress rather than overburden stress, it seems more probable that solution planes which are symmetrical with respect to bedding or a plane vertical to bedding developed from overburden stress. The even spacing of solution planes is enigmatic. Perhaps their spacing became increasingly uniform during pressure solution.

Conclusions

The forms in the Newland gray microspar and black chert-bearing microspar interpreted by Walcott (1914) as organic, by Fenton and Fenton (1936) as both organic forms and forms resulting from goundwater dissolution, and by Gutstadt (1975) as pseudofossils and dubiofossils, resulting in part from fracturing and weathering, are here reinterpreted as pressure solution forms. Solution seams between many of the forms are oblique to bedding, but are either symmetric about a vertical plane, as in plates, or are symmetric about a vertical axis, as in hemispheroids and the cherty frond-like forms in Deep Creek Canyon. For those reasons, they are interpreted to be pressure solution seams that formed in response to overburden stress, rather than tectonic stress. Features called molar-tooth structure and algal structures by Boyce (1975), Verrall (1955), and McMannis (1963) in the Newland carbonates in the Horseshoe Hills and northern Bridger Range are all pressure solution features similar to those in Deep Creek Canyon and in the Little Birch

Creek section. No molar-tooth structure as described by O'Connor (1972) and Eby (1977) occur in any exposed Helena embayment Belt carbonates except those in Chamberlain-like shale in the Neihart and Moose Creek areas and in the lower Newland in the Smith River Section.

CHAPTER V

DIAGENESIS

Pressure Solution

Pressure solution features unlike those discussed in Chapter IV occur in the upper Newland in Unit IV at Little Birch Creek and in Unit VII at Newlan Creek. These two intervals appear nearly identical. Both contain silty microspar beds interbedded with black calcareous shales and some discontinuous silty microspar beds with nodular silty microspar in the intervening shales (Figs. 11, 13). Laminations can be traced from the nodules and terminating beds into the shales. Some nodules are disc-shaped, which seems to preclude a tensional pull-apart mechanism for the development of the discontinuous beds and nodules. Also, detached load structures in the beds indicate that they probably lacked the competency to break apart from each other and would instead have flowed under tensional stress, unless each was cemented before deposition of the overlying bed. In the Newland Creek section, small clots of sand, shaped like saucers or inverted cones, occur in the shale beds between the carbonate beds. My interpretation of these relationships is that the shale interbeds are a result of pressure solution, and that the nodules of silty microspar represent remnants of largely dissolved carbonate beds. The sands in the shales are remnants of sandy ripples or load structures deposited in the now dissolved microspar.

The shaly interval underlying the gray microspar of Unit VI at Little Birch Creek may have developed from pressure solution of a pre-existing carbonate body. Evidence for this is the increased number of limestone nodules in the shale just below the gray microspar, the arrangement of limestone nodules along specific bedding horizons, and the dissimilarity of the fissile gray shale to any of the detrital silty shale in the Newland. Black microspar nodules in the silty shale of Unit V may be the remnants of dissolved microspar beds. Pressure solution of microspar beds in the silty shale intervals may provide the small amount of calcareous cement found in laminated quartz sandstone in the silty shale units, which are otherwise noncalcareous. In places, the black microspar nodules contain silty laminations and ripple cross-laminations, indicating that earlier silty microspar beds have been dissolved away. The surrounding shale contains no sedimentary structures formed by traction transport of silt or sand across a depositional surface.

Dolomitization

The lower Newland and Units I through III are mostly dolomite in the Newlan Creek, Decker Gulch, and Smith River sections, while the overlying units contain very little dolomite. The dolomite consists of interlocking microspar-sized dolomite grains. In more modern rocks, this would suggest very early dolomitization. Dunham and Olson (1980) interpret such a dolomite fabric in the Ordivician-Silurian Hanson Creek Formation of central Nevada as an indication that dolomitization preceded recrystallization of the original carbonate-mud matrix to

impermeable microspar. They believe dolomitization in the Hanson Creek Formation resulted from meteoric water-marine pore water mixing below the meteoric-sediment water interface.

Dolomite is rare in the rest of the Newland sections. In the Little Birch Creek and Deep Creek sections, scattered quartz-replaced dolomite rhombs occur in the carbonate, indicating slight dolomitization followed by silicification of the dolomite.

Silicification

The number of silicification events in the Newland is difficult to establish. The light gray and white cherts in the lower Newland in the Smith River section precipitated very early, as evidenced by their involvement in soft sediment slumping. Chert-cored microspar clasts (Fig. 47) overlying chert lenses in microspar laminations in thinly laminated microspar in Unit IV in Decker Gulch contain dolomite rhombs near their edges (Fig. 48). Walker (1962) reports such textures as good criteria for recognition of dolomite replacement of chert, but Knauth (1979) points out that this may not be true if the water were supersaturated with dolomite during chert precipitation. Silicified dolomitic beds in the lower Newland in the Smith River section indicate silicification after dolomitization.

Calcitization

Some silicified dolomite in the Smith River section contains matrix-supported spar-sized calcite crystals several millimeters in diameter in the aphanitic silicified dolomite matrix. The calcite crystals

Figure 47. Clasts of elongate chert-cored (dark) microspar (light) in a microspar matrix. Clasts may be a result of dissolution of the carbonate layer around them, rather than a result of transport and restacking in so unlikely a position. Field of view is 3.84 mm X 2.3 mm, crossed nichols. Unit IV, Decker Gulch section.

Figure 48. Microspar-sized dolomite rhombs in a chert nodule from Unit III, Decker Gulch section. Field of view is 2.4 mm X 1.44 mm, plain light

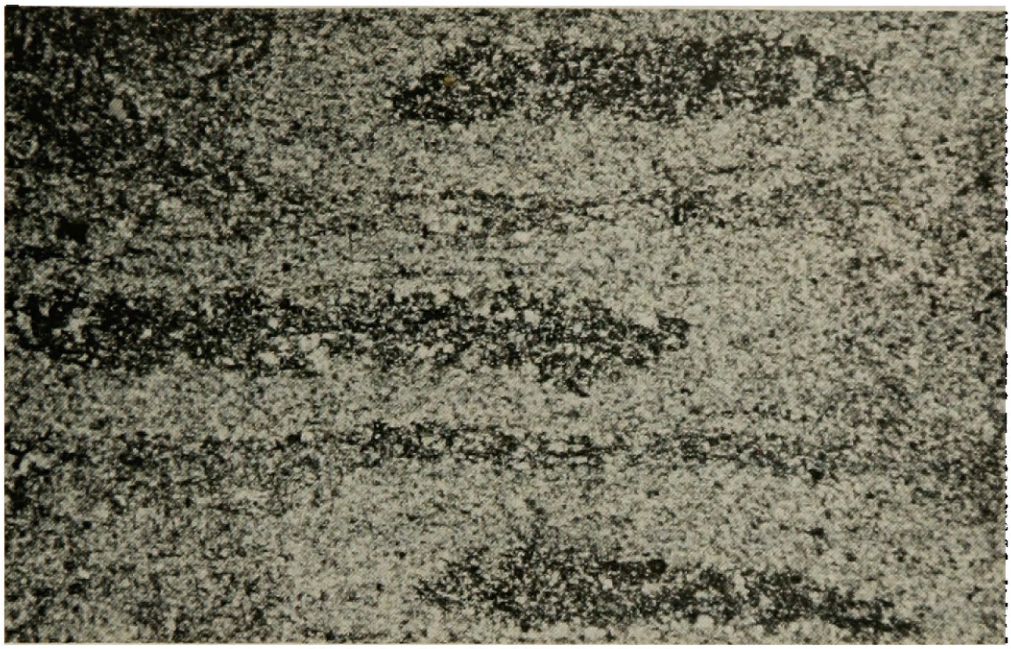

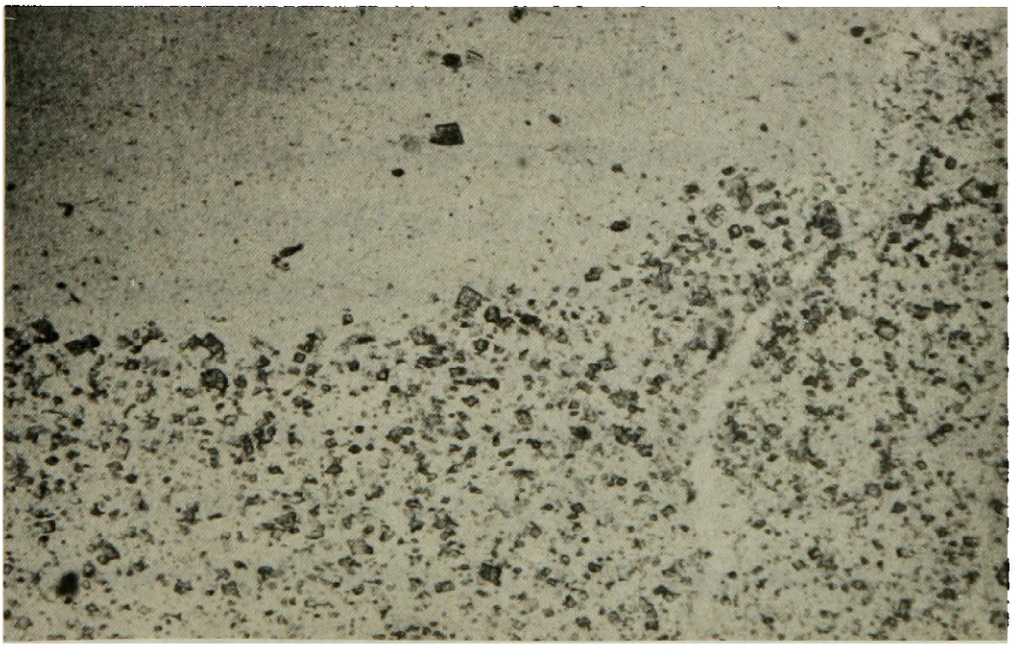

comprise up to 10% of the rock where they occur, and in hand sample, the rock appears oolitic. Adjacent sparite crystals are typically optically continuous and many appear rhomb-shaped. They probably represent a late dedolomitization event.

Diagenetic Relationships at Little Birch Creek

The most abundant and complex diagenetic textures involving silicification and dolomitization are associated with the pressure solution features in Unit III in the Little Birch Creek section. Here, black chert forms the matrix between many of the ropes and plates, but in many places abruptly changes to a clay-rich matrix (Fig. 32) or a radialaxial calcite matrix. Fractures within the ropes and curved plates are filled with granoblastic quartz. Granoblastic quartz seldom occurs in the matrix, except in a few places in the chert. The ropes and plates have rims of radialaxial calcite up to 5 mm thick which is similar to radialaxial that described by Bathurst (1959, 1979) (Figs. 32, 49). The radialaxial calcite is further rimmed by feathery fibrous calcite crystals which are often uniformly oriented at low angles to the surface of the radialaxial calcite rim. In some places, growth of granoblastic quartz in fractures has forced the radialaxial calcite rims out into the cherty matrix (Fig. 50), indicating that either the chert was pliable during growth of granoblastic quartz, or that the matrix was some other pliable material later replaced by chert.

Both microspar- and spar-sized rhomb-shaped calcite crystals with ragged edges occur in the chert (Fig. 51). These appear to be

Figure 49. Radialaxial calcite rimming microspar in a chert (light) matrix. Unit III, Little Birch Creek section. Field of view is 3.84 mm X 2.3 mm, plain light.

Figure 50. Growth of granoblastic quartz in radialaxial calcite rimming a microspar plate has forced part of the radialaxial calcite rim into the plastic matrix, which is now chert (dark). Field of view is 3.84 mm X 2.3 mm, crossed nicols, Unit III, Little Birch Creek section.

Figure 51. Microspar-sized and spar-sized rhombs of calcite in chert, indicating dedolomitization. Field of view is 3.84 mm X 2.3 mm, plain light, Unit III, Little Birch Creek section.

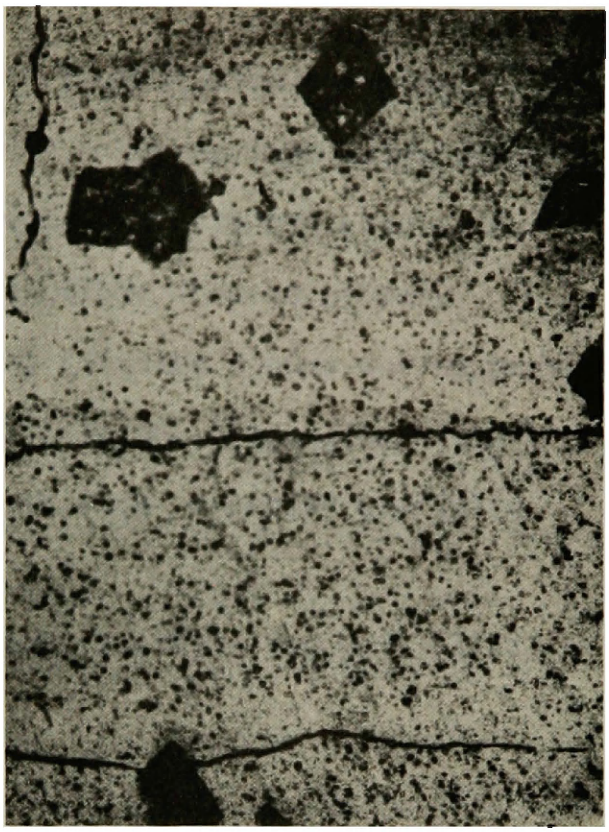

pseudomorphs after dolomite and may result from dedolomitization. Supporting evidence for dedolomitization is a strong iron oxide stain on many bedding plane surfaces. Also associated with the cherts are a few clots of medium-grained sand. These clots show no primary structure and were probably isolated along solution planes during pressure solution. The presence of chert very early in the diagenetic history of Unit III is evidenced by chert grains in sand directly overlying the unit.

A possible sequence of complex diagenetic events for Unit III at Little Birch Creek is as follows:

1) Early silicification
2) Neomorphism + pressure solution $\pm$ dolomitization; the timing of neomorphism is unclear, but it seems reasonable for it to accompany pressure solution, and the intimate association of dolomitization and pressure solution has been pointed out by Wanless (1979).
3) Development of radialaxial calcite rims on the pressure solution forms, with a later feathery calcite growth on these.
4) Growth of gransblastic quartz in fractures in the ropes and curved plates.
5) Final silicification resulting in black chert between the pressure solution forms.

6) Dolomitization of some of the chert, producing some spar-sized dolomite crystals.
7) Dedolomitization of the rhombs in the chert, perhaps as a result of weathering of the outcrops.

Interpretation

General interpretations for Newland Limestone diagenesis are as follows. Silicification was in some places very early. Dolomitization was pervasive along the northern edge of the basin and was probably also very early. An evaporite-related model for dolomitization in the Newland does not fit the data well, because evidence for extensive evaporites in the Newland is lacking, and because the dolomitization occurred in sediments below wave base. It has been shown by Baker and Kastner (1980) that dolomite will form from calcite in the absence of dissolved silica and SO_4^- and in the presence of abundant dissolved Mg^{+2}. They infer that the microbial reduction of sulfate in organic-rich sediments accelerates dolomite precipitation. If the pore fluids of the Newland sediments were either low in sulfate or if much of the sulfate were being reduced, and if silica was precipitated as a sufficient rate, then the Newland may have been pervasively dolomitized by Mg^{+2} ions replacing Ca^{+2} ions in the calcite.

Dorag dolomitization (dolomitization by the mixing of fresh water and seawater described by Hanshaw and others, 1971, Land, 1973, and Badiozamani, 1973) may account for dolomitization in the northern Newland sections. Undoubtedly, some fresh water was introduced by the embayment

along its northern margins, but the composition of the basinal waters remains in question. This model does not explain why the uppermost Newland units were not dolomitized.

The degree of silicification also decreases basinward. Very little chert occurs in the Deep Creek section. In the Birch Creek section, chert is abundant in Unit III, but is nearly absent in the other units. Silicification in the northern sections is more pervasive, resulting in chert in the lower Newland, in Unit III and to some extent in Unit IV. It is interesting to note that increased silica precipitation occurred in areas of increased dolomite formation. This favors the model of Baker and Kastner (1980) for dolomitization of the Newland sediments.

Knauth (1979) has proposed a model for chert replacement of carbonates by marine-meteoric water mixing much like that proposed for dolomitization by Hanshaw and others (1971), Land (1973), and Badiozamani (1973). In his model, he suggests that meteoric water moving through carbonate sediments along a coast would become increasingly saturated with silica due to dissolution of silicic biogenic materials. During mixing of this water with seawater, the waters become supersaturated with silica and undersaturated with calcium carbonate. Under these conditions, silica will replace the carbonate sediments, forming chert nodules, and dolomite will precipitate. Forster (1977) describes a similar process for joint dolomitization and silicification of the Ordivician Manitou Formation in Colorado. Such a model could

account for the increased dolomite and silica in the Newland along the northern edge of the embayment.

Removal of the silica from the waters around and below the sediment-water interface might allow dolomite precipitation if sulfate in the system were reduced, as shown by Baker and Kastner (1980). Dolomite would also be readily precipitated by the Dorag model together with the silica, as Forster (1977) and Knauth (1979) suggest.

Discoid Nodules

The origin of the discoid nodules of radiating fibrous calcite with cone-in-cone structure in Unit IV exposed in the head of Lake Creek east of the Newlan Creek section is unclear. Their centers consist of anomolous structures, such as sand lenses, interrupting the carbonate laminations. In some places, the sand appears to have intruded the laminated carbonate, and may have been the result of a sand dike piercing the carbonate laminations. The size of the fibrous calcite crystals increases outward from microspar size in the nodule centers to elongate crystals over 1 cm long on the nodule edges. Crystal sizes abruptly double across well-defined boundaries concordant to the nodule shape. Most boundaries are marked by very thin discontinuous clay seams which also occur along the cone-in-cone fracturing. Where original laminations are visible, some appear spread apart by the growth of the fibrous crystals.

Nodules of radiating, fibrous black calcite occur in the lower Newland in the Wagner Gulch area in the Big Belt Mountains. These are

flat on the bottom, and are shaped like the upper hemisphere of a discoid nodule. All occur as float, and so may have been broken. Crystals are roughly the same size throughout the nodule and reach sizes of over 1 cm in length. Cone-in-cone fracturing is superimposed on the radiating structure. In some nodules, deformed but continuous shale laminations are trapped within the structure and are roughly concordant with the shape of the nodule. The degree of cone-in-cone fracturing characteristically changes on either side of the trapped laminations. The outsides of the nodules often have a fibrous white calcite coating with the long axes of the crystals normal to the nodule surface and in apparent crystallographic continuity with the fibrous black calcite. The contact between the black and white calcite aggregates is very even and sharp. The white calcite is probably a secondary growth on the nodule surfaces.

In Deep Creek canyon in the lower Newland, fibrous black calcite occurs in thin layers parallel to shale bedding with the long axes of the calcite crystals perpendicular to bedding. In some places, the upper or lower one-half of a layer may consist of fibrous white calcite with identical structure. At the junction of the Castle Fork and the Russel Fork of Deep Creek, pyrite-bearing aggregates of radiating fibrous black calcite occur as pods along both shale bedding and in fractures. The occurrence of the calcite along the fractures indicates a post-tectonic origin for the black calcite.

Whether or not the black calcite nodules in the lower Newland are related to those in Unit IV is unclear. Important differences are the

color of the calcite, the variation in fibrous calcite grain sizes in the Univ IV nodules as opposed to relatively uniform grain sizes in the black calcite nodules, the presence of structural anomalies in the centers of the nodules in Unit IV, and the types of occurrences.

The nodules in Unit IV may have a late origin like the nodules in the lower Newland, or may result from calcite replacement of evaporite nodules, or may be a result of introduction of waters supersaturated with calcium carbonate and subsequent fibrous calcite growth around structural anomalies with the laminated carbonates relatively early in diagenesis, as suggested by the deformation of the laminations.

Conclusions

Diagenesis of the Newland Limestone involved pressure solution of the microspar intervals, pervasive dolomitization along the northern margin of the embayment, perhaps several silicification events, and some dedolomitization.

The small grain size and texture of the dolomite and the incorporation of chert into transported sands and slumps indicate that dolomitization and silicification may have occurred quite early in the diagenetic history of the Newland. Dolomitization and silicification were both most pervasive along the embayment's northern margin, suggesting that they may have resulted from meteoric water-embayment water mixing.

The black chert-bearing microspar in the Little Birch Creek section records a complex diagenetic history involving pressure solution,

dolomitization, silicification, calcite recrystallization and dedolomitization. Further study is required to unravel the timing and complexities of diagenesis of the Newland Limestone.

REFERENCES

Aitken, J.P., 1967, Classification and environmental significance of cryptalgal limestones and dolomites with illustrations from the Cambrian and Ordivician of southwestern Alberta: Jour. Sed. Petrology, v. 37, p. 1163-1178.

Alexander, R.G., 1955, Geology of the Whitehall area, Montana: Yellowstone-Bignorn Research Project, Contribution 195, 107 p.

Badiozamani, K., 1973, The Dorag dolomitization model-Application to the Middle Ordivician of Wisconsin: Jour. Sed. Petrology, v. 43, p. 965-984.

Baker, P.A., and Kastner, M., 1980, The origin of dolomite in marine sediments: Geol. Soc. America Abs. with Programs, v. 12, no. p. 381-382.

Barthurst, R.G., 1979, Carbonate Sediments and their Diagenesis: Developments in Sedimentology 12, 2nd. ed., Elsevier Scientific.

Bathurst, R.G., 1959, The cavernous structure of some Mississippian Stromatactis reefs in Lancashire, England: Jour. Sed. Petrology, v. 67, p. 506-521.

Billings, M.P., 1972, Structural Geology, Prentice-Hall.

Birkholz, D.O., 1967 Geology of the Camas Creek area, Meagher County, Montana: M.S. thesis, Montana College of Mineral Science and Technology.

Blatt, H., Middleton, G.V., and Murray, R.C., 1980, Origin of Sedimentary Rocks, 2nd. ed., Prentice-Hall.

Bonnett, A., 1979, Depositional sequences and sedimentary-tectonic implications of the limestone-rich interval of the LaHood Formation (Precambrian Y), southwestern Montana: Geol. Soc. America Abs. with Programs, v. 11, no. 6, p. 266-267.

Boyce, , 1975, Depositional systems in the LaHood Formation, Belt Supergroup, Precambrian, southwestern Montana: Ph.D. dissertation, University of Texas at Austin.

Burwash, R.A., Baadsgaard, H., and Peterman, Z.E., 1962, Precambrian K-Ar dates from the western Canada sedimentary basin: Jour. Geophys. Res., v. 67, no. 4, pp. 1617-1625.

Catanzaro, E.J., and Kulp, J.L., 1964, Discordant zircons from the Little Belt (Montana), Beartooth (Montana), and Santa Catalina (Arizona) Mountains: Geochim. Cosmochim. Acta, v. 28, pp. 87-124.

Dahl, G.G., Jr., 1971, General geology of the area drained by the North Fork of the Smith River, Meagher County, Montana: M.S. thesis, Montana College of Mineral Science and Technology.

Dunham, J.B., and Olson, E.R., 1980, Shallow subsurface dolomitization of subtidally deposited sediments in the Hanson Creek Formation (Ordivician-Silurian) of central Nevada: Soc. Ec. Paleon. Mineralogists Spec. Pub. no. 28, pp. 139-161.

Eby, D.E., 1977, Sedimentation and early diagenesis within eastern portions of the 'Middle Belt Carbonate Interval' (Helena Formation), Belt Supergroup (Precambrian Y), western Montana: Ph.D. dissertation, State University of New York at Stoney Brook.

Fenton, C.R., and Fenton, M.A., 1936, Walcott's "Pre-Cambrian Algonkian algal flora" and associated animals: Geol. Soc. America, Bull., v. 47, p. 609-620.

Folk, R.L., 1974, Petrology of Sedimentary Rocks, Hemphill Publishing Co., Austin, Texas.

Forster, J.R., 1977, Diagenesis of the lower Ordivician Manitou Formation, El Paso County, Colorado: M.S. Thesis, University of Montana.

Giletti, B.J., 1966, Isotopic ages from southwestern Montana: Jour. Geophys. Research, v. 71, no. 16, p. 4029-4036.

Glaessner, M.F., 1962, Pre-Cambrian fossils: Cambridge Phil. Soc., Cambridge, England, Biol. Reviews, v. 37, p. 467-494.

Groff, S.L., 1967, A summary description of geology in the Smith River Valley, Meagher Co., Montana: Montana Geol. Soc., 18th Ann. Field Conf., Guidebook.

Gutstadt, A.M., 1975, Pseudo- and dubiofossils from the Newland Limestone (Belt Supergroup, Late Precambrian), Montana: Jour. Sed. Petrology, v. 45, no. 2, p. 405-414.

Hanshaw, B.B., Back, W., and Deike, R.G., 1971, A geochemical hypothesis for dolomitization by groundwater: Econ. Geology, v. 66, p. 710-724.

Harrison, J.E., 1972, Precambrian Belt basin of the northwestern United States: Its geometry, sedimentation, and copper occurrences: Geol. Soc. America, Bull., v. 83, no. 5, p. 1215-1240.

Hayden, R.J. and Wehrenberg, J.P., 1960, A^{40}-K^{40} dating of igneous and metamorphic rocks in western Montana: Jour. of Geology, v. 68, no. 1, pp. 94-97.

Hawley, D., 1973, Sedimentary environment of the LaHood Formation, a southeastern facies of the Belt supergroup, Montana, in Belt Symposium 1973, Idaho Bur. Mines and Geology, 322 p.

Hoffman, J., and Hower, J., 1979, Clay mineral assemblages as low grade metamorphic geothermometers: Application to the thrust faulted disturbed belt of Montana, U.S.A.: in Aspects of Diagenesis, SEPM Spec. Pub. No. 26, p. 55-79.

Holtedahl, O., 1921, On the occurrence of structures like Walcott's Algonkian algae in the Permian of England: Amer. Jour. Sci., ser. 5, v. 1, p. 195-206.

Horodyski, R.J., 1980, Middle Proterozoic shale-facies microbiota from the lower Belt Supergroup, Little Belt Mountains, Montana: Jour. Paleontology, v. 54, no. 4, p. 649-663.

Hruska, D.C., 1967, Geology of the Dry Range area, Meagher County, Montana: M.S. thesis, Montana College of Mineral Science and Technology.

Keefer, W.R., 1972, Geologic map of the west half of the Neihart quadrangle, Montana: U.S. Geol. Survey Misc. Geol. Inv. Map I-726.

Klemme, H.D., 1949, The geology of the Sixteenmile Creek area, Montana: Ph.D. dissertation, Princeton University.

Knauth, L.P., 1979, A model for the origin of chert in limestone: Geology, v. 7, p. 274-277.

Land, L.S., 1973, Contemporaneous dolomitization of middle Pleistocene reefs by meteoric water, North Jamaica: Bull. of Marine Science, v. 231, p. 64-91.

McClernan, H.G., 1969, Geology of the Sheep Creek area, Meagher County, Montana: M.S. thesis, Montana College of Mineral Science and Technology.

McIlreath, I.A., and James, N.P., 1979, Carbonate Slopes: in Facies Models, Geoscience Canada, Reprint Series 1.

McMannis, W.J., 1963, LaHood Formation - A coarse facies of the Belt series in southwestern Montana: Geol. Soc. America Bull., v. 74, p. 407-436.

McMannis, W.J., 1952, Geology of the Bridger Range area: Ph.D. dissertation, Princeton University.

_____, 1955, Geology of the Bridger Range, Montana: Geol. Soc. America Bull., v. 66, p. 1385-1430.

Maxwell, D.T., 1964, Diagenetic-metamorphic trends of layer silicates in the Precambrian Belt series: Ph.D. dissertation, University of Montana.

_____ and Hower, J., 1967, High-grade diagenesis and low-grade metamorphism of illite in the Precambrian Belt Series: Am. Mineralogist, v. 52, nos. 5-6, pp. 843-857.

Mertie, J.B., Fisher, R.P., and Hobbs, S.W., 1951, Geology of the Canyon Ferry quadrangle, Montana: U.S. Geol. Survey Bull. 972.

Nelson, W.H., 1963, Geology of the Duck Creek Pass quadrangle, Montana: U.S. Geol. Survey Bull. 1121-J.

Obradovich, J.D., and Peterman, Z.E., 1968, Geochronology of the Belt Series, Montana: Canadian Jour. Earth Sci., v. 5, no. 3, pt. 2, pp. 737-747.

O'Connor, M.P., 1972, Classification and environmental interpretation of the Cryptalgal organosedimentary "Molar-Tooth" structure from the later Precambrian Belt-Purcell Supergroup: Jour. Geology, v. 80, p. 592-610.

Phelps, G.B., 1969, Geology of the Newlan Creek area, Meagher County, Montana: M. S. thesis, Montana College of Mineral Science and Technology.

Raymond, P.E., 1935, Precambrian life: Geol. Soc. America Bull., v. 46, p. 375-392.

Reineck, H.E., and Singh, I.B., 1980, Depositional Sedimentary Environments, 2nd ed., Springer-Verlag.

Reynolds, M.W., 1979, Character and extent of basin-range faulting, western Montana and east-central Idaho: RMAG-UGA 1979 Basin and Range Symposium.

_____ and Lindsey, D.A., 1979, Eastern extent of the Proterozoic Y Belt basin, Montana: U.S. Geol. Survey Prof. Paper 1150, p. 68.

Skipp, B., and Peterson, A.D., 1965, Geologic map of the Maudlow quadrangle, southwest Montana: U.S. Geol. Survey Misc. Inv. Geol. Map I-452.

Smith, A.G. and Barnes, W.C., 1966, Correlation of and facies changes in the carbonaceous, calcareous, and dolomitic formations of the Precambrian Belt-Purcell Supergroup: Geol. Soc. America Bull., v. 77, no. 12, p. 1399-1426.

Sosman, R.B., 1927, The Properties of Silica, New York.

Till, R., 1978, Arid shorelines and evaporites, in Sedimentary Environments and Facies, H.G. Reading, ed., Blackwell Scientific.

Velde, B., 1965, Experimental determination of muscovite polymorph stabilities: Am. Mineralogist, v. 50, p. 436-449.

Verrall, P., 1955, Geology of the Horseshoe Hills area, Montana: Ph.D. dissertation, Princeton University.

Walcott, C.D., 1914, Cambrian geology and paleontology, III, no. 2, Pre-Cambrian Algonkian algal flora: Smithsonian Misc. Collections, v. 64, no. 2, pp. 77-140.

_____, 1899, Pre-Cambrian fossiliferous formations: Geol. Soc. America Bull., v. 10, p. 199-244.

Walker, T.R., 1962, Reversible nature of chert-carbonate replacement in sedimentary rocks: Geol. Soc. America Bull., v. 73, pp. 237-242.

Walter, M.R., Oehler, J.H., and Oehler, D.Z., 1976, Megascopic algae 1300 million years old from the Belt supergroup, Montana: A reinterpretation of Walcott's Helminthoidichnites: Jour. Paleontology, v. 50, pp. 872-881.

Wanless, H.R., 1979, Limestone response to stress: pressure solution and dolomitization: Jour. Sed. Petrology, v. 49, no. 2, pp. 437-462.

Weed, W.H., 1900, Geology of the Little Belt Mountains, Montana: U.S. Geol. Survey Ann. Report, v. 20, pt. 3, p. 257-461.

_____, 1899, Little Belt Mountains, Montana: U.S. Geol. Survey Folio 56.

_____ and Pirsson, L.V., 1896, Geology of the Castle Mountains mining districts: U.S. Geol. Survey Bull. 139.

Winston, D., Jacobs, P., Baldwin, D., and Reid, J., Late Precambrian faulting in the Belt Basin, Montana and Idaho, and its effects on Cretaceous and Tertiary thrusting: unpublished.

Woodward, L.E., 1981, Tectonic framework of disturbed belt of west-central Montana: American Assoc. Petrol. Geologists Bull., v. 65, no. 2, pp. 291-302.

Yoder, H.S., and Eugster, H.P., 1955, Synthetic and natural muscovites: Geochim. Cosmochim. Acta, v. 8, pp. 225-280.

APPENDIX I

SECTION LOCATIONS

Location of sections (Fig. 2 in text) are as follows:

Newlan Creek section -- center and south center of section 29, R. 7 E., T. 11 N.; Coxcombe Butte and Charcoal Gulch 7.5 minute quadrangles, on the west side of U. S. Highway 89. This is the Newland Limestone type section of Walcott (1899). The area has been mapped by Phelps (1969).

Decker Gulch section -- east 1/2 of section 7, R. 6 E., T. 11 N.; Whitetail Reservoir 7.5 minute quadrangle. This area has been mapped by Phelps (1969).

Smith River section -- west 1/2 of section 1, R. 4 E., T. 11 N.; Fort Logan 7.5 minute quadrangle, bluff on the west side of the Smith River. This area has been mapped by Hruska (1967).

Little Birch Creek section -- SW 1/4 of section 15, NE 1/4 of section 21, NE 1/4 of section 16, and SW 1/4 of section 22, R. 5 E., T. 9 N.; Hanson Reservoir 7.5 minute quadrangle, cliffs on east side of Little Birch Creek, ridge between Little Birch Creek and Big Birch Creek, and the butte to the south. The geology of this area is unmapped.

Deep Creek section -- from the center of the SE 1/4 of section 30 eastward to the center of section 29, R. 4 E., T. 7 N.; Duck Creek Pass 15 minute quadrangle, along the north side of U. S. Highway 12. This area is mapped by Nelson (1963).

APPENDIX II

1. Tan calcareous shale

   Mineralogy and texture: equidimensional microspar-sized calcite and/or dolomite, illite ± chlorite, and scattered quartz, feldspar, and muscovite silt grains.

   Color: gray on fresh break, tan and gray weathering.

   Bedding: thinly- to thickly-laminated (< 0.3 cm to 0.5 cm).

   Comments: This rock type comprises most of the lower Newland. Carbonaceous films occur parallel to bedding planes.

2. Black calcareous shale

   Mineralogy and texture: microspar-sized calcite, clay and scattered quartz, feldspar, and muscovite silt grains.

   Color: black and dark gray both on fresh and weathered surfaces.

   Bedding: thinly- to thickly-laminated (<0.3 to .5 cm); fissil in some places.

   Comments: Interbedded with microspar layers and often grades laterally into microspar nodules and discontinuous beds.

3. Gray shale

   Mineralogy and texture: illite ± chlorite, scattered quartz, feldspar, and muscovite silt grains.

   Color: medium to dark gray on fresh and weathered surfaces.

   Bedding: thinly laminated (<0.3 cm); usually fissile.

   Comments: Generally occurs adjacent to microspar intervals and in places contains black microspar nodules. However, this rock type also occurs in the lower Newland in the Smith River section.

4. Silty shale

Mineralogy and texture: illite ± chlorite, quartz, feldspar, muscovite, and minor biotite silt and some sand grains. Composition ranges from clay rich to silty or sandy.

Color: Generally gray on a fresh break, and brown, gray, rusty, and green weathering. In places laminations alternate from light pink to light green.

Bedding: generally thinly- to thickly-laminated (0.2 cm to 1 cm) graded silt-to-clay couplets; where sandy, the bedding is wavy to lenticular (Reineck and Singh, 1980), and sandstone lenses are ripple cross-laminated.

Comments: This shale is identical to shale in much of the Greyson. Other sedimentary structures are load structures. The shale contains carbonaceous films parallel to lamination planes.

5. Black shale

Mineralogy and texture: illite, chlorite ± kaolinite (Maxwell and Hower, 1967); scattered quartz, feldspar, and muscovite silt grains.

Color: black to dark gray on a fresh break, weathers black to dark greenish gray.

Bedding: thinly- to thickly-laminated (0.2 to 1 cm); laminations are wavy and irregular.

Comments: Carbonaceous films occur parallel to black shale laminations. This rock type comprises all Belt shale in the

Neihart area in sections described as Chamberlain, Newland, and Greyson by Walcott (1899) and Keefer (1972) and in addition Spokane by Weed (1900).

6. Red shale

Mineralogy and texture: illite ± chlorite, iron oxides, and in places high percentages of microspar-sized calcite.
Color: red on fresh and weathered surfaces.
Bedding: thinly- to thickly-laminated ($\lesssim$0.3 cm to .5 cm).
Comments: This rock type occurs only interlaminated with tan calcareous shale. In Unit II in the Little Birch Creek section, red shale and white shale of identical composition but lacking iron oxides occur together.

7. Dolomitic mudstone

Mineralogy and texture: microspar-sized dolomite with scattered clay and quartz and feldspar silty grains.
Color: tan and gray on both fresh and weathered surfaces.
Bedding: thinly- to thickly-laminated (0.1 cm to 1 cm).
Comments: Dolomitic mudstone is a lower Newland lithology exposed only in the Smith River section. The mudstone lacks the shaly parting characteristic of tan calcareous shale, and instead weathers into blocky fragments. It contains gray laminated chert nodules and lenses, and laminations rich in matrix-supported gray chert sand grains. The mudstone contains many soft sediment folds.

8. Green claystone

Mineralogy and texture: illite and chlorite with muscovite, quartz, and tourmaline silty grains, and some pyrite cubes up to 0.5 cm in diameter.

Color: dark green on a fresh bread, and dark green, brown and rusty weathering.

Bedding: generally medium- to thickly-bedded (20 cm to 40 cm), but in some places thickly-laminated (0.3 cm to 1 cm).

Comments: This rock type is exposed only in the Deep Creek area in the lower Newland. The claystone contains carbonaceous films parallel to bedding. Pyrite cubes are numerous along fracture planes and account for the rusty weathering.

9. Black siltstone

Mineralogy and texture: illite $\pm$ chlorite with scattered quartz and muscovite silt grains.

Color: black on fresh and weathered surfaces.

Bedding: thinly- to thickly-laminated (0.1 cm to 1 cm).

Comments: Black siltstone appears identical to green claystone in thin section, but, in addition to its color, contains a higher percentage of silt grains. Black siltstone is exposed only in the lower Newland of the Deep Creek area.

10. Gray microspar

Mineralogy and texture: equidimensional microspar-sized calcite with scattered quartz, feldspar, muscovite, and biotite silt grains and clay aggregates. Calcite comprises more than 95% of the rock. In some places, the microspar is dolomitic.

Color: dark gray on a fresh break, light gray weathering.

Bedding: thinly bedded (6 cm to 8 cm); thin beds are themselves thinly to thickly laminated (0.2 cm to 1 cm). In a few places, silt-rich laminations are finely ripple cross-laminated.

Comments: This rock type is characteristic of the upper Newland and in many places contains pressure solution features.

11. Black chert bearing microspar

Mineralogy and texture: equidimensional microspar-sized calcite and/or dolomite with scattered quartz, feldspar, muscovite, and minor biotite silt grains, and clay aggregates.

Color: dark gray on fresh and weathered surfaces when calcite; medium gray on afresh break and light brown or gray weathering when dolomitic.

Bedding: thickly-laminated to thin bedded (0.5 to 6 cm).

Comments: Dolomite comprises from 0 to 100% of the carbonate content regionally. Black chert nodules are everywhere present. Pressure solution features are numerous where nondolomitic.

12. Silty microspar

Mineralogy and textures: equidimensional or elongate microspar-sized calcite with quartz, feldspar, muscovite, and minor biotite silt grains and silt-sized clay aggregates. Slightly dolomitic in some places.

Color: dark gray on a fresh break; tan and gray weathering.

Bedding: thinly to thickly bedded (1 cm to 25 cm) with thin to thick laminations (0.2 to 1 cm); laminations typically grade upward from silty bottoms to microspar tops. Many beds contain 1 cm to 6 cm sets of fine cross laminations.

Comments: Beds of silty microspar are separated by interbeds of black calcareous shale or tan calcareous shale where thicker bedded. Carbonaceous films occur parallel to bedding planes. In a few places, small black chert nodules occur along bedding.

13. Black laminated microspar

Mineralogy and texture: equidimensional microspar-sized calcite containing scattered quartz, feldspar, muscovite, and clay aggregate silt grains.

Color: Black on fresh and weathered surfaces.

Bedding: thinly to thickly laminated (0.2 cm to .8 cm) thin beds (4 cm to 8 cm).

Comments: Black laminated microspar contains carbonaceous films parallel to bedding, and overlies silty microspar in Unit IV in the Little Birch Creek section.

14. Nodular black microspar

Mineralogy and texture: equidimensional to elongate microspar-sized calcite with scattered quartz, feldspar, muscovite, and clay aggregate silt grains.

Color: black to dark gray on a fresh break; dark to rusty brown weathering.

Bedding: nodular; nodules are thin to thickly laminated (0.2 cm to 1 cm).

Comments: Nodular black microspar occurs in silty shales widely scattered in gray shale and silty shale.

15. Black dolomite

Mineralogy and texture: microspar-sized dolomite with scattered quartz and clay aggregate silt grains; silicified.

Color: black on a fresh break; dark brown or gray weathering.

Bedding: medium to thickly bedded (10 cm to 40 cm).

Comments: Black dolomite occurs with molar tooth-bearing dolomite in the Smith River section.

16. Molar tooth-bearing dolomite

Mineralogy and texture: microspar-sized dolomite with scattered quartz and feldspar silt grains. In many places, contains ribbons and pods of mosaically-textured microspar-sized calcite (molar tooth structure; O'Connor, 1972; Eby, 1977).

Color: dark gray on a fresh break, and tan, yellowish tan, and light gray weathering; molar tooth structure is dark gray.

Bedding: thin to thick bedded (8 cm to 35 cm).

Comments: Molar tooth-bearing dolomite is exposed only in the lower Newland in the Smith River section and in exposures underlying the lower Newland and overlying the Chamberlain Shale.

17. Intrasparite

Mineralogy and texture: microspar-sized calcite and/or dolomite intraclasts in a sparry calcite matrix with small amounts of quartz, feldspar, muscovite, biotite, and chert silt and sand grains, and ooids.

Color: dark gray on a fresh break, tan and light gray weathering.

Bedding: bedding is lenticular; intraclasts are imbricated in some places.

Comments: Intraclasts are coarse sand- to pebble-sized, and are generally associated with small amounts of calcitic quartz sandstone in silty microspar. Some of the intraclasts contain or consist wholly of molar tooth structure.

18. Sandy sparite

Mineralogy and texture: over 50% sparry calcite and/or dolomite matrix containing fine- to medium-sand grains of quartz with small amounts of microcline, orthoclase, plagioclase, muscovite, biotite, chert, ooids, and molar tooth structure clasts.

Color: medium gray on a fresh break; light gray to light tan weathering.

Bedding: generally thickly laminated to thinly bedded (015 cm to 4 cm).

Comments: This rock type comprises the megaripple at the base of Unit VII in the Little Birch Creek section.

19. Calcitic quartz sandstone

Mineralogy and texture: rounded fine- to medium-grained sand composed of quartz with small amounts of orthoclase, microcline, plagioclase, muscovite, biotite, zircon, metamorphic rock fragments, ooids, and in some cases chert, generally matrix-supported in 15 to 50% sparry calcite and/or dolomite matrix.

Color: gray on a fresh break; light gray or tan weathering.

Bedding: lenticular or thinly laminated to thickly bedded (0.2 cm to 60 cm).

Comments: This rock type is characteristic of turbidites throughout the Newland and is also contained in silty microspar.

20. Laminated quartz sandstone

Mineralogy and texture: rounded to angular very fine to fine sand-sized grains of quartz with smaller amounts of feldspar, muscovite, and biotite; grains are grain supported; matrix is clay, calcite, and in places iron oxide.

Color: black, brown, and light gray on both fresh and weathered surfaces.

Bedding: thinly laminated to thinly bedded (0.2 cm to 5 cm) beds (6 cm to 10 cm). Laminations and thin beds are generally straight and evenly spaced.

Comments: Black laminations contain clay and carbonaceous cement, brown laminations contain iron oxide cement, and gray ones contain calcite cement. Beds of laminated quartz sandstone occur in silty shale and are widely spaced.

21. Quartz sandstone

Mineralogy and texture: medium-grained sand to pebble-sized grains of quartz, and smaller amounts of feldspar and metamorphic rock fragments with scattered patches of clay and calcite cement; overgrowths on the grains fill most of the original space between grains.

Color: gray to white on fresh break; gray weathering.

Bedding: medium to thickly bedded (12 cm to 40 cm) with some cross-laminations; beds fine upward.

Comments: The sand grains were probably matrix supported prior to overgrowth development. This sandstone occurs only in the lower Newland in the Smith River section.

22. Gray laminated chert

Mineralogy and texture: dominantly chert with inclusions of quartz and feldspar silt grains, microspar-sized dolomite, clay and muscovite flakes, and carbonaceous films; chert shows a preferred orientation of microcrystalline quartz grains resulting in a fibrous appearance and optical continuity; optical characteristics match those of lutecite (Sosman, 1927) with the exception that this chert show a negative optic sign, rather than the positive sign described by Sosman for lutecite.

Color: gray to white

Bedding: nodular and lenticular; thin to thick laminations (0.1 cm to 1 cm) are defined by silt concentrations and carbonaceous films.

Comments: This chert occurs only in dolomitic mudstone in the lower Newland of the Smith River section. Sand grains of the chert are matrix supported along some mudstone laminations.

23. Black chert

Mineralogy and texture: chert with inclusions of muscovite and microspar-sized calcite and dolomite grains, and in some places clots of quartz, feldspar and oolitic sand grains.

Color: black or dark brown on both fresh and weathered surfaces.

Bedding: nodular, lenticular, and bedded stringers; within the chert, thin laminations ($<$0.3 cm) are defined by varying muscovite populations.

Comments: Contained in black chert-bearing microspar.

24. Noncalcareous argillites

Mineralogy and texture: dominantly clay with scattered quartz, feldspar, and muscovite silt grains and iron oxides.

Color: brown, gray, tan white, and rusty on both fresh and weathered surfaces.

Bedding: thick clay laminations (0.3 cm to 1 cm) separated by thin silty iron oxide-rich thin laminations ($<$0.3 cm); laminations are often irregular in thickness.

Comments: This rock type is exposed only in the lower Newland in a quarry at the mouth of Miller Gulch along Newlan Creek, where the argillite contains abundant soft sediment folds.

APPENDIX III

SECTION PROFILES

The section profiles are divided into two parts. These are a graphic representation of the section in the right column, containing lithologic symbols for the rock types and showing the weathering profile, and to the left a table of 10 columns containing data on thickness, rock types, bedding, color, mineralogy, grain size, amount of bedload transport, sedimentary structures, diagenetic features, and unit numbers used in the correlations.

Lithologic symbols are generalized, and are blocky patterns for carbonate, slanted block patterns for dolomite, broken horizontal line patterns for shale, and stippled patterns for sandstone. Blank areas with X's indicate covered intervals.

Column 1 is divided into a right half, showing the measured thickness in feet, and a left half showing the measured thickness in meters. The scale is 40 feet to the inch.

Column 2 is divided into a right half with numbers corresponding to rock types in Appendix II, and a left half with symbols for bedding. TNL = thinly laminated (0.3 cm); TKL = thickly laminated (0.3-1 cm); TNB = thin bedded (1-10 cm); MB = medium bedded (10-30 cm); TKB = thickly bedded (30-100 cm).

Column 3 contains symbols for the rock types fresh and weathering colors. T = tan, G = gray; Gr = Green; B = brown; Bl = black; Ru = rusty; R = red; W = white; and the prefix D = dark and L = light.

Column 4 shows carbonate content, both dolomitic and calcitic. L = low; M = moderate; H = high; and the prefix V = very.

Column 5 shows dolomite content. The symbols are the same as in column 4.

The right half of column 6 shows clay content, and the left half shows terrigenous silt and sand content. The symbols are the same as in column 4.

Column 7 shows the amount of bedload transport, based on the abundance of hydraulically formed primary sedimentary structures. The symbols are the same as in column 4.

Column 8 shows the types of sedimentary structures. R = ripple cross-laminations; LS = load structures; MR = megaripples; SSD = soft sediment deformation from compression; FC = flute casts.

Column 9 shows types of diagenetic structures in the carbonates discussed in Chapter IV. R = ropes; CP = curved plates; H = hemispheroids; IH = inverted hemispheroids; O = ovoids; TLS = thinly laminated structures; M = mottling; and OM = oriented mottling.

The Roman numerals in column 10 correspond to the lithologic units discussed in Chapter II and used in the correlations. O = lower Newland.

The arrows indicate the range of the characteristic indicated by the symbol at the base of an arrow. Symbols in parentheses indicate that that characteristic is confined to that specific corresponding horizon, and are used with thin but significant layers.

Newlan Creek section

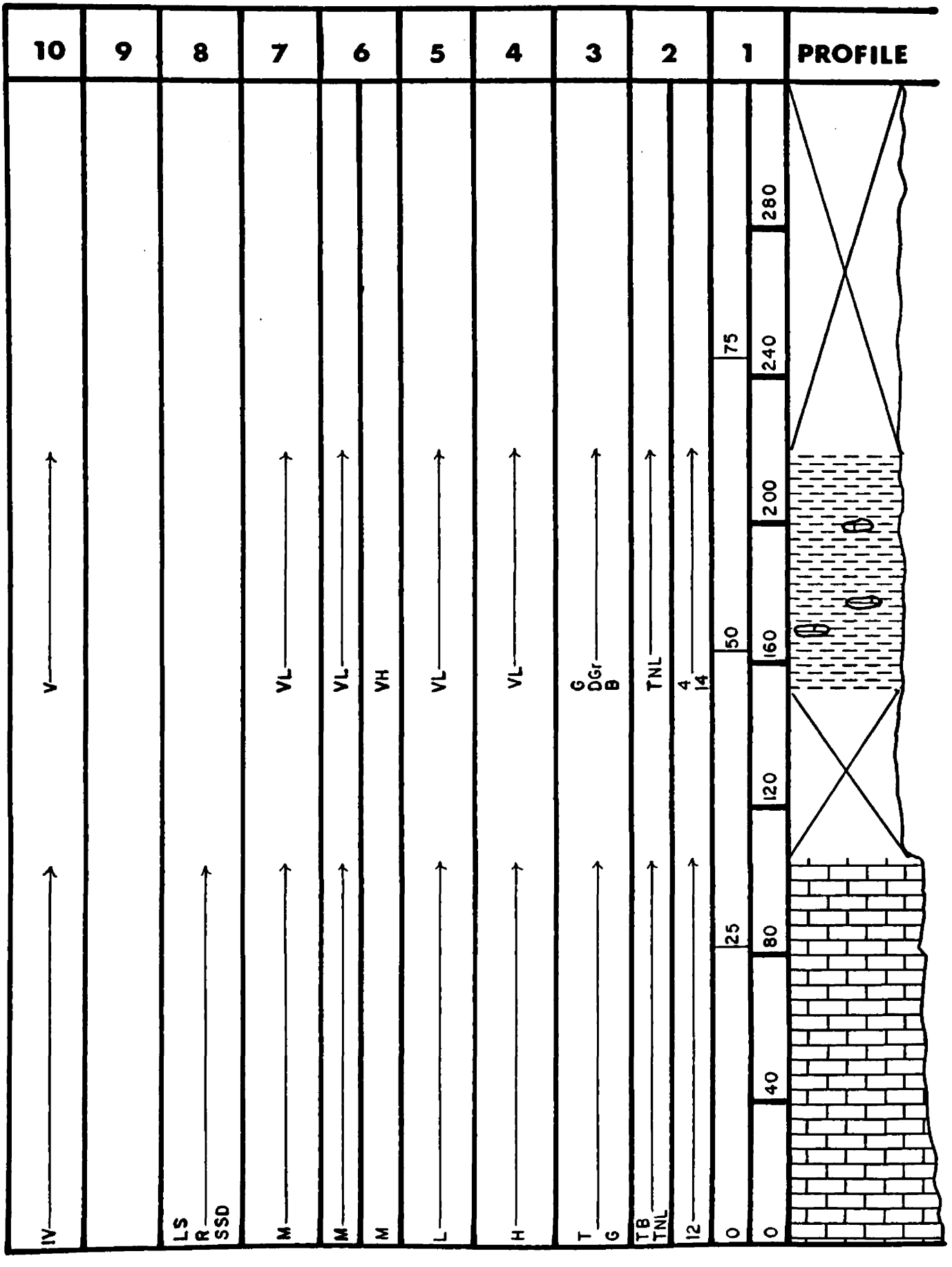

Newlan Creek section

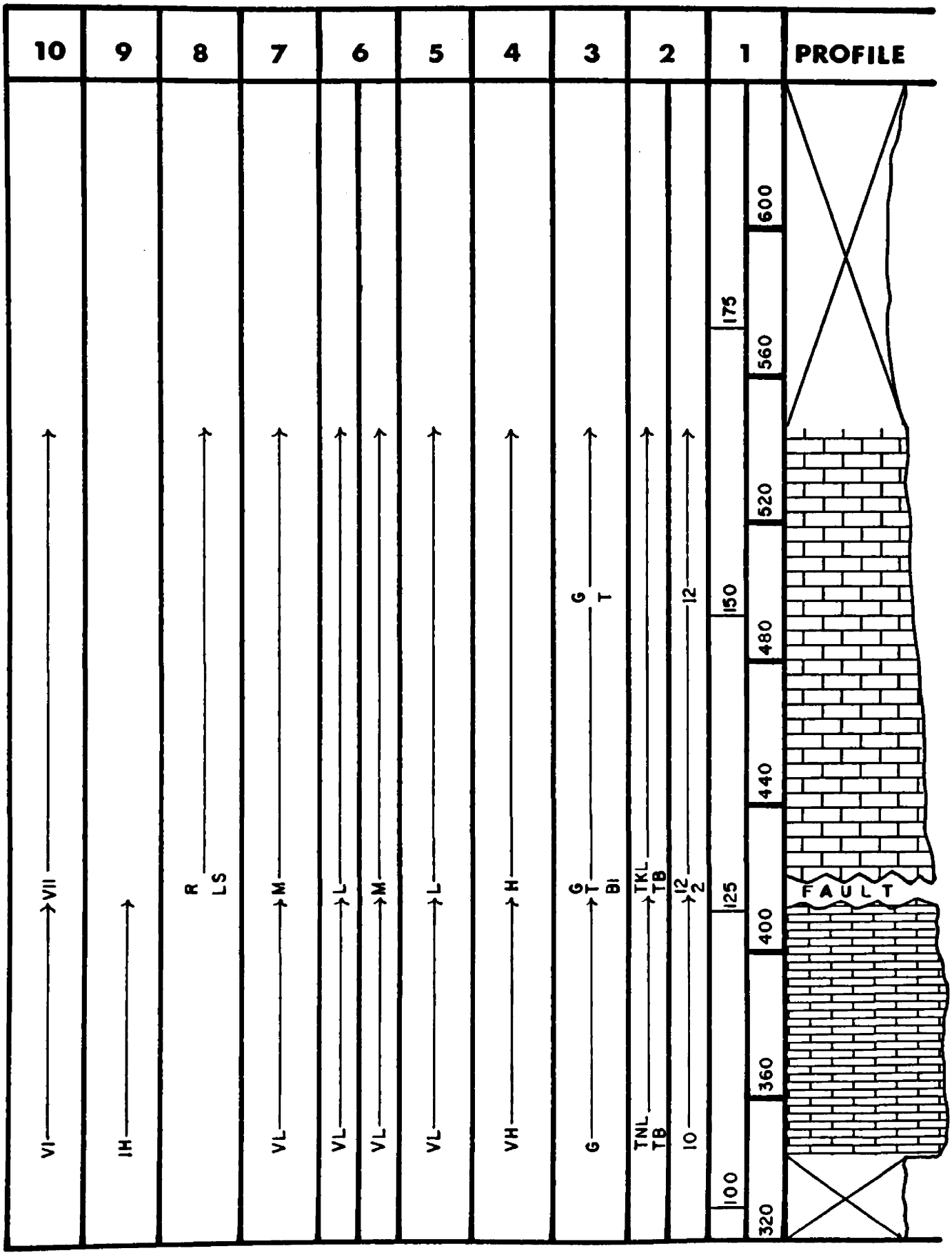

Decker Gulch section

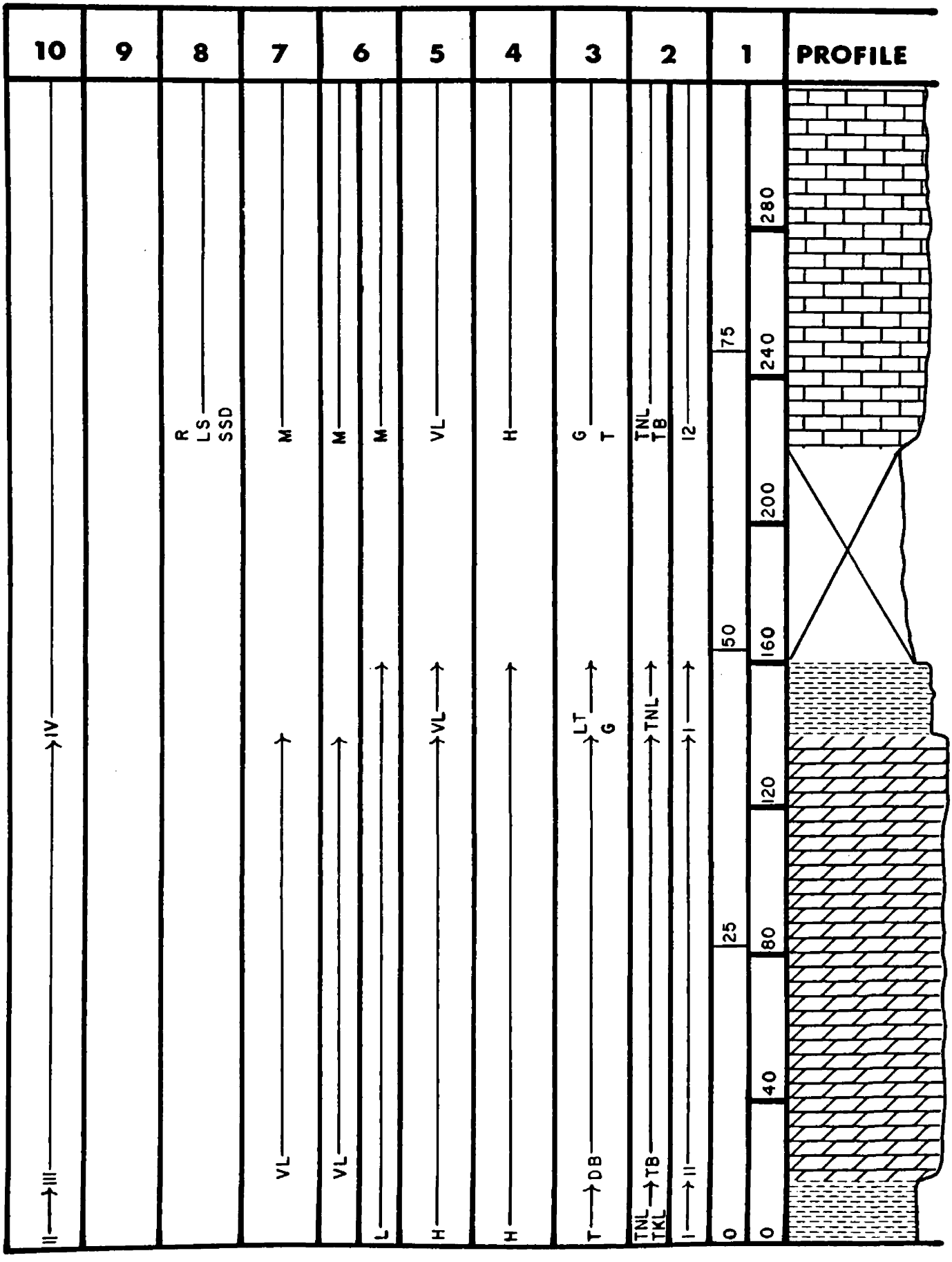

Decker Gulch section

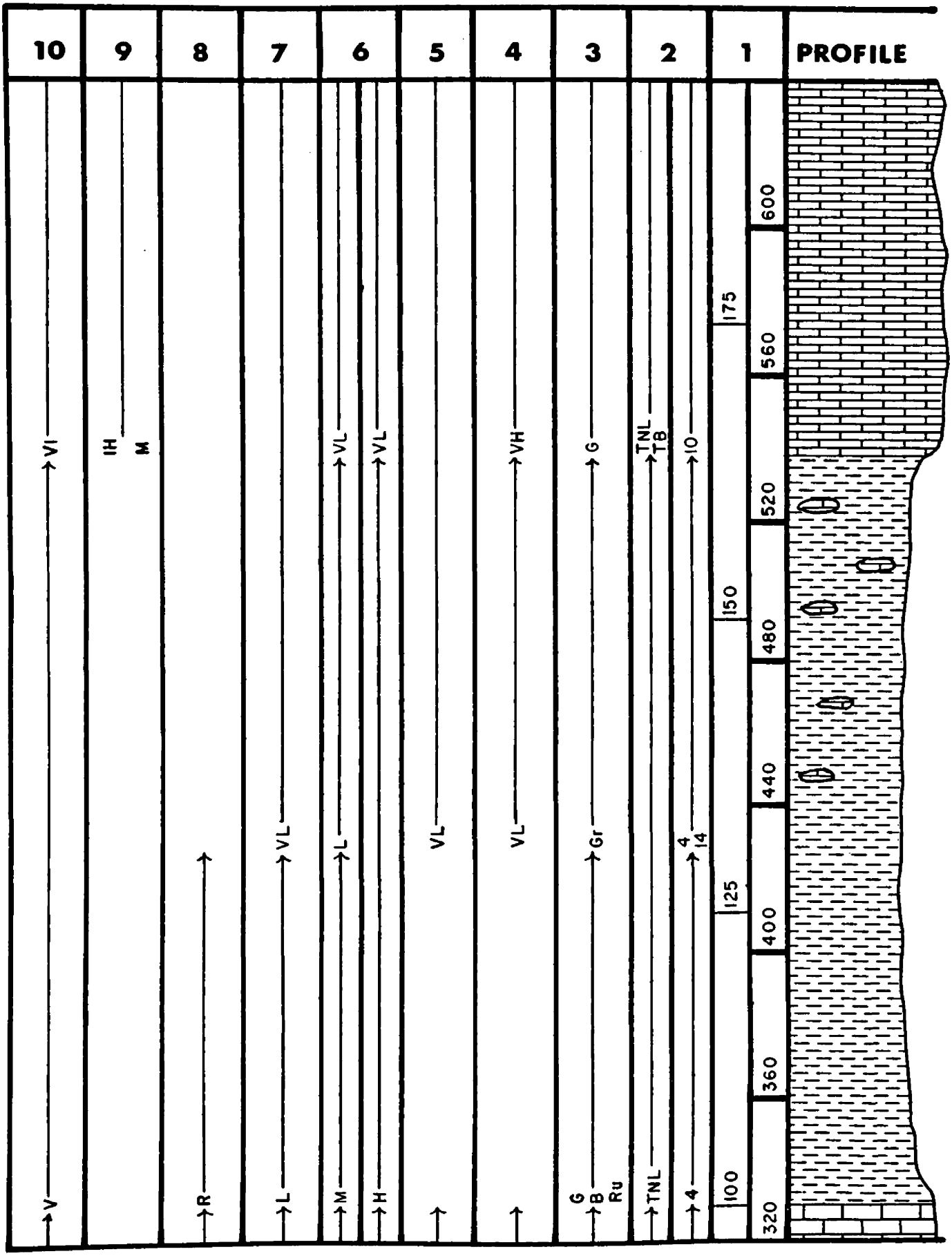

Decker Gulch section

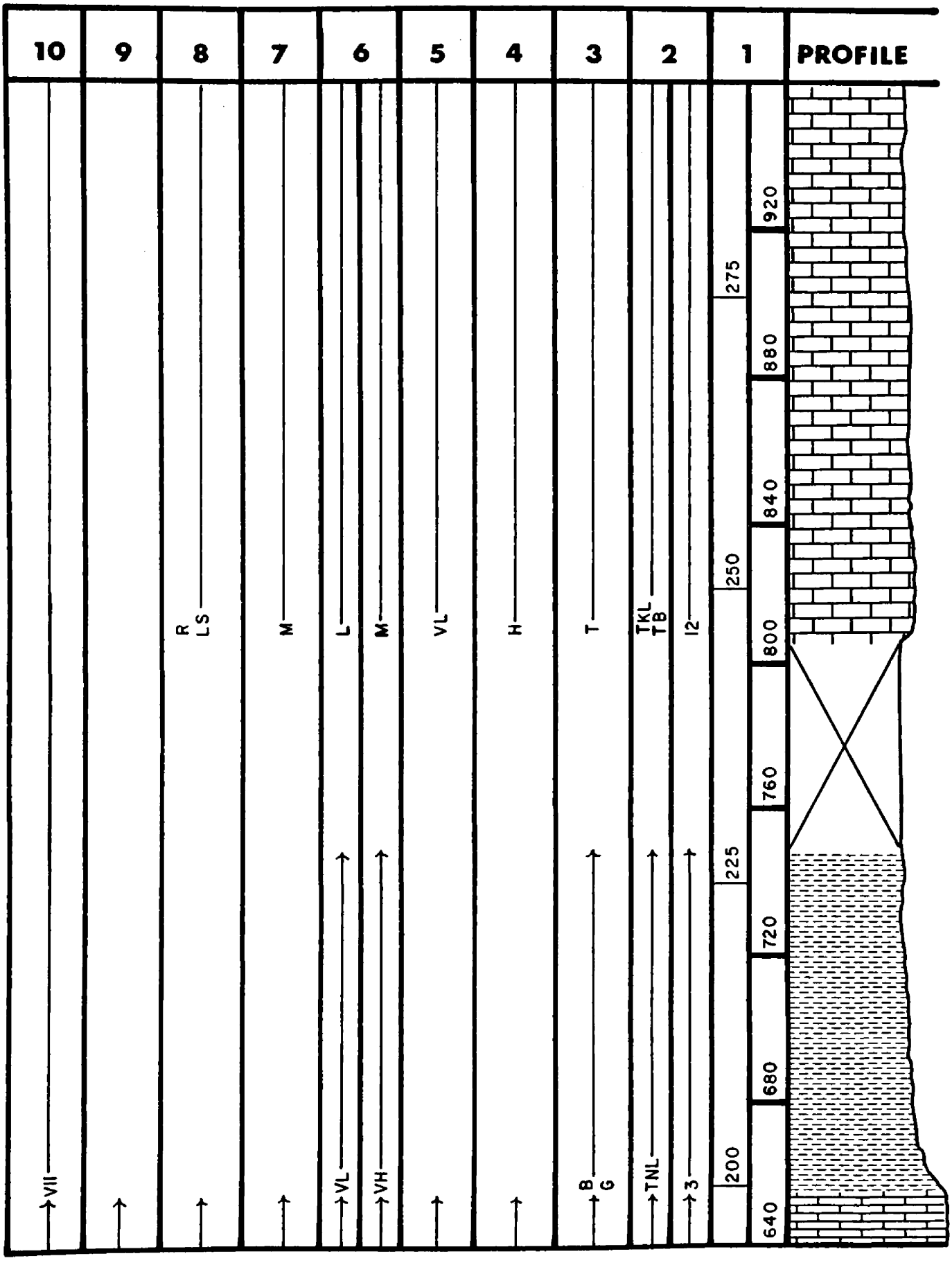

Decker Gulch section

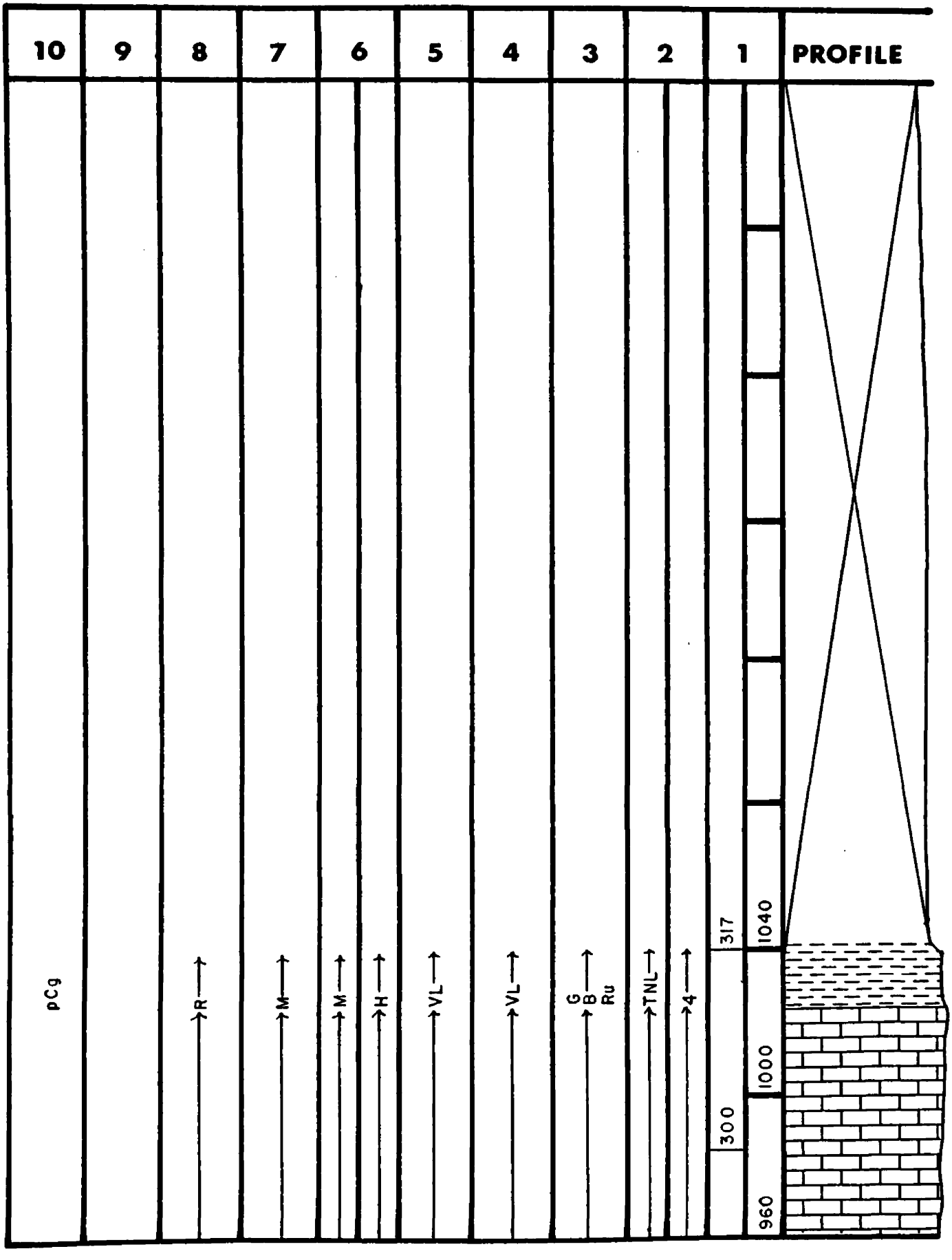

Smith River Section

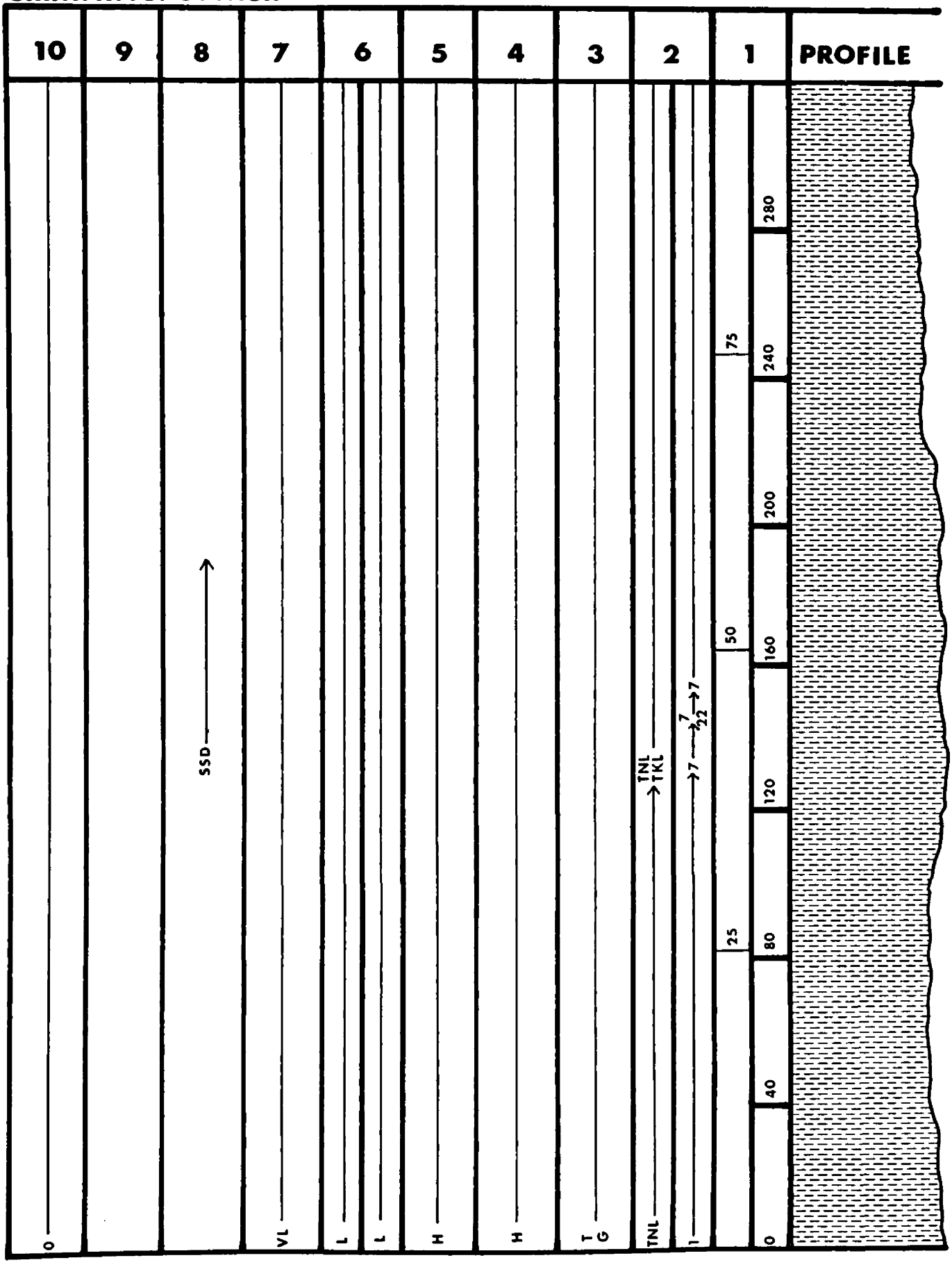

Smith River Section

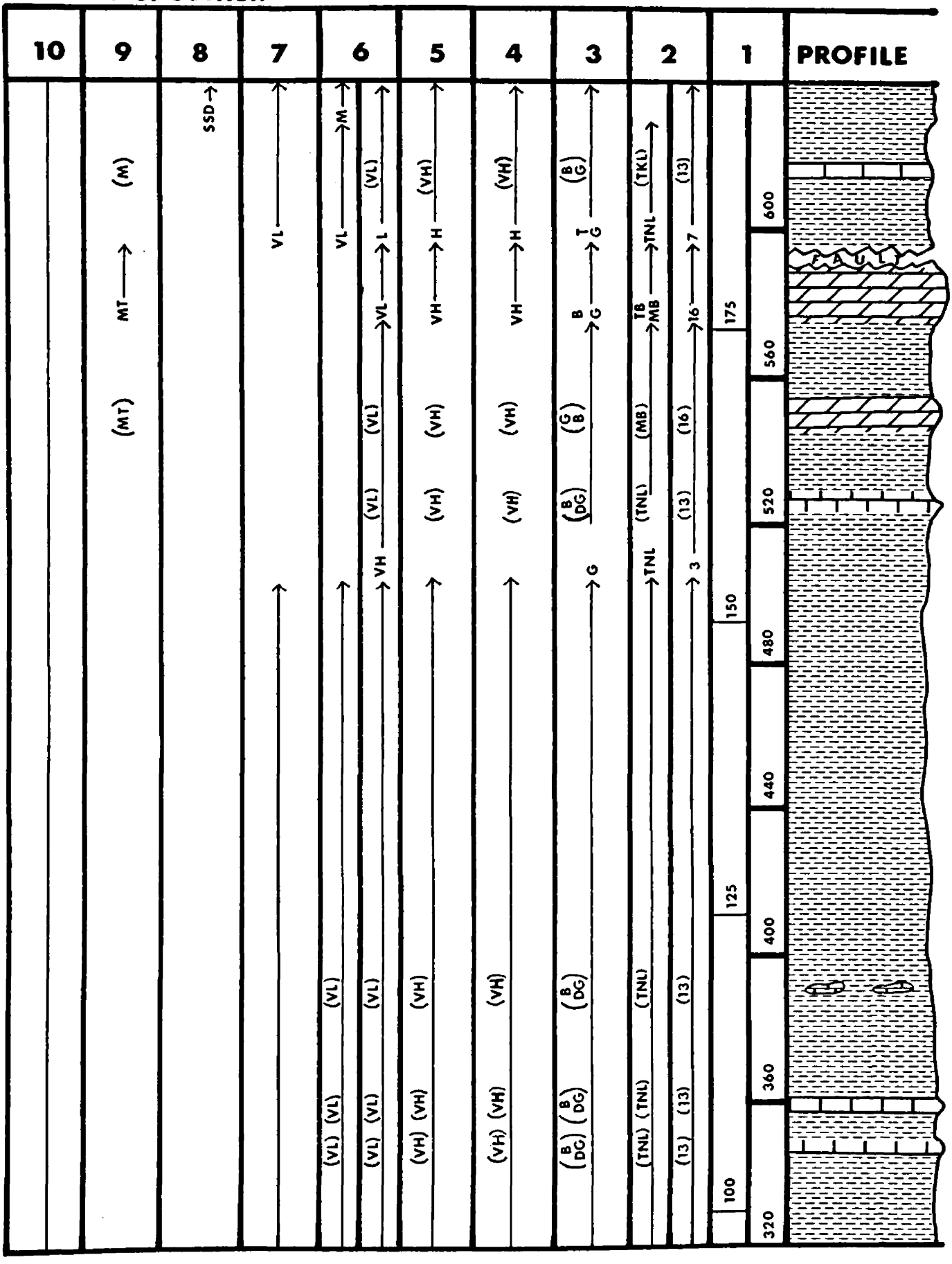

Smith River section

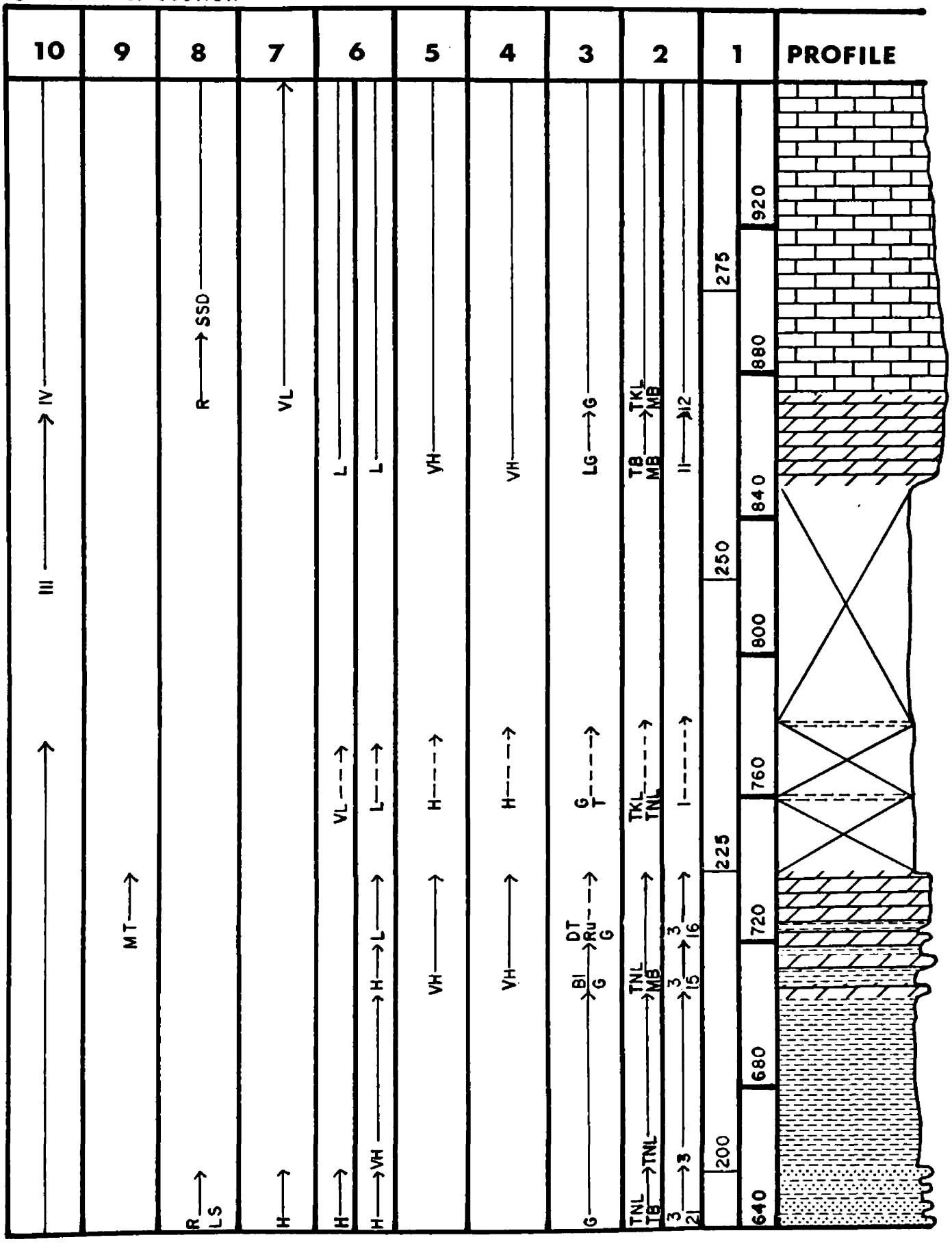

Smith River section

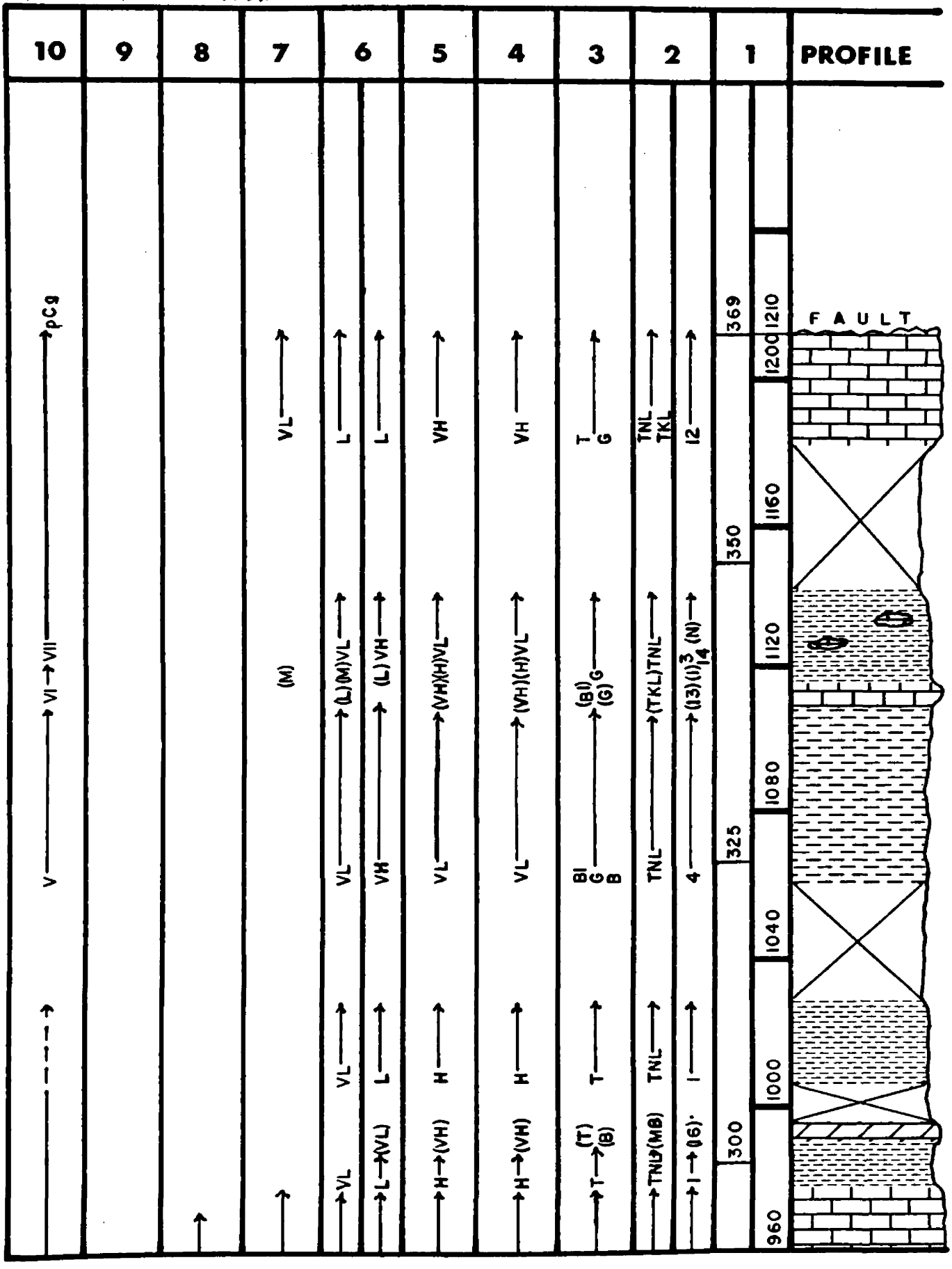

Little Birch Creek section

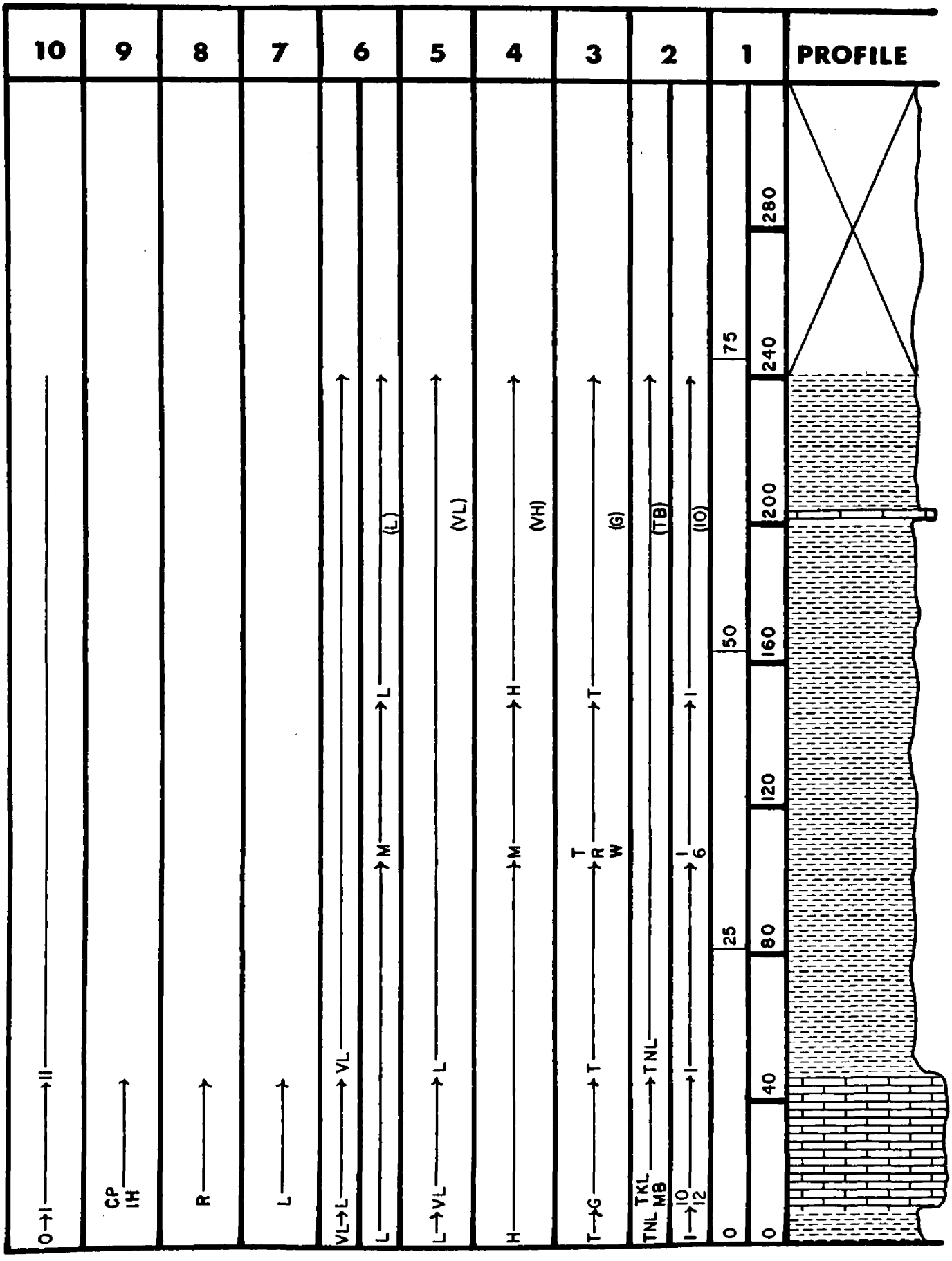

Little Birch Creek section

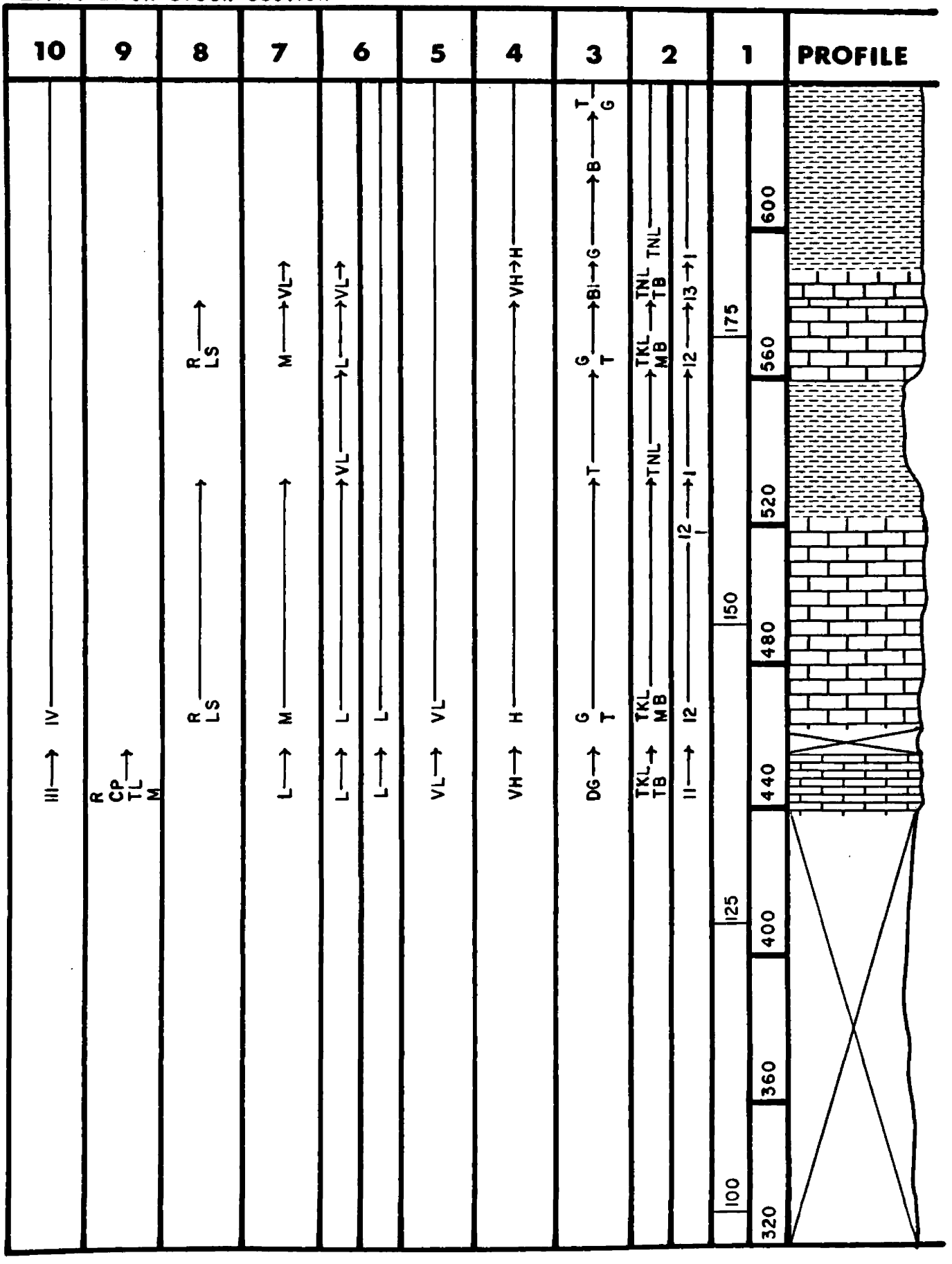

Little Birch Creek

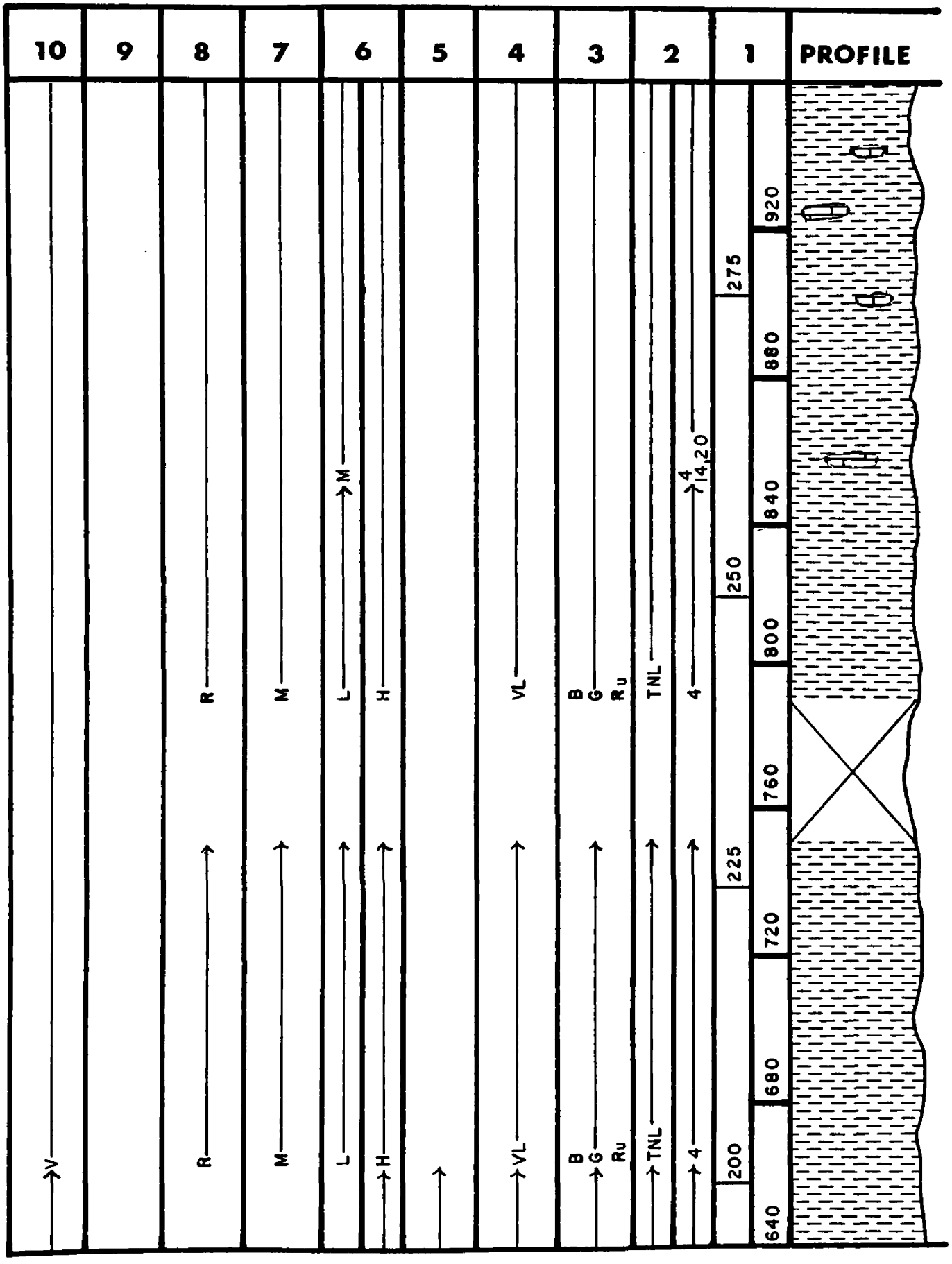

Little Birch Creek section

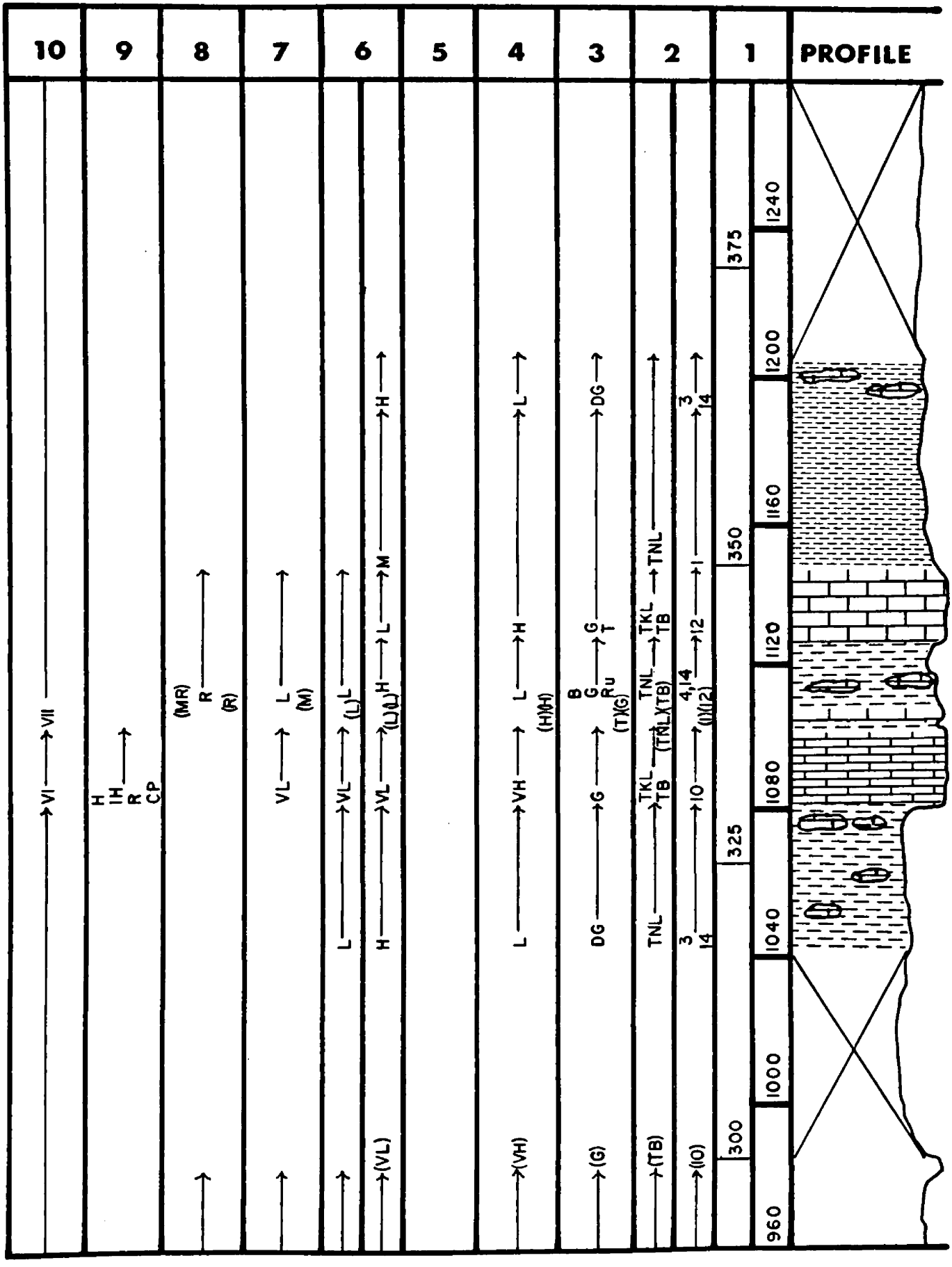

Little Birch Creek section

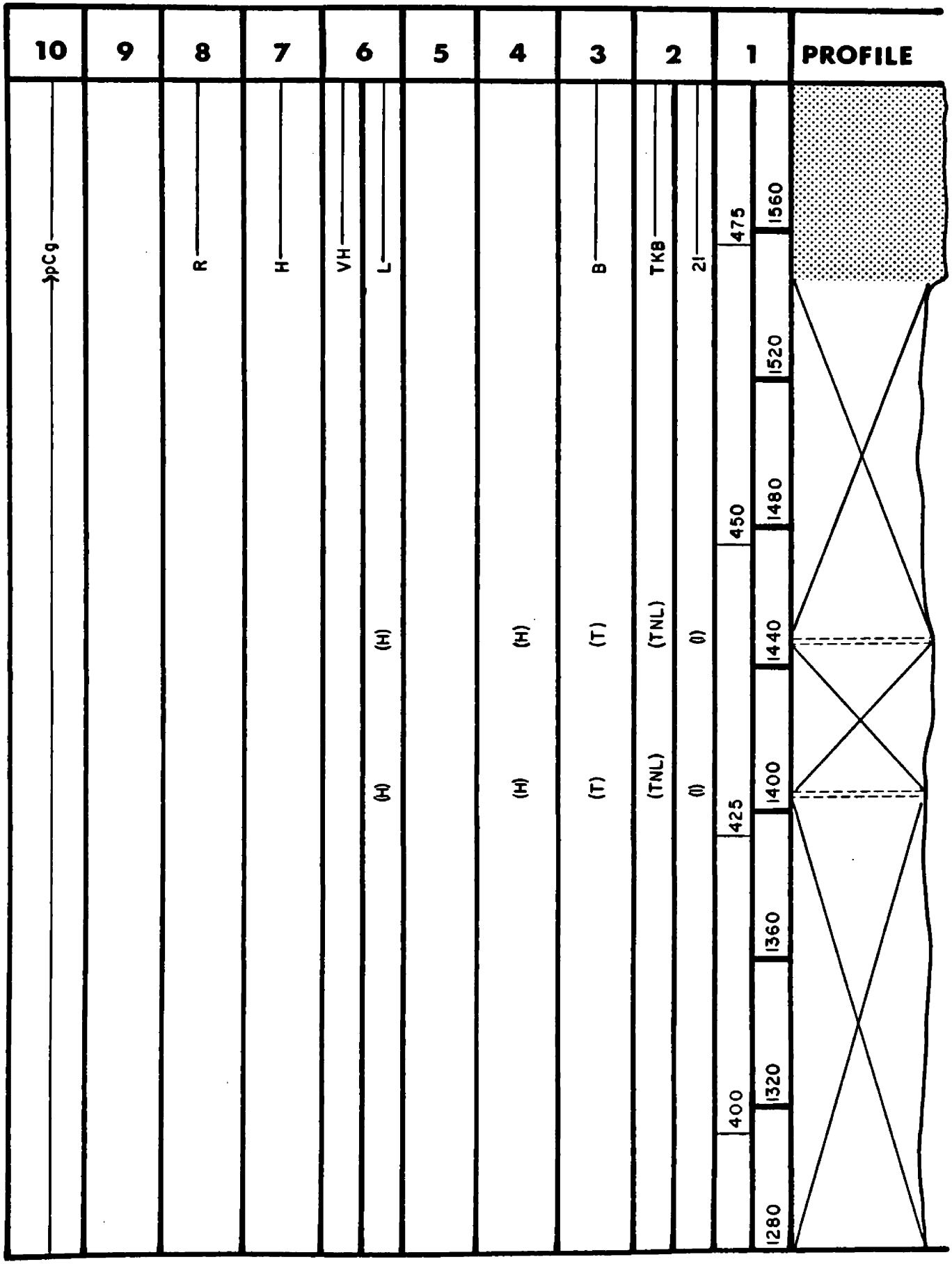

Little Birch Creek section

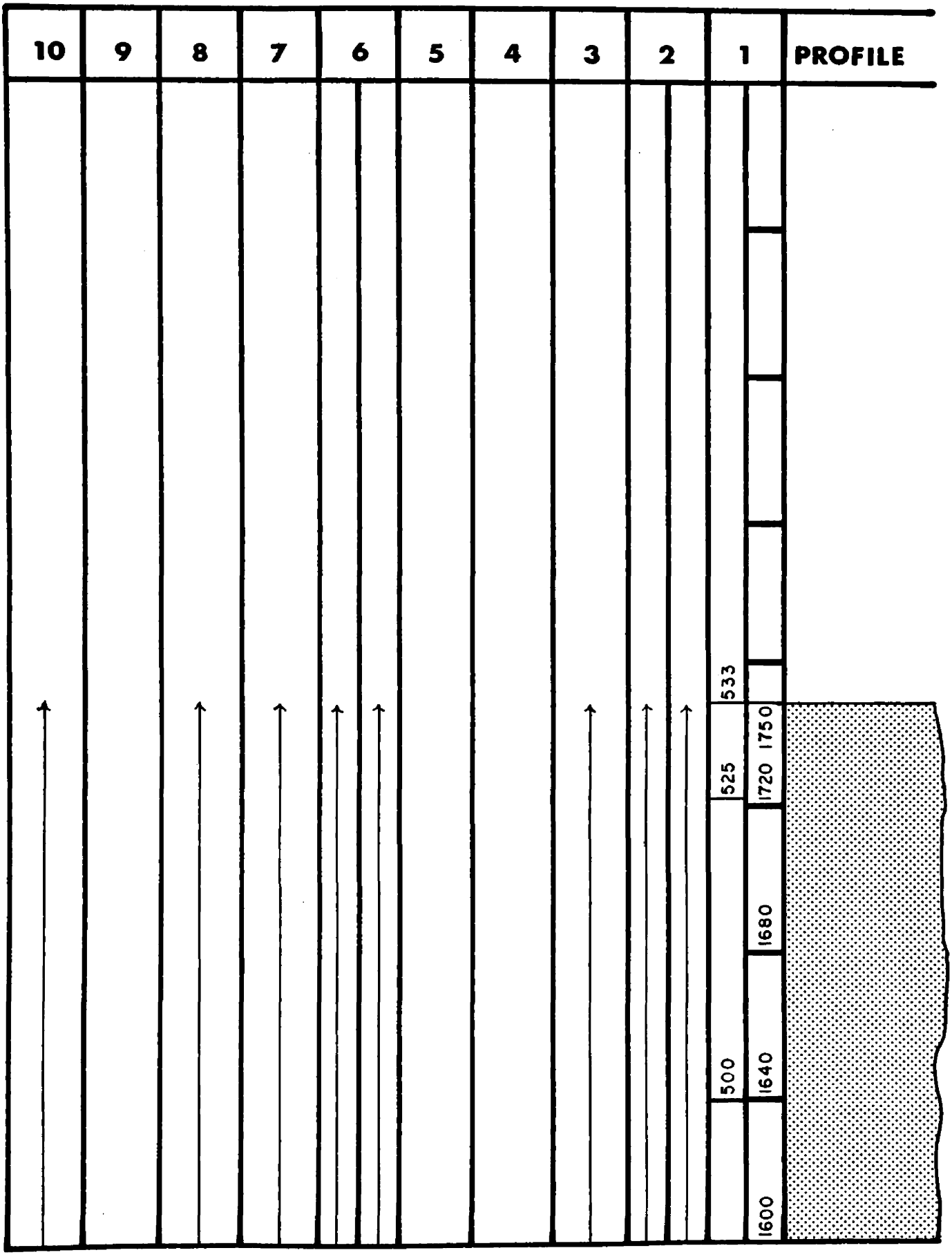

Deep Creek section

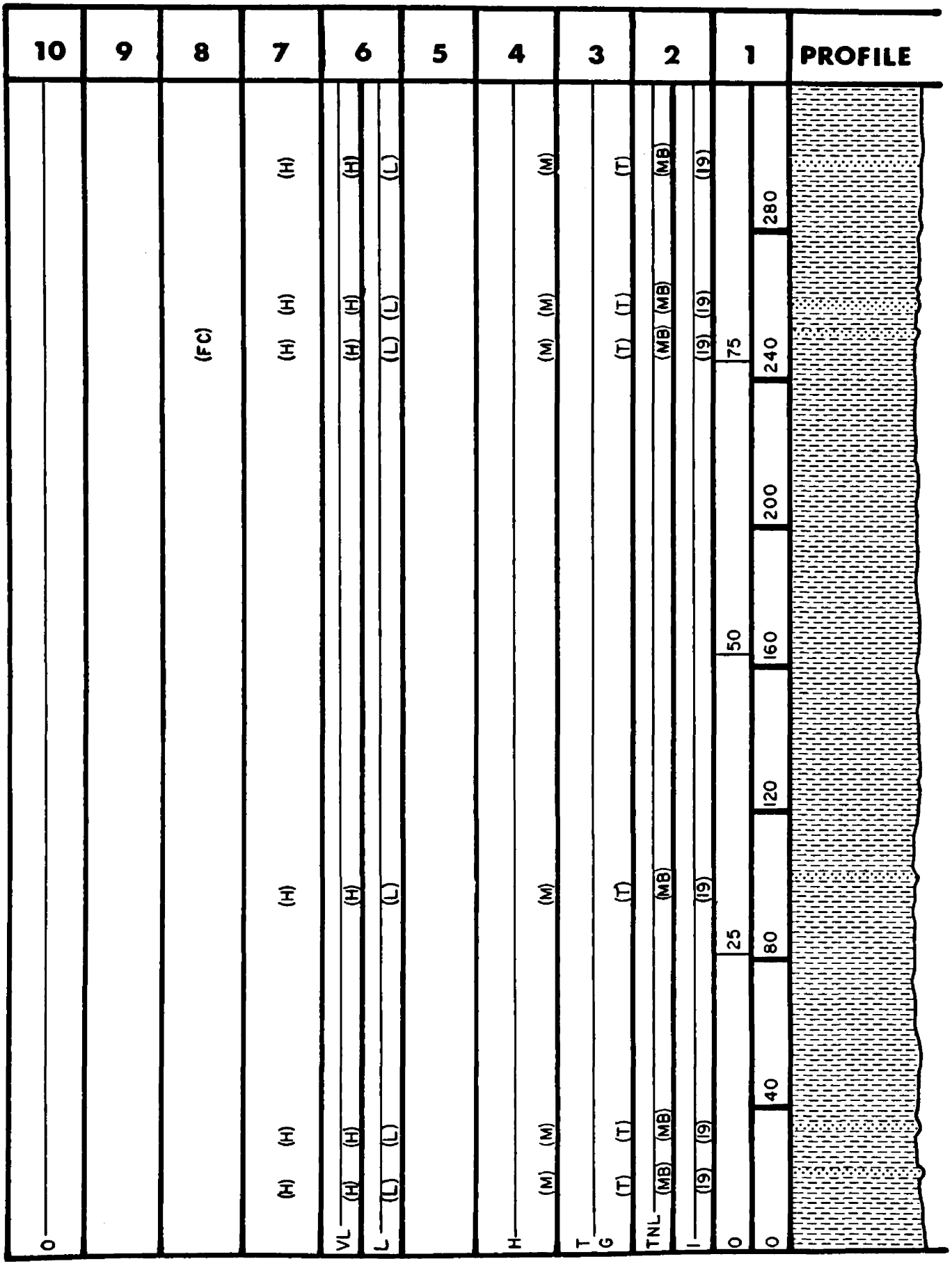

Deep Creek section

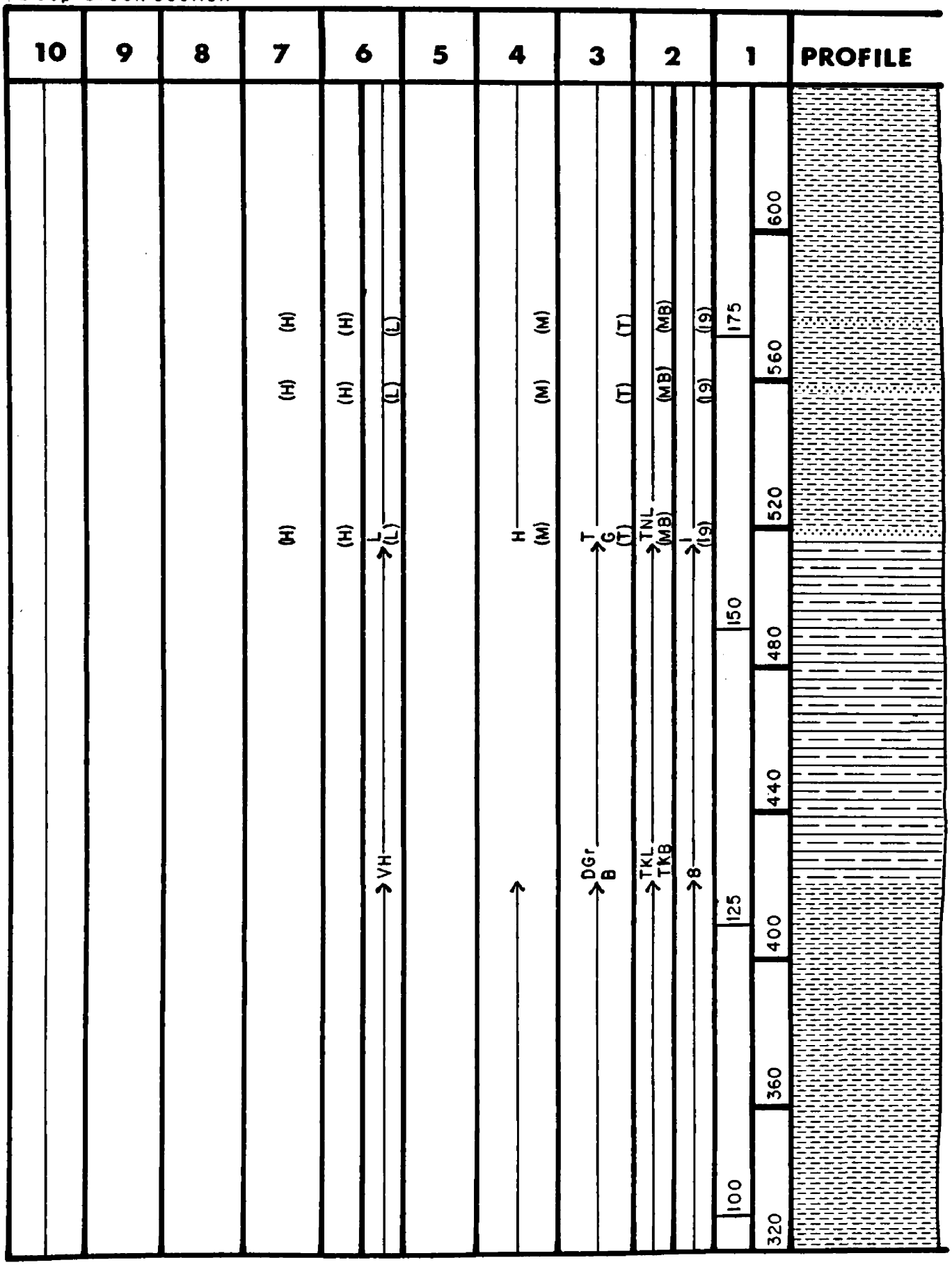

Deep Creek section

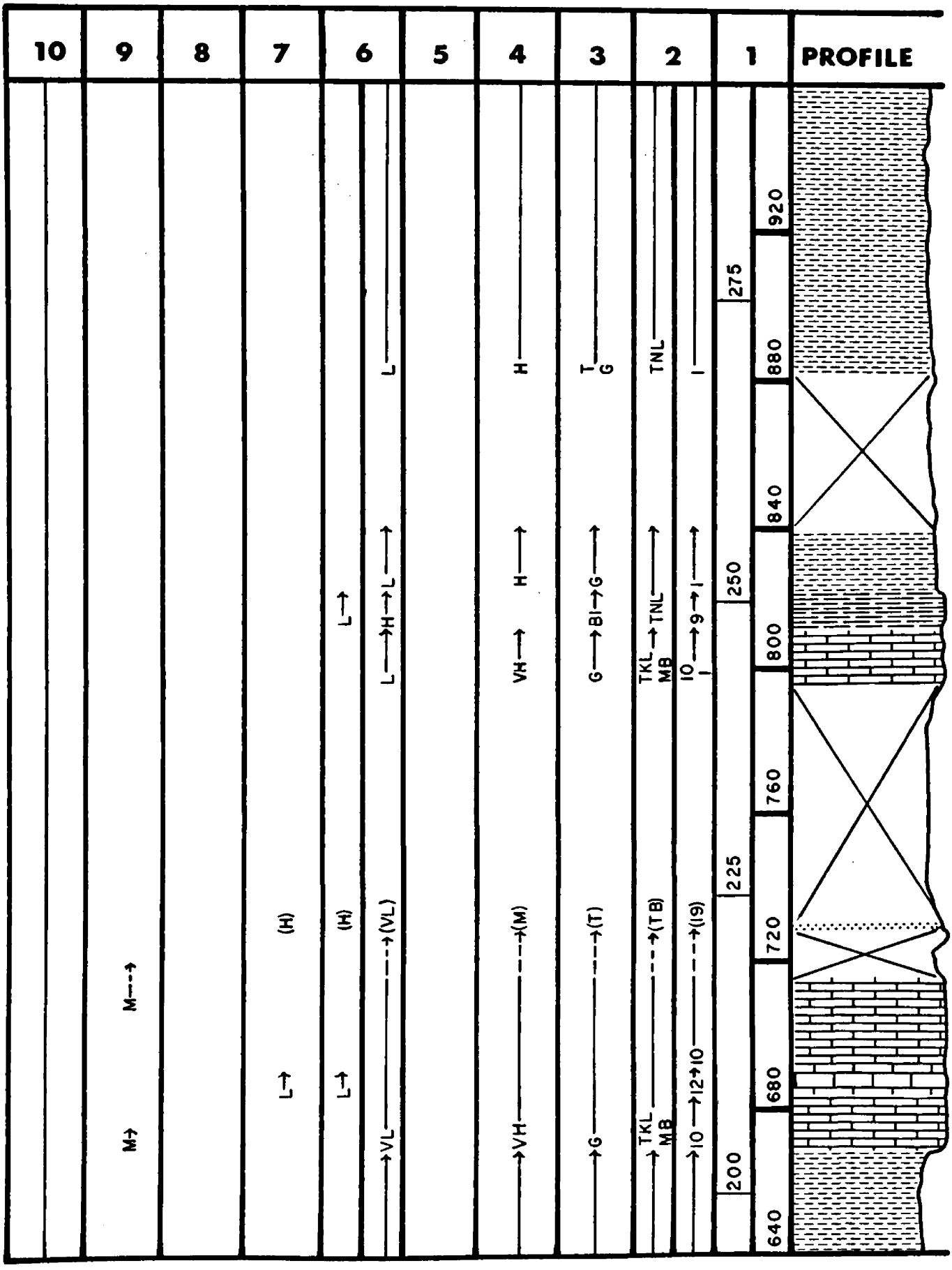

Deep Creek section

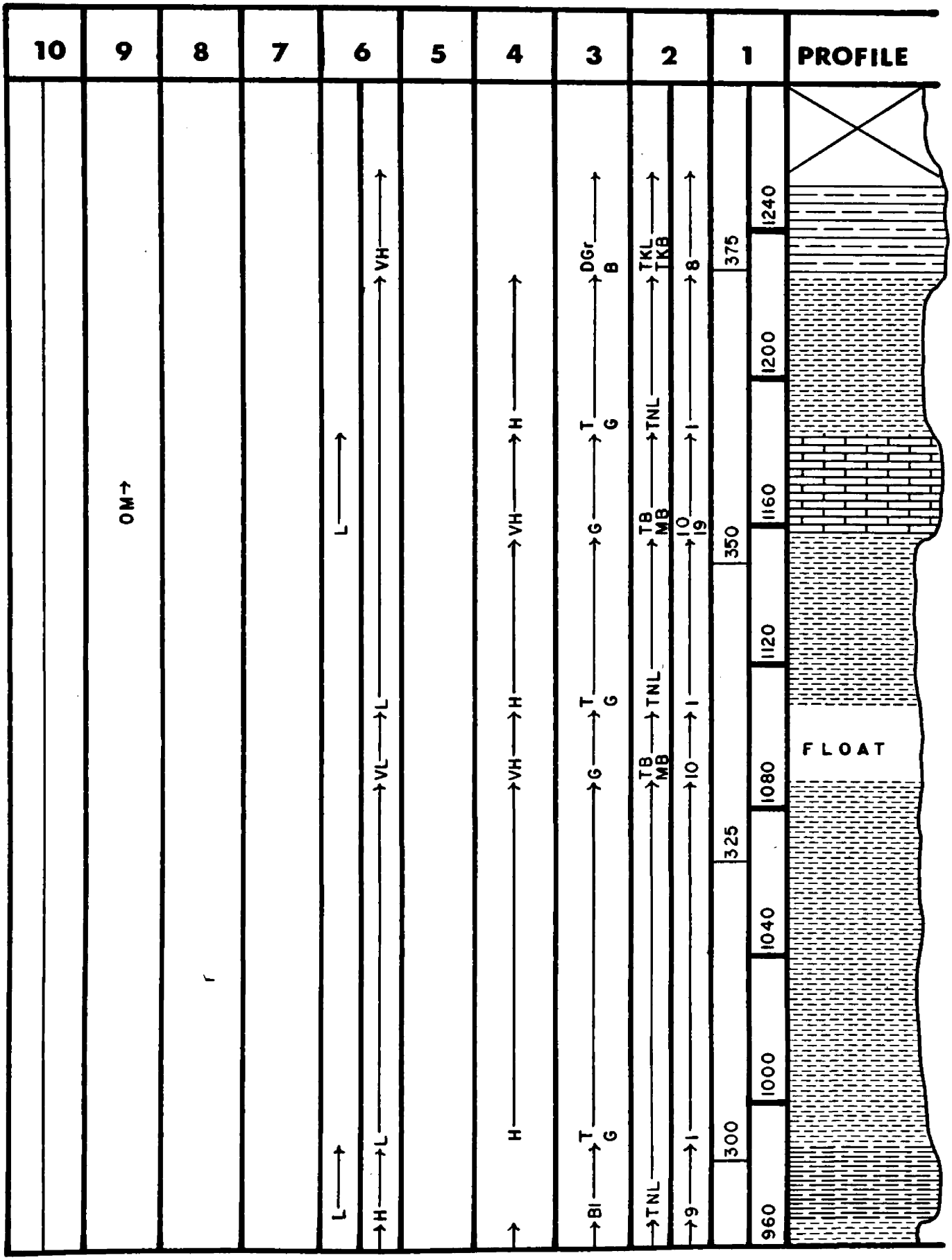

Deep Creek section

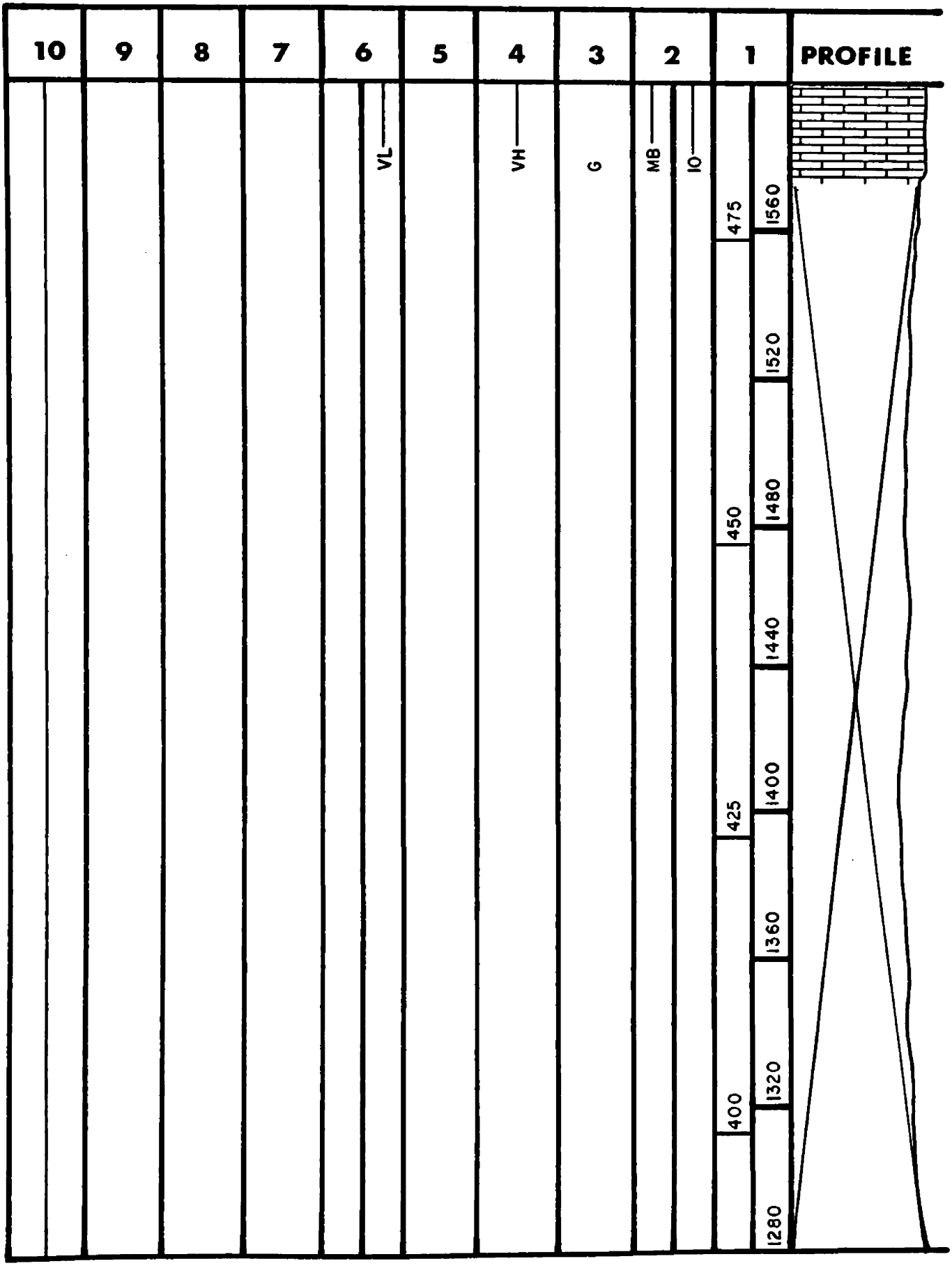

Deep Creek section

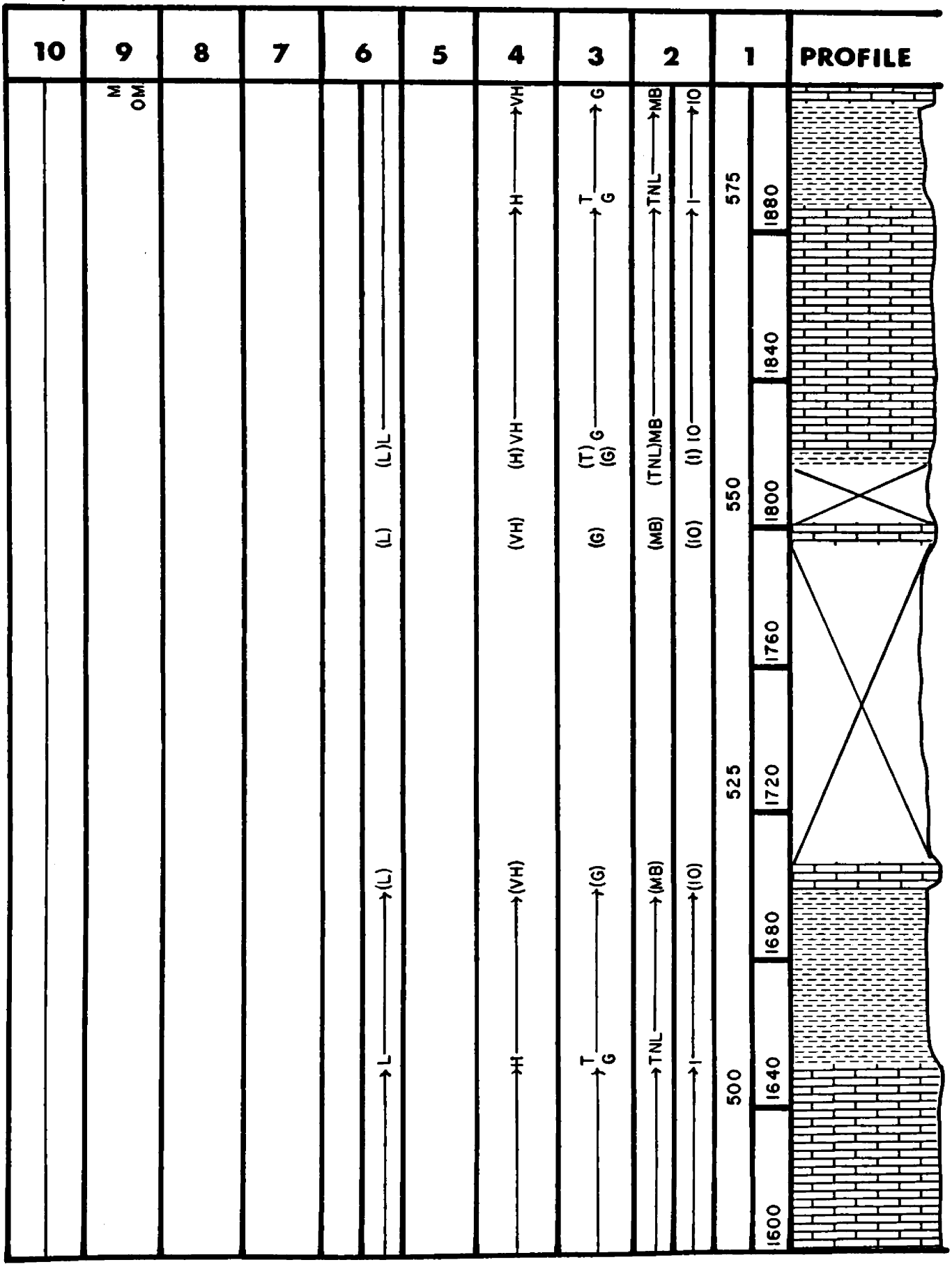

Deep Creek section

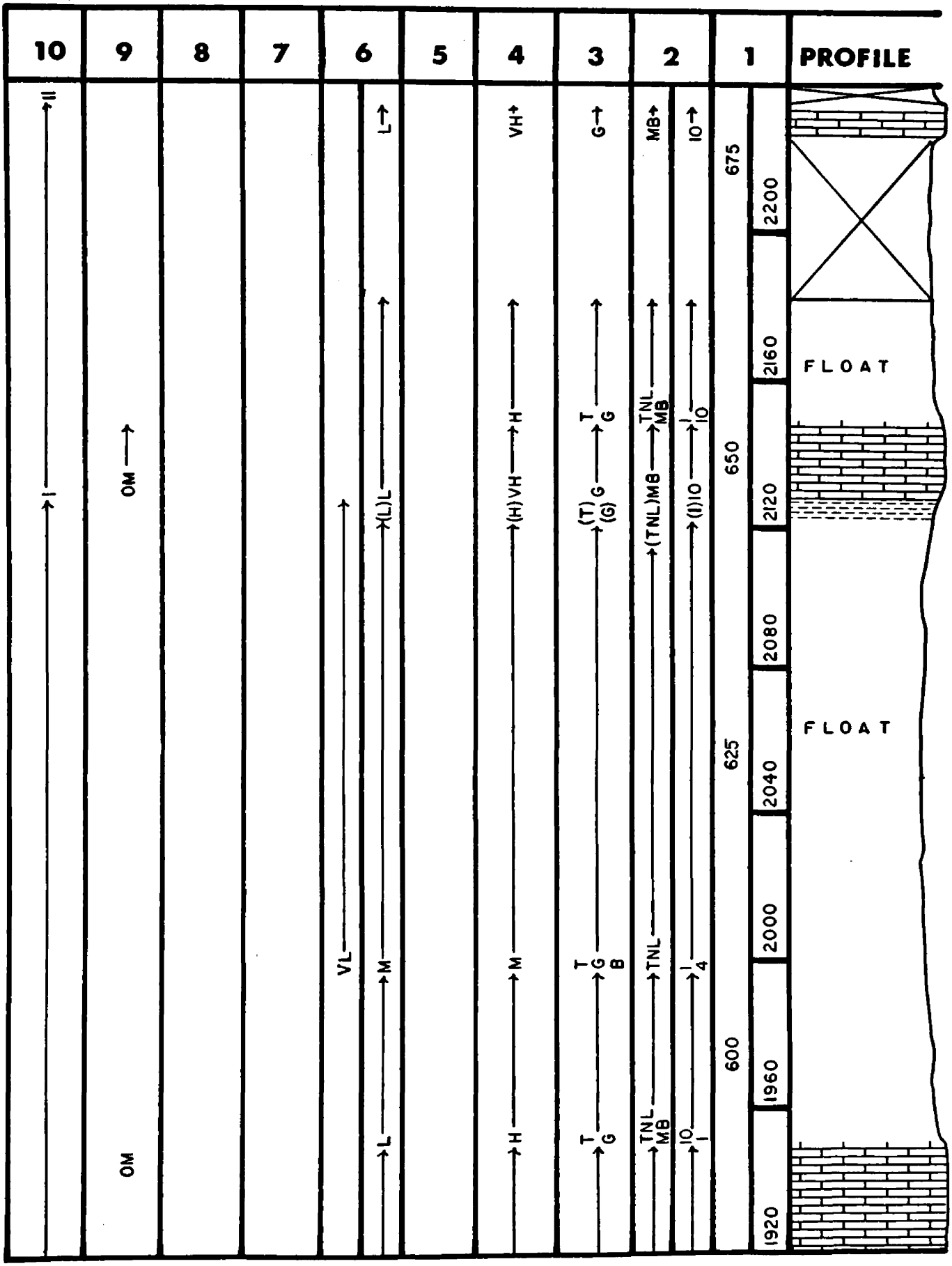

Deep Creek section

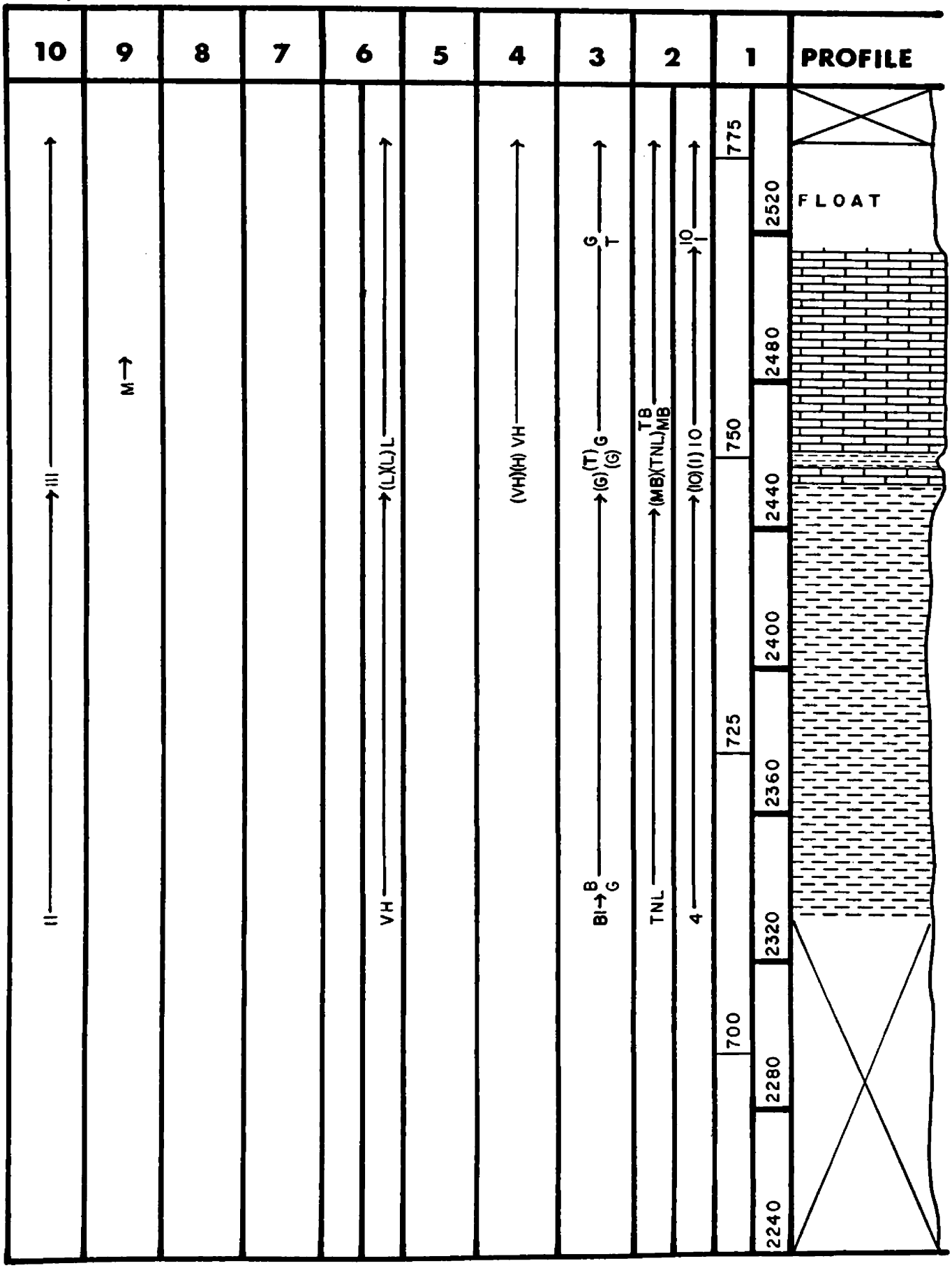

Deep Creek section

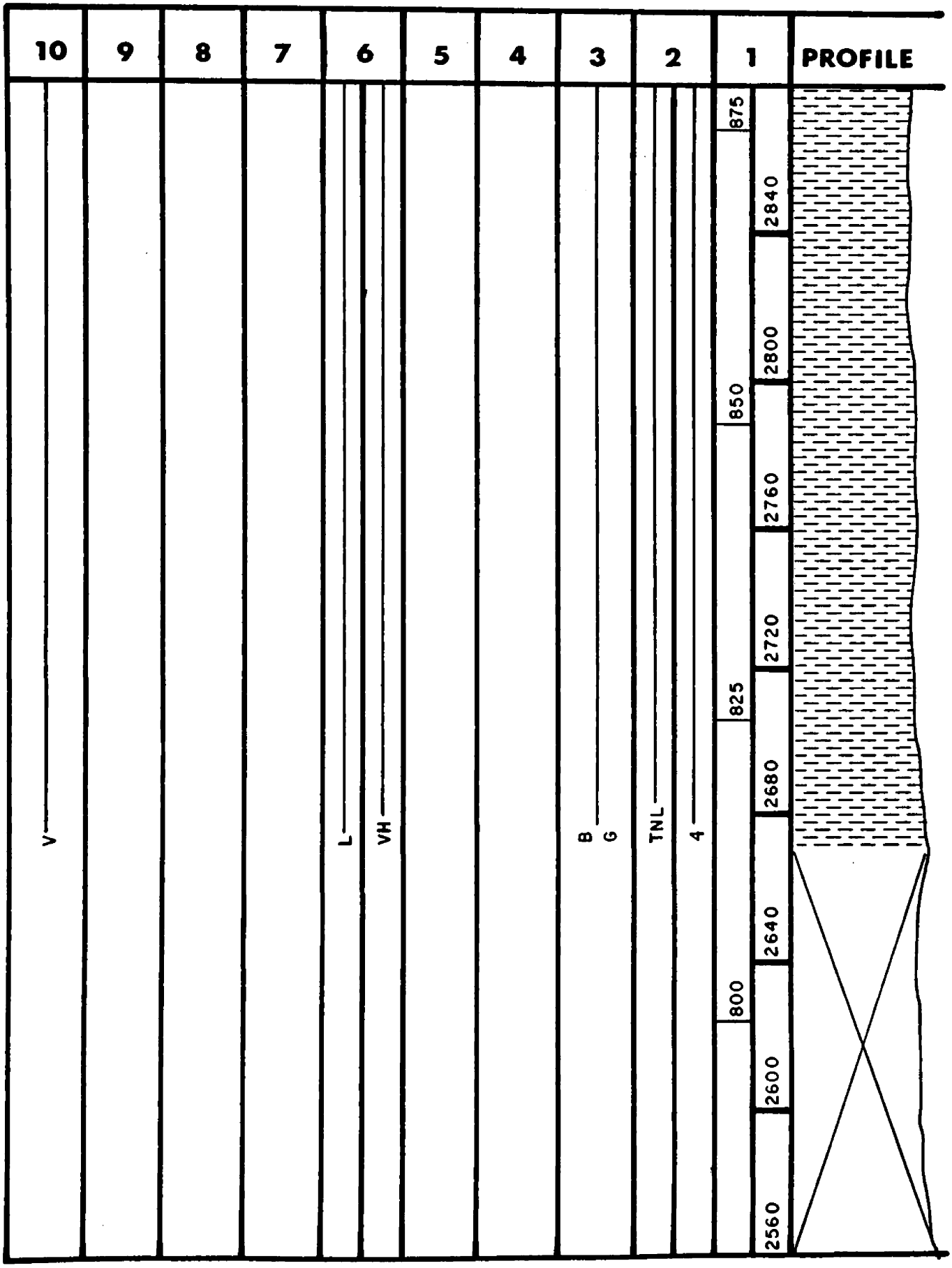

Deep Creek section

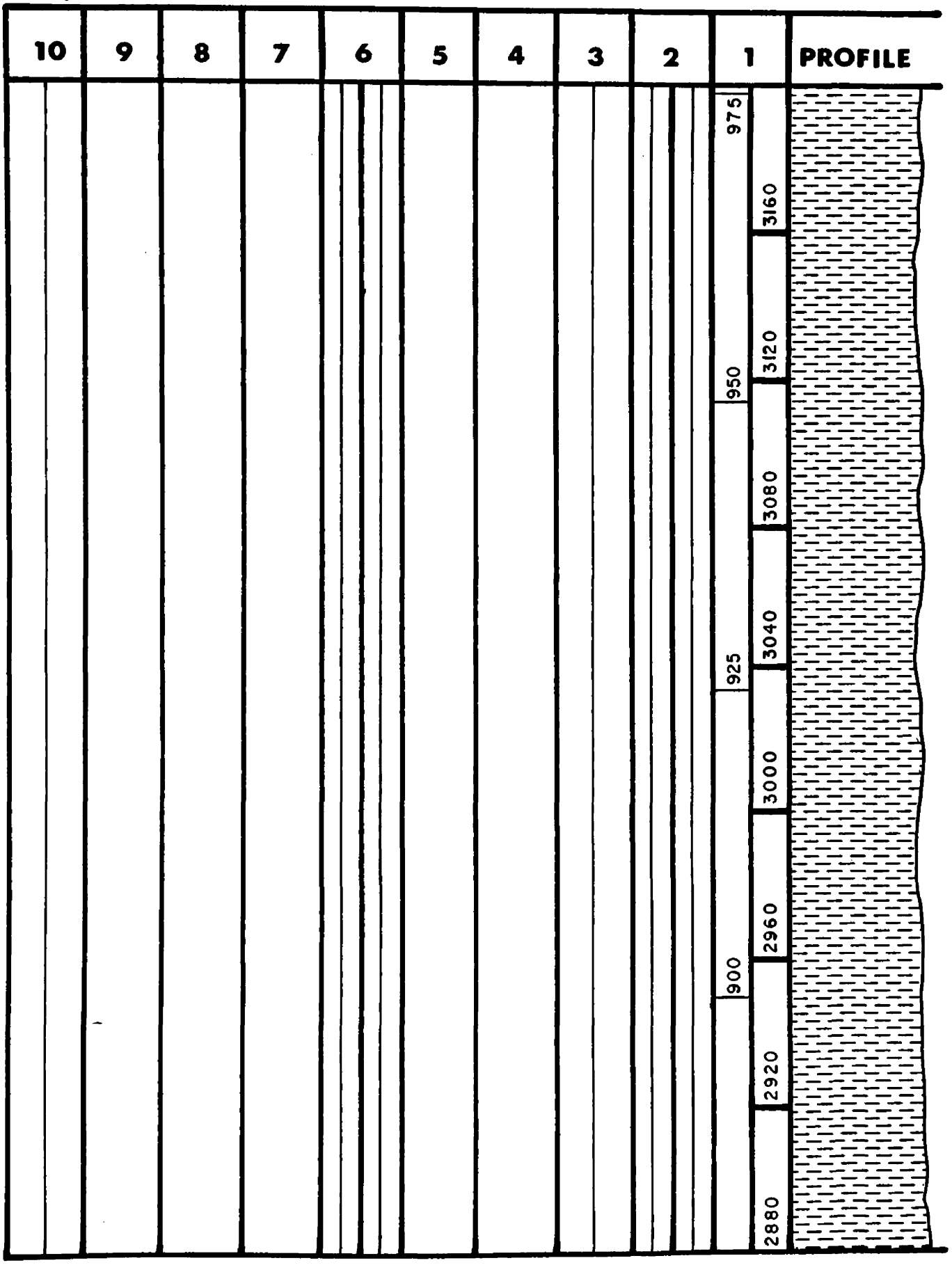

Deep Creek section

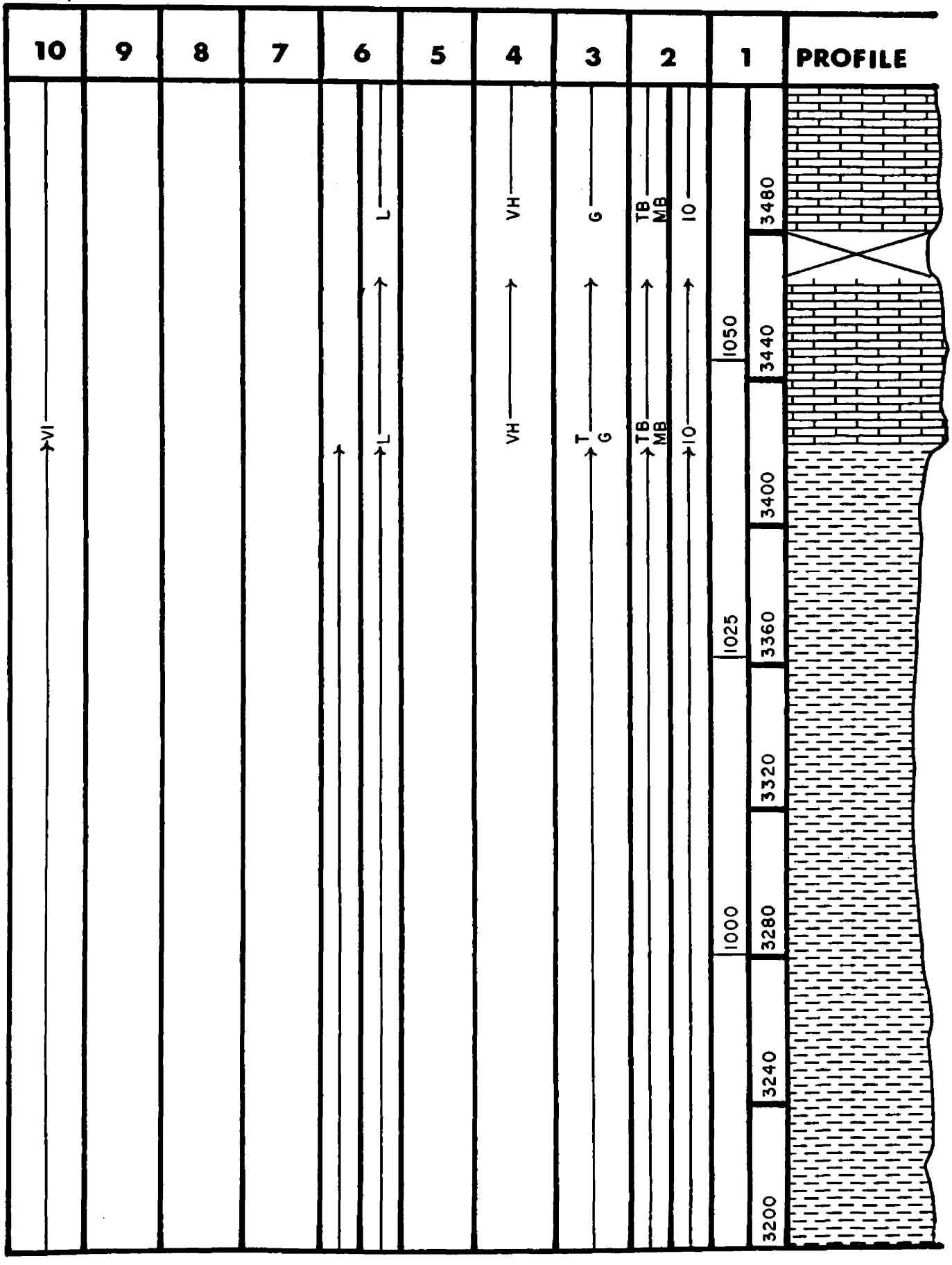

Deep Creek section

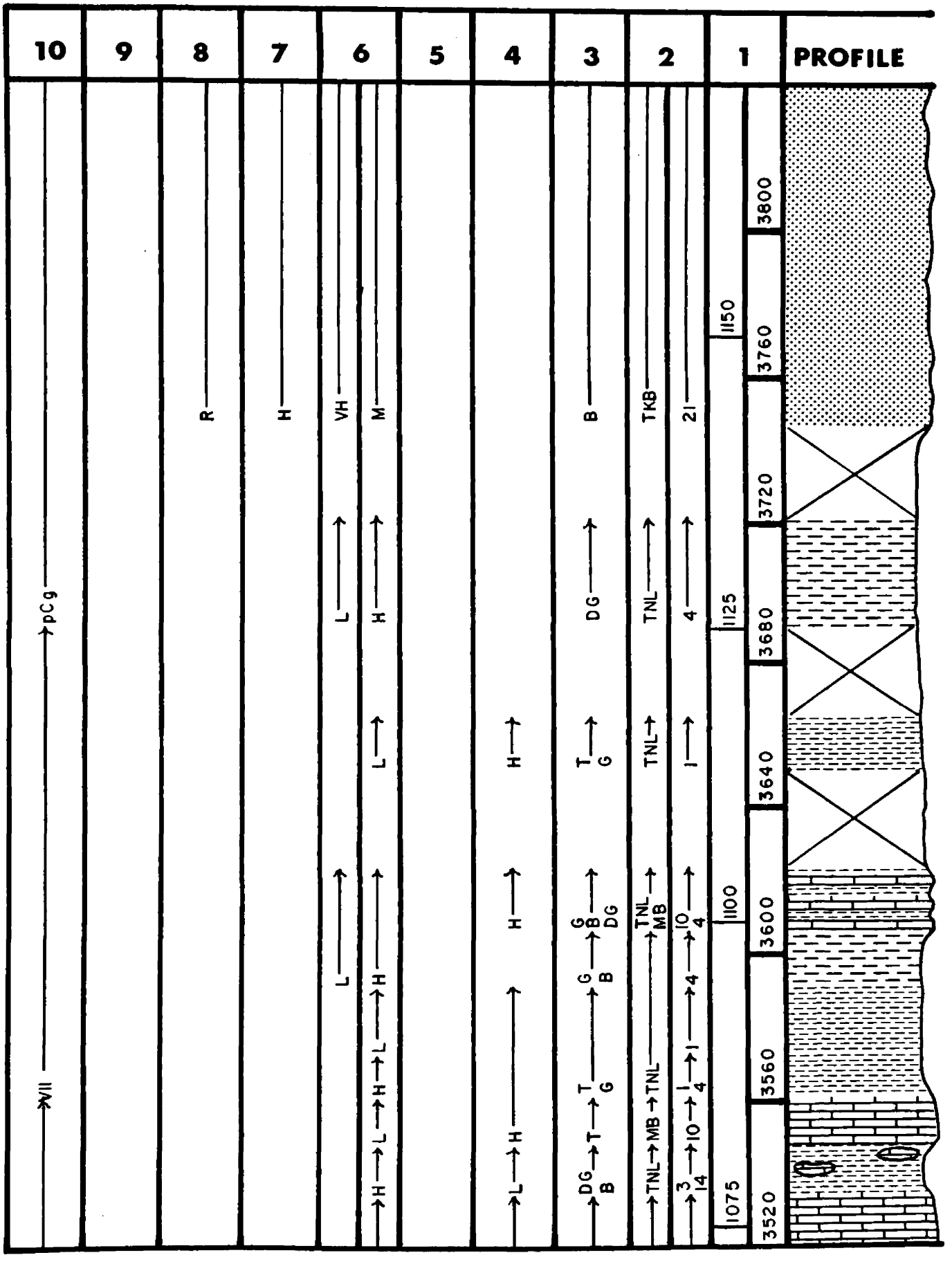
10
9
8
7
6
5
4
3
2
1
PROFILE
pCg
VII
R
H
VH
L
M
H
L
H
L
H
L
H
H
L
H
H
L
H